RADC-TR-80-362
Phase Report
November 1980

AN H-FIELD SOLUTION FOR A CONDUCTING BODY OF REVOLUTION

Syracuse University

Joseph R. Mautz
Roger F. Harrington

APPROVED FOR PUBLIC RELEASE; DISTRIBUTION UNLIMITED

ROME AIR DEVELOPMENT CENTER
Air Force Systems Command
Griffiss Air Force Base, New York 13441

This report has been reviewed by the RADC Public Affairs Office (PA) and is releasable to the National Technical Information Service (NTIS). At NTIS it will be releasable to the general public, including foreign nations.

RADC-TR-80-362 has been reviewed and is approved for publication.

APPROVED: Roy F. Stratton

ROY F. STRATTON
Project Engineer

APPROVED: David C. Luke

DAVID C. LUKE, Colonel, USAF
Chief, Reliability & Compatibility Division

FOR THE COMMANDER: John P. Huss

JOHN P. HUSS
Acting Chief, Plans Office

If your address has changed or if you wish to be removed from the RADC mailing list, or if the addressee is no longer employed by your organization, please notify RADC (RBCT) Griffiss AFB NY 13441. This will assist us in maintaining a current mailing list.

Do not return this copy. Retain or destroy.

UNCLASSIFIED

SECURITY CLASSIFICATION OF THIS PAGE (When Data Entered)

REPORT DOCUMENTATION PAGE

READ INSTRUCTIONS BEFORE COMPLETING FORM

1. REPORT NUMBER: RADC-TR-80-362	2. GOVT ACCESSION NO: AD-A096313
3. RECIPIENT'S CATALOG NUMBER	
4. TITLE (and Subtitle): AN H-FIELD SOLUTION FOR A CONDUCTING BODY OF REVOLUTION	5. TYPE OF REPORT & PERIOD COVERED: Phase Report
	6. PERFORMING ORG. REPORT NUMBER: N/A
7. AUTHOR(s): Joseph R. Mautz, Roger F. Harrington	8. CONTRACT OR GRANT NUMBER(s): F30602-79-C-0011
9. PERFORMING ORGANIZATION NAME AND ADDRESS: Syracuse University, Department of Electrical and Computer Engineering, Syracuse NY 13210	10. PROGRAM ELEMENT, PROJECT, TASK AREA & WORK UNIT NUMBERS: 62702F, 23380317
11. CONTROLLING OFFICE NAME AND ADDRESS: Rome Air Development Center (RBCT), Griffiss AFB NY 13441	12. REPORT DATE: November 1980
	13. NUMBER OF PAGES: 92
14. MONITORING AGENCY NAME & ADDRESS (if different from Controlling Office): Same	15. SECURITY CLASS. (of this report): UNCLASSIFIED
	15a. DECLASSIFICATION/DOWNGRADING SCHEDULE: N/A

16. DISTRIBUTION STATEMENT (of this Report)

Approved for public release; distribution unlimited.

17. DISTRIBUTION STATEMENT (of the abstract entered in Block 20, if different from Report)

Same

18. SUPPLEMENTARY NOTES

RADC Project Engineer: Roy F. Stratton (RBCT)

19. KEY WORDS (Continue on reverse side if necessary and identify by block number)

Body of revolution
Computer programs
H-Field solution
Method of moments
Software

20. ABSTRACT (Continue on reverse side if necessary and identify by block number)

The magnetic field integral equation for electromagnetic scattering from a perfectly conducting body of revolution is solved by the method of moments. A Fourier series in ϕ is used. The t dependence of the expansion functions is subsectional. Pulses are used for the ϕ component of the unknown electric current induced on the surface S of the body of revolution. Triangles divided by the cylindrical coordinate radius are used for the t component. Here, t and ϕ are orthogonal coordinates

(Cont'd)

DD FORM 1 JAN 73 1473 EDITION OF 1 NOV 65 IS OBSOLETE

UNCLASSIFIED

SECURITY CLASSIFICATION OF THIS PAGE (When Data Entered)

406139

Item 20 (Cont'd)

on S, t being the arc length along the generating curve of S and ϕ the azimuthal angle.

A numerical solution is obtained by means of a computer program which is described and listed. This computer program is designed to handle oblique plane wave incidence efficiently.

CONTENTS

PART ONE

SOLUTION PROCEDURE AND NUMERICAL RESULTS

I. INTRODUCTION

The purpose of the present report is to develop an H-field solution which can be used alone or used in conjunction with the E-field solution in [1] to obtain a combined field solution which is hopefully more accurate than the one in [2]. Here, H-field solution means a solution to the magnetic field integral equation for a perfectly conducting body immersed in an incident electric field. Similarly, E-field solution means a solution to the electric field integral equation. In [1] and in the present report, solution is by the method of moments with a Fourier series in ϕ. For compatibility, the expansion functions used in the present report must be the same as those in [1]. In [1] and in the present report, the t dependence of the expansion functions is subsectional. Pulses are used for the ϕ component of the unknown electric current induced on the surface S of the body of revolution. Triangles divided by the cylindrical coordinate radius are used for the t component. Here, t and ϕ are orthogonal coordinates on S, t being the arc length along the generating curve of S and ϕ the azimuthal angle.

Computations indicate that the E-field solution of [1] is more accurate than the E-field solution of [2] and that the present H-field solution is nearly as accurate as the H-field solution of [2]. Hence, the combined field solution obtained by putting together the present H-field solution and the E-field solution of [1] should compare favorably with the combined field solution of [2].

Early work on H-field solutions is summarized in [3]. Two recent H-field solutions are presented in [4] and [2]. The solution in [4] uses pulse expansion functions for both t and ϕ components of the unknown electric current induced on S. H-field formulations are basic ingredients in solutions to problems of scattering by a dielectric body of revolution [5], [6], [7] and a dielectrically clad conducting body of revolution [8]. The expansion functions in [5] and [8] are triangles divided by the cylindrical

coordinate radius for both components of the current. The H-field formulation of [2] is used in [6] and [9]. The expansion functions in [7] are pulses for the ϕ component of current and shifted pulses divided by the cylindrical coordinate radius for the t component.

The magnetic field integral equation for a perfectly conducting body of revolution illuminated by an incident magnetic field $\underline{H}^i$ is

$$-\underline{n} \times \underline{H}^s(\underline{J}) = \underline{n} \times \underline{H}^i \quad \text{just inside S} \tag{1}$$

where S is the surface of the body of revolution and $\underline{n}$ is the unit vector which is normal to S and which points outward from S. In (1), $\underline{J}$ is the electric current induced on S and $\underline{H}^s(\underline{J})$ is the magnetic field due to $\underline{J}$ radiating in the absence of the body of revolution. It is assumed that the medium outside S is linear, isotropic, and homogeneous. "Outside S" means outside the body of revolution and "inside S" means inside it. "Absence of the body of revolution" means that the body of revolution has been removed and that the ensuing void has been filled with the outside medium. The incident magnetic field $\underline{H}^i$ is the field which would exist in the absence of the body of revolution.

Equation (1) states that the tangential components of the total magnetic field $(\underline{H}^s + \underline{H}^i)$ vanish just inside S. Consequently, (1) is valid only if S is closed. By contrast, the E-field integral equation (40) of [2] is valid for both open and closed surfaces of revolution.

II. METHOD OF MOMENTS SOLUTION

Equation (1) is solved by the method of moments. The moments solution to (1) is approached by writing

$$\underline{J} = \sum_n \left(\sum_j I^t_{nj} \underline{J}^t_{nj} + \sum_j I^\phi_{nj} \underline{J}^\phi_{nj} \right) \tag{2}$$

where $\underline{J}^t_{nj}$ and $\underline{J}^\phi_{nj}$ are expansion functions defined by

$$\underline{J}_{nj}^{t} = \underline{u}_t \frac{T_j(t)}{\rho} e^{jn\phi} \qquad \begin{cases} n = 0, \pm 1, \pm 2, \ldots \\ j = 1,2,\ldots P-2 \end{cases} \tag{3a}$$

$$\underline{J}_{nj}^{\phi} = \underline{u}_\phi \frac{P_j(t)}{\rho_j} e^{jn\phi} \qquad \begin{cases} n = 0, \pm 1, \pm 2, \ldots \\ j = 1, 2, \ldots P-1 \end{cases} \tag{3b}$$

and where I_{nj}^{t} and I_{nj}^{ϕ} are unknown constants to be determined. The subscript j which runs from 1 to either (P-2) or (P-1) in (3) is not to be confused with the j which appears in the argument of the exponential in (3). The latter j is $\sqrt{-1}$. The variables t and ϕ are orthogonal curvilinear coordinates on S. Specifically, t is the arc length along the generating curve of S and ϕ is the azimuthal angle. The generating curve of S is the plane curve which, when rotated about the z axis, generates S. In (3), $\underline{u}_t$ and $\underline{u}_\phi$ are unit vectors in the t and ϕ directions, respectively. These directions are chosen so that

$$\underline{n} = \underline{u}_\phi \times \underline{u}_t \tag{4}$$

The function $T_j(t)$ is the triangle function defined by

$$T_j(t) = \begin{cases} (t - \bar{t}_j)/\Delta_j & , \quad \bar{t}_j \le t \le \bar{t}_{j+1} \\ (\bar{t}_{j+2} - t)/\Delta_{j+1} & , \quad \bar{t}_{j+1} \le t \le \bar{t}_{j+2} \\ 0 & , \quad \text{otherwise} \end{cases} \tag{5}$$

and $P_j(t)$ is the pulse function defined by

$$P_j(t) = \begin{cases} 1 & , \quad \bar{t}_j \le t < \bar{t}_{j+1} \\ 0 & , \quad \text{otherwise} \end{cases} \tag{6}$$

Here, $\bar{t}_1$, $\bar{t}_2$, ... $\bar{t}_P$ are consecutive but not necessarily equally spaced points on the generating curve of S. $\bar{t}_1$ is the value of t at the beginning of the generating curve and $\bar{t}_P$ is the value of t at the end. Henceforth, the generating curve is assumed to be a series of straight line segments joining the points $\bar{t}_1$, $\bar{t}_2$,... $\bar{t}_P$. In (5),

$$\Delta_j = t_{j+1}^- - t_j^- \tag{7}$$

In (3), ρ is the distance of the point t on the generating curve from the z axis and ρ_j is the value of ρ at $t = t_j$ where

$$t_j = \frac{1}{2}(t_j^- + t_{j+1}^-) \tag{8}$$

It is assumed that all the ρ_j's are positive.

The moments solution to (1) is obtained by substituting (2) into (1), integrating over S the dot product of (1) with each member of a set of testing functions, and solving the resulting matrix equation for I_{nj}^t and I_{nj}^ϕ. There are two kinds of testing functions, $\underline{W}_{ni}^t$ and $\underline{W}_{ni}^\phi$ defined by

$$\underline{W}_{ni}^t = \underline{u}_t \frac{T_i(t)}{\rho} e^{-jn\phi} \quad \begin{cases} n = 0, \pm 1, \pm 2, \ldots \\ i = 1,2,\ldots P-2 \end{cases} \tag{9a}$$

$$\underline{W}_{ni}^\phi = \underline{u}_\phi \frac{P_i(t)}{\rho_i} e^{-jn\phi} \quad \begin{cases} n = 0, \pm 1, \pm 2, \ldots \\ i = 1,2,\ldots P-1 \end{cases} \tag{9b}$$

The matrix equation for I_{nj}^t and I_{nj}^ϕ decomposes into

$$\begin{bmatrix} Y_n^{tt} & Y_n^{t\phi} \\ Y_n^{\phi t} & Y_n^{\phi\phi} \end{bmatrix} \begin{bmatrix} \vec{I}_n^t \\ \vec{I}_n^\phi \end{bmatrix} = \begin{bmatrix} \vec{I}_n^{it} \\ \vec{I}_n^{i\phi} \end{bmatrix}, \quad n = 0, \pm 1, \pm 2, \ldots \tag{10}$$

where the superscripted $\vec{I}_n$'s are column vectors and the superscripted Y_n's are submatrices. The jth element of $\vec{I}_n^t$ is I_{nj}^t and the jth element of $\vec{I}_n^\phi$ is I_{nj}^ϕ. The ith elements of $\vec{I}_n^{it}$ and $\vec{I}_n^{i\phi}$ are given by

$$I_{ni}^{it} = \int dt\ T_i(t) \int_0^{2\pi} d\phi(\underline{u}_\phi \cdot \underline{H}^i) e^{-jn\phi} \tag{11a}$$

$$I_{ni}^{i\phi} = -\frac{1}{\rho_i} \int dt\, \rho\, P_i(t) \int_0^{2\pi} d\phi(\underline{u}_t \cdot \underline{H}^i) e^{-jn\phi} \tag{11b}$$

The second subscript on I in (11) denotes the ith element. The superscript i on I in (11) is the same as that in (10). This superscript indicates dependence on the incident magnetic field $\underline{H}^i$.

For a particular value of n in (10), the matrix of the superscripted Y_n's on the left-hand side of (10) is called the moment matrix for that value of n. The ijth elements of the superscripted Y_n's are given by

$$(Y_n^{tt})_{ij} = \pi \int_{\bar{t}_i}^{\bar{t}_{i+2}} \frac{T_i(t)\ T_j(t)}{\rho} dt + k^3 \int_{\bar{t}_i}^{\bar{t}_{i+2}} dt\ T_i(t) \int_{\bar{t}_j}^{\bar{t}_{j+2}} dt'\ T_j(t')$$

$$[((\rho'-\rho)\cos v' - (z'-z)\sin v')\ G_2 - G_1\, \rho \cos v'] \tag{12a}$$

$$(Y_n^{\phi t})_{ij} = \frac{jk^3}{\rho_i} \int_{\bar{t}_i}^{\bar{t}_{i+1}} dt\, \rho\, P_i(t) \int_{\bar{t}_j}^{\bar{t}_{j+2}} dt'\ T_j(t')(\rho' \sin v \cos v'$$

$$- \rho \sin v' \cos v - (z'-z) \sin v \sin v')G_3 \tag{12b}$$

$$(Y_n^{t\phi})_{ij} = \frac{jk^3}{\rho_j} \int_{\bar{t}_i}^{\bar{t}_{i+2}} dt\ T_i(t) \int_{\bar{t}_j}^{\bar{t}_{j+1}} dt'\ \rho'\ P_j(t')(z'-z)G_3 \tag{12c}$$

$$(Y_n^{\phi\phi})_{ij} = \frac{\pi}{\rho_i \rho_j} \int_{\bar{t}_i}^{\bar{t}_{i+1}} \rho\, P_i(t) P_j(t) dt + \frac{k^3}{\rho_i \rho_j} \int_{\bar{t}_i}^{\bar{t}_{i+1}} dt\, \rho\, P_i(t) \int_{\bar{t}_j}^{\bar{t}_{j+1}} dt' \rho' P_j(t')$$

$$[((\rho'-\rho)\cos v - (z'-z)\sin v)G_2 + G_1 \rho' \cos v] \tag{12d}$$

The derivation of (12) is not included here because it is similar to that of (20)-(23) of [2]. Actually, (12) was obtained by replacing $f_i(t)$ by $\frac{1}{\rho} T_i(t)$ in (20) and (22) and by $\frac{1}{\rho_i} P_i(t)$ in (21) and (23) and by replacing $f_j(t')$ by $\frac{1}{\rho'} T_j(t')$ in (20) and (21) and by $\frac{1}{\rho_j} P_j(t')$ in (22) and (23). The equations (20)-(23) referred to in the previous sentence are in [2].

In (12), k is the propagation constant in the medium outside S. Also, v is the angle between the tangent to the generating curve and the z axis. v is positive if the generating curve is moving away from the z axis. Otherwise, $v \leq 0$. In (12), ρ, z, and v are evaluated at the point t on the generating curve and ρ', z', and v' are the values of ρ, z, and v at the point t'. The subscripted G's in (12) are given by

$$G_1 = 2 \int_0^{\pi} G \sin^2(\phi/2) \cos(n\phi) d\phi \tag{13a}$$

$$G_2 = \int_0^{\pi} G \cos \phi \cos(n\phi) d\phi \tag{13b}$$

$$G_3 = \int_0^{\pi} G \sin \phi \sin(n\phi) d\phi \tag{13c}$$

where

$$G = \frac{1 + jkR}{k^3 R^3} e^{-jkR} \tag{14}$$

where

$$R = \sqrt{(\rho'-\rho)^2 + (z'-z)^2 + 4\rho\rho' \sin^2(\phi/2)} \tag{15}$$

The regions of integration in (12a)-(12c) overlap. To avoid integrating more than once over the same region, we account for the contributions in (12a)-(12c) by regions of integration rather than by matrix elements. If A_q is the region which $\bar{t}_q \leq t \leq \bar{t}_{q+1}$, then A_q contributes

$$(\dot{Y}_n^{tt})_{ij} = \pi \int_{t_q^-}^{t_{q+1}^-} \frac{T_i(t)\ T_j(t)}{\rho}\, dt \tag{16}$$

to the single integral with respect to t in (12a). Because the domains of the triangle functions are limited, (16) is nonzero only for

$$\left.\begin{array}{l} i = q-1,\ q \\ i \neq 0 \\ i \neq P-1 \end{array}\right\} \tag{17a}$$

$$\left.\begin{array}{l} j = q-1,\ q \\ j \neq 0 \\ j \neq P-1 \end{array}\right\} \tag{17b}$$

The dot on the left-hand side of (16) indicates that (16) is not all of (12a) but only the contribution due to A_q.

If A_{pq} is the region for which

$$t_p^- \leq t \leq t_{p+1}^-$$

$$t_q^- \leq t' \leq t_{q+1}^- ,$$

then the contributions to (12a)-(12c) due to A_{pq} are given by

$$(\overset{*}{Y}{}_n^{tt})_{ij} = k^3 \int_{t_p^-}^{t_{p+1}^-} dt\ T_i(t) \int_{t_q^-}^{t_{q+1}^-} dt' T_j(t')\ [((\rho'-\rho)\cos v' - (z'-z)\sin v')G_2$$

$$- G_1\, \rho \cos v'\} \tag{18a}$$

$$(\overset{*}{Y}{}_n^{\phi t})_{pj} = \frac{jk^3}{\rho_p} \int_{t_p^-}^{t_{p+1}^-} dt\, \rho\, P_p(t) \int_{t_q^-}^{t_{q+1}^-} dt'\ T_j(t')(\rho' \sin v \cos v'$$

$$- \rho \sin v' \cos v - (z'-z)\sin v \sin v')G_3 \tag{18b}$$

$$(\overset{*}{Y}{}^{t\phi}_{n})_{iq} = \frac{jk^3}{\rho_q} \int_{t_p^-}^{t_{p+1}^-} dt\ T_i(t) \int_{t_q^-}^{t_{q+1}^-} dt'\rho'\ P_q(t')(z'-z)G_3 \tag{18c}$$

where

$$\left.\begin{array}{l} i = p-1,\ p \\ i \neq 0 \\ i \neq P-1 \end{array}\right\} \tag{19a}$$

and

$$\left.\begin{array}{l} j = q-1,\ q \\ j \neq 0 \\ j \neq P-1 \end{array}\right\} \tag{19b}$$

The asterisks on the left-hand sides of (18a)-(18c) indicate contributions due to A_{pq}. For instance, (18a) is not all of (12a) but only the contribution due to A_{pq}. Equation (12d) is suitable for calculation as is because it has no overlapping intervals. However, to obtain a notation consistent with that in (18a)-(18c), we replace ij by pq in (12d). The result is

$$(Y^{\phi\phi}_{n})_{pq} = \frac{\pi}{\rho_p^2}\,\delta_{pq} \int_{t_p^-}^{t_{p+1}^-} \rho P_p^2(t)dt + \frac{k^3}{\rho_p\rho_q} \int_{t_p^-}^{t_{p+1}^-} dt\rho P_p(t) \int_{t_q^-}^{t_{q+1}^-} dt'\rho' P_q(t')$$

$$[((\rho'-\rho)\cos v - (z'-z)\sin v)G_2 + G_1\rho'\cos v] \tag{18d}$$

where

$$\delta_{pq} = \begin{cases} 1\ , & p = q \\ 0\ , & p \neq q \end{cases} \tag{20}$$

The fact that the pulses (6) do not overlap was used to obtain the δ_{pq} term in (18d).

Each integral with respect to t in (18) is approximated by sampling the pertinent integrand at $t = t_p$ and multiplying by Δ_p. Next, the definitions (5) and (6) of the triangle and pulse functions are substituted into (18). Because the portion of the generating curve for $t_q^- \le t' \le t_{q+1}^-$ is assumed to be a straight line, v' is constant there so that

$$\left.\begin{aligned} \rho' &= \rho_q + (t' - t_q)\sin v_q \\ z' &= z_q + (t' - t_q)\cos v_q \end{aligned}\right\} \quad t_q^- \le t' \le t_{q+1}^- \tag{21}$$

where z_q is the value of z' at $t' = t_q$. Equations (21) are also substituted into (18). As a result, (18) becomes

$$(\overset{*}{Y}{}_n^{tt})_{ij} = \frac{k^3\Delta_p}{4}\int_{t_q^-}^{t_{q+1}^-}\left(1 + (-1)^{q-j}\,\frac{2(t'-t_q)}{\Delta_q}\right)\left[((\rho_q-\rho_p)\cos v_q - (z_q-z_p)\sin v_q)G_2 - G_1\rho_p\cos v_q\right]dt' \tag{22a}$$

$$(\overset{*}{Y}{}_n^{\phi t})_{pj} = \frac{jk^3\Delta_p}{2}\int_{t_q^-}^{t_{q+1}^-}\left(1 + (-1)^{q-j}\,\frac{2(t'-t_q)}{\Delta_q}\right)(\rho_q\sin v_p\cos v_q - \rho_p\sin v_q\cos v_p - (z_q-z_p)\sin v_p\sin v_q)G_3\,dt' \tag{22b}$$

$$(\overset{*}{Y}{}_n^{t\phi})_{iq} = \frac{jk^3\Delta_p}{2}\int_{t_q^-}^{t_{q+1}^-}\left(1 + \frac{(t'-t_q)\sin v_q}{\rho_q}\right)(z_q-z_p + (t'-t_q)\cos v_q)G_3\,dt' \tag{22c}$$

$$(Y_n^{\phi\phi})_{pq} = \frac{\pi\Delta_q}{\rho_q}\delta_{pq} + k^3\Delta_p\int_{t_q^-}^{t_{q+1}^-}\left(1 + \frac{(t'-t_q)\sin v_q}{\rho_q}\right)\Big[((\rho_q-\rho_p)\cos v_p - (z_q-z_p)\sin v_p + (t'-t_q)(\sin v_q\cos v_p - \cos v_q\sin v_p))G_2 + G_1\rho_q\left(1+\frac{(t'-t_q)\sin v_q}{\rho_q}\right)\cos v_p\Big]dt'$$

d)

The ranges of values of i and j in (22) are given by (19). Because ρ is linear in t, the process of sampling the integrand at $t = t_p$ and multiplying by Δ_p gave the exact value of the first integral in (18d).

The integral in (16) can be approximated either by sampling the integrand at $t = t_q$ and multiplying by Δ_q or by applying Gaussian quadrature. Gaussian quadrature was chosen because it gave more accurate values of electric currents induced on the sphere and cone-sphere examples in Section V. Thanks to (5) and (21), the Gaussian quadrature formula for the integral in (16) becomes

$$(\dot{Y}_n^{tt})_{q-1,q-1} = \frac{\pi\Delta_q}{8} \sum_{\ell=1}^{n_t} \frac{A_\ell^{(n_t)}(1 - x_\ell^{(n_t)})^2}{\hat{\rho}_\ell} \tag{23a}$$

$$(\dot{Y}_n^{tt})_{q,q-1} = (\dot{Y}_n^{tt})_{q-1,q} = \frac{\pi\Delta_q}{8} \sum_{\ell=1}^{n_t} \frac{A_\ell^{(n_t)}(1 - x_\ell^{(n_t)})(1 + x_\ell^{(n_t)})}{\hat{\rho}_\ell} \tag{23b}$$

$$(\dot{Y}_n^{tt})_{q,q} = \frac{\pi\Delta_q}{8} \sum_{\ell=1}^{n_t} \frac{A_\ell^{(n_t)}(1 + x_\ell^{(n_t)})^2}{\hat{\rho}_\ell} \tag{23c}$$

where $$\hat{\rho}_\ell = \rho_q + \frac{\Delta_q x_\ell^{(n_t)}}{2} \sin v_q \tag{23d}$$

The abscissas $x_\ell^{(n_t)}$ and weights $A_\ell^{(n_t)}$ in (23) are given in Appendix A of [10] for several values of n_t.

Equations (22) can be rewritten as

$$(\overset{*}{Y}{}_n^{tt})_{ij} = \frac{k^3\Delta_p\Delta_q}{8} [((\rho_q-\rho_p)\cos v_q - (z_q-z_p)\sin v_q)G_{21} - G_{11}\,\rho_p \cos v_q]$$

$$+ (-1)^{q-j} \frac{k^3\Delta_p\Delta_q}{8} [((\rho_q-\rho_p)\cos v_q - (z_q-z_p)\sin v_q)G_{22} - G_{12}\rho_p\cos v_q] \tag{24a}$$

$$(\overset{*}{Y}{}_n^{\phi t})_{pj} = \frac{jk^3\Delta_p\Delta_q}{4} (\rho_q \sin v_p \cos v_q - \rho_p \sin v_q \cos v_p -$$

$$- (z_q-z_p)\sin v_p \sin v_q)(G_{31} + (-1)^{q-j}G_{32}) \tag{24b}$$

$$(\overset{*}{Y}{}_n^{t\phi})_{iq} = \frac{jk^3\Delta_p\Delta_q}{4}\left[(z_q-z_p)\left(G_{31} + \frac{\Delta_q \sin v_q}{2\rho_q} G_{32}\right) + \frac{\Delta_q \cos v_q}{2}\left(G_{32} + \frac{\Delta_q \sin v_q}{2\rho_q} G_{33}\right)\right] \tag{24c}$$

$$(Y_n^{\phi\phi})_{pq} = \frac{\pi\Delta_p}{\rho_p}\delta_{pq} + \frac{k^3\Delta_p\Delta_q}{2}\left[((\rho_q-\rho_p)\cos v_p-(z_q-z_p)\sin v_p)\left(G_{21}+ \frac{\Delta_q \sin v_q}{2\rho_q} G_{22}\right)\right.$$

$$+ \frac{\Delta_q}{2}(\sin v_q \cos v_p - \cos v_q \sin v_p)\left(G_{22} + \frac{\Delta_q \sin v_q}{2\rho_q} G_{23}\right) +$$

$$\left. + \rho_q \cos v_p\left(G_{11} + \frac{\Delta_q \sin v_q}{\rho_q} G_{12} + \left(\frac{\Delta_q \sin v_q}{2\rho_q}\right)^2 G_{13}\right)\right] \tag{24d}$$

where

$$G_{m\alpha} = \left(\frac{2}{\Delta_q}\right)^{\alpha} \int_{t_q^-}^{t_{q+1}^-} (t'-t_q)^{\alpha-1} G_m(t'-t_q)dt' \ , \quad \begin{cases} m = 1,2,3 \\ \alpha = 1,2,3 \end{cases} \tag{25}$$

Here,

$$G_1(u) = 2\int_0^{\pi} G(u,\phi)\sin^2(\phi/2)\cos(n\phi)d\phi \tag{26a}$$

$$G_2(u) = \int_0^{\pi} G(u,\phi)\cos\phi\cos(n\phi)d\phi \tag{26b}$$

$$G_3(u) = \int_0^{\pi} G(u,\phi)\sin\phi\sin(n\phi)d\phi \tag{26c}$$

where

$$G(u,\phi) = \frac{1 + jkR(u,\phi)}{k^3R^3(u,\phi)} e^{-jkR(u,\phi)} \tag{27}$$

where

$$R(u,\phi) = \sqrt{(\rho'-\rho_p)^2 + (z'-z_p)^2 + 4\rho_p\rho' \sin^2(\phi/2)} \tag{28}$$

where

$$\rho' = \rho_q + u \sin v_q \tag{29a}$$

$$z' = z_q + u \cos v_q \tag{29b}$$

III. NUMERICAL EVALUATION OF THE INTEGRALS $G_{m\alpha}$

The integrals $G_{m\alpha}$ of (25) are now evaluated by means of either pure Gaussian quadrature or Gaussian quadrature fortified by the method of elimination of the singularity of the integrand. The proximity of the singularity of $G(u,\phi)$ of (26) to the region of integration falls into one of four different cases defined in this section.

If

$$\left.\begin{array}{c} p \neq q \\ \frac{1}{2} c_t \Delta_q \leq d_o \\ c_\phi \rho_q \leq d_o \end{array}\right\} \quad \begin{array}{c}\text{Case 1} \\ \text{Pure quadrature}\end{array} \tag{30}$$

then pure Gaussian quadrature is used to evaluate the integrals in (25) and (26). In (30), c_t and c_ϕ are constants for which the values

$$\left.\begin{array}{l} c_t = 2. \\ c_\phi = 0.1 \end{array}\right\} \tag{31}$$

are suggested. Also in (30),

$$d_o = \begin{cases} d^* & , \quad |t_o^*| \leq \frac{1}{2} \Delta_q \\ \sqrt{(|t_o^*| - \frac{1}{2} \Delta_q)^2 + (d^*)^2} & , \quad |t_o^*| > \frac{1}{2} \Delta_q \end{cases} \tag{32}$$

where

$$t_o^* = (\rho_q - \rho_p)\sin v_q + (z_q - z_p)\cos v_q \tag{33}$$

$$d^* = |(\rho_q - \rho_p)\cos v_q - (z_q - z_p)\sin v_q| \tag{34}$$

The quantity d_o defined by (32) is the minimum value of $R(u,\phi)$ for the ranges $|u| \leq \frac{1}{2} \Delta_q$ and $0 \leq \phi \leq \pi$ of values of u and ϕ in (26). Equations (30)-(34) were taken from pages 24 and 25 of [1].

The Gaussian quadrature formulas for the integrals in (25) and (26) are

$$G_{m\alpha} = \sum_{\ell'=1}^{n_t} A_{\ell'}^{(n_t)} \left(x_{\ell'}^{(n_t)}\right)^{\alpha-1} G_m\left(\frac{1}{2}\Delta_q x_{\ell'}^{(n_t)}\right) , \begin{cases} m = 1,2,3 \\ \alpha = 1,2,3 \end{cases} \tag{35}$$

$$G_1(u) = \pi \sum_{\ell=1}^{n_\phi} A_\ell^{(n_\phi)} G(u,\phi_\ell)\sin^2\left(\frac{1}{2}\phi_\ell\right)\cos(n\phi_\ell) \tag{36a}$$

$$G_2(u) = \frac{\pi}{2} \sum_{\ell=1}^{n_\phi} A_\ell^{(n_\phi)} G(u,\phi_\ell)\cos\phi_\ell \cos(n\phi_\ell) \tag{36b}$$

$$G_3(u) = \frac{\pi}{2} \sum_{\ell=1}^{n_\phi} A_\ell^{(n_\phi)} G(u,\phi_\ell)\sin\phi_\ell \sin(n\phi_\ell) \tag{36c}$$

where $G(u,\phi_\ell)$ is given by (27)-(29) with ϕ replaced by ϕ_ℓ. Here,

$$\phi_\ell = \frac{\pi}{2}\left(x_\ell^{(n_\phi)} + 1\right) \tag{37}$$

The abscissas $x_{\ell'}^{(n_t)}$ and $x_\ell^{(n_\phi)}$ and weights $A_{\ell'}^{(n_t)}$ and $A_\ell^{(n_\phi)}$ in (35) and (36) are given in Appendix A of [10] for several values of n_t and n_ϕ.

If (30) is not true, then the singularity due to the kernel (27) is eliminated [11] before applying Gaussian quadrature to the integrals in (25) and (26). The singularity analysis presented here is more general than that in [7] because the one in [7] was carried out only for $p = q$. Substitution of

$$e^{-jkR} = 1 - jkR - \frac{k^2R^2}{2}$$

into (27) reveals that, near $R = 0$, (27) behaves like a function G^s given by

$$G^s = \frac{1}{k^3R^3} + \frac{1}{2kR} \tag{38}$$

Three different methods of eliminating the singularity are used. If

$$\left.\begin{array}{r} p \neq q \\ \frac{1}{2}\, c_t \Delta_q > d_o \\ c_\phi \rho_q \leq d_o \end{array}\right\} \begin{array}{l} \text{Case 2} \\ \text{Method 1} \\ \; \end{array} \tag{39}$$

then method 1 is used. In method 1, the orders of integration in (25) are interchanged to obtain

$$G_{1\alpha} = 2\int_0^\pi H_\alpha(\phi)\sin^2(\phi/2)\cos(n\phi)d\phi \tag{40a}$$

$$G_{2\alpha} = \int_0^\pi H_\alpha(\phi)\cos\phi\,\cos(n\phi)d\phi \qquad \alpha = 1,2,3 \tag{40b}$$

$$G_{3\alpha} = \int_0^\pi H_\alpha(\phi)\sin\phi\,\sin(n\phi)d\phi \tag{40c}$$

where

$$H_\alpha(\phi) = \left(\frac{2}{\Delta_q}\right)^\alpha \int_{\bar{t}_q}^{\bar{t}_{q+1}} (t'-t_q)^{\alpha-1}\, G(t'-t_q,\phi)dt' \tag{41}$$

In method 1, the singular part of the integrand in (41) is integrated analytically, the remaining part is integrated by means of Gaussian quadrature, and then Guassian quadrature is applied to the integrations with respect to ϕ in (40). The singular part of a singular integrand is a function which behaves like the integrand near its singularity. Evidently, the singular part is not unique.

Guided by (38) in our choice of the singular part of the integrand in (41), we write

$$H_\alpha(\phi) = \left(\frac{2}{\Delta_q}\right)^\alpha \int_{\bar{t}_q}^{\bar{t}_{q+1}} (t'-t_q)^{\alpha-1}\left(G(t'-t_q,\phi) - \frac{1}{k^3R^3(t'-t_q,\phi)} - \frac{1}{2kR(t'-t_q,\phi)}\right)dt' + I_\alpha \tag{42}$$

where

$$I_\alpha = \left(\frac{2}{\Delta_q}\right)^\alpha \int_{\bar{t}_q}^{\bar{t}_{q+1}} (t'-t_q)^{\alpha-1} \left(\frac{1}{k^3R^3(t'-t_q,\phi)} + \frac{1}{2kR(t'-t_q,\phi)}\right)dt' \tag{43}$$

Application of Gaussian quadrature to the first integral in (42) gives

$$H_\alpha(\phi) = \sum_{\ell'=1}^{n_t} A_{\ell'}^{(n_t)} (x_{\ell'}^{(n_t)})^{\alpha-1} \left(G(\tfrac{1}{2}\Delta_q x_{\ell'}^{(n_t)},\phi) - \frac{1}{k^3R^3(\frac{1}{2}\Delta_q x_{\ell'}^{(n_t)},\phi)}\right.$$

$$\left. - \frac{1}{2kR(\frac{1}{2}\Delta_q x_{\ell'}^{(n_t)},\phi)}\right) + I_\alpha \tag{44}$$

Equation (43) can be rewritten as

$$I_\alpha = \left(\frac{2}{\Delta_q}\right)^\alpha \int_{t_o-\frac{1}{2}\Delta_q}^{t_o+\frac{1}{2}\Delta_q} (w-t_o)^{\alpha-1} \left[\frac{1}{k^3(w^2+d^2)^{3/2}} + \frac{1}{2k(w^2+d^2)^{1/2}}\right]dw \tag{45}$$

where

$$t_o = (\rho_q-\rho_p)\sin v_q + (z_q-z_p)\cos v_q + 2\rho_p \sin v_q \sin^2(\phi/2) \tag{46a}$$

$$d^2 = r_{pq}^2 - t_o^2 \tag{46b}$$

$$r_{pq}^2 = (\rho_q-\rho_p)^2 + (z_q-z_p)^2 + 4\rho_p\rho_q \sin^2(\phi/2) \tag{46c}$$

Application of formulas 200.01., 200.03., and sequel in [12] to (45) gives

$$I_1 = \frac{2}{k\Delta_q}\left[\frac{w}{k^2d^2r} + \frac{1}{2}\log(w+r)\right]_{t_o-\frac{1}{2}\Delta_q}^{t_o+\frac{1}{2}\Delta_q} \tag{47a}$$

$$I_2 = \left(\frac{2}{k\Delta_q}\right)^2 \left[\frac{kr}{2} - \frac{1}{kr}\right]_{t_o - \frac{1}{2}\Delta_q}^{t_o + \frac{1}{2}\Delta_q} - \frac{2t_o}{\Delta_q} I_1 \tag{47b}$$

$$I_3 = \left(\frac{2}{k\Delta_q}\right)^3 \left[kw\left(\frac{kr}{4} - \frac{1}{kr}\right) + \left(1 - \frac{k^2 d^2}{4}\right)\log(w+r)\right]_{t_o - \frac{1}{2}\Delta_q}^{t_o + \frac{1}{2}\Delta_q}$$

$$- \frac{4t_o I_2}{\Delta_q} - \left(\frac{2t_o}{\Delta_q}\right)^2 I_1 \tag{47c}$$

where

$$r = \sqrt{w^2 + d^2} \tag{47d}$$

If $\phi = 0$ in (42), then (30) guarantees that the variable t' of integration in (42) passes close to the singularity of $G(t'-t_q,\phi)$. In this case, (44) and (47) are necessary. However, as ϕ moves toward π, r_{pq} may become so large that the variable t' in (42) never comes close to the singularity of $G(t'-t_q,\phi)$. In this case, (44) and (47) are no longer necessary. Their calculation is always time consuming regardless of the value of r_{pq}. Even worse, the calculation of (44) and (47) is subject to excessive roundoff error whenever r_{pq} is appreciably larger than Δ_q. It was decided to restrict use of (44) and (47) to

$$r_{pq} < \frac{1}{2} c_t \Delta_q + \frac{1}{2} \Delta_q \tag{48}$$

For larger values of r_{pq}, recourse is to the Gaussian quadrature formula

$$H_\alpha(\phi) = \sum_{\ell'=1}^{n_t} A_{\ell'}^{(n_t)} \left(x_{\ell'}^{(n_t)}\right)^{\alpha-1} G\left(\frac{1}{2}\Delta_q x_{\ell'}^{(n_t)},\phi\right) \tag{49}$$

The term $\frac{1}{2}\Delta_q$ on the right-hand side of (48) is necessary to assure that the distance $R(t'-t_q,\phi)$ used in (41) is at least as large as $\frac{1}{2} c_t \Delta_q$ for all values of t' in (41) before (49) is invoked. This distance enters (41) through (27).

In method 1, $G_{m\alpha}$ of (40) is approximated by

$$\left.\begin{aligned}
G_{1\alpha} &= \pi \sum_{\ell=1}^{n_\phi} A_\ell^{(n_\phi)} H_\alpha(\phi_\ell)\sin^2(\tfrac{1}{2}\phi_\ell)\cos(n\phi_\ell) && \text{(50a)}\\
G_{2\alpha} &= \frac{\pi}{2} \sum_{\ell=1}^{n_\phi} A_\ell^{(n_\phi)} H_\alpha(\phi_\ell)\cos\phi_\ell \cos(n\phi_\ell) && \text{(50b)}\\
G_{3\alpha} &= \frac{\pi}{2} \sum_{\ell=1}^{n_\phi} A_\ell^{(n_\phi)} H_\alpha(\phi_\ell)\sin\phi_\ell \sin(n\phi_\ell) && \text{(50c)}
\end{aligned}\right\} \quad \alpha = 1,2,3$$

where $H_\alpha(\phi_\ell)$ is given by either (44) of (49).

If

$$\left.\begin{aligned} p &\neq q && \text{case 3}\\ c_\phi \rho_q &> d_o && \text{Method 2}\end{aligned}\right\} \qquad (51)$$

then method 2 is used to eliminate the singularity due to the kernel (27). In method 2, the singular parts of the integrands in (26) are integrated analytically, the remaining parts are integrated by means of Gaussian quadrature, and then (25) is approximated by the Gaussian quadrature formula (35).

Integration of (38) with respect to ϕ is difficult. With a view toward replacement of (38) by a function which behaves like (38) near $\phi = 0$ but is easier to integrate, we rewrite (28) as

$$R(u,\phi) = a\sqrt{1-b} \qquad (52)$$

where

$$a = \sqrt{(\rho'-\rho_p)^2 + (z'-z_p)^2 + \rho_p\rho'\phi^2} \qquad (53a)$$

$$b = \frac{\rho_p\rho'}{a^2}(\phi^2 - 4\sin^2(\phi/2)) \qquad (53b)$$

where ρ' and z' are given by (29). Near $\phi = 0$,

$$0 \le b \lesssim \phi^2/12 \tag{54}$$

The left-hand side of (54) is a consequence of the fact that $|x| \geq |\sin x|$ for any value of x. The right-hand side of (54) was obtained by setting $a^2 = \rho_p\rho'\phi^2$ in (53b). Substitution of (52) into (38) and subsequent expansion of (38) in powers of b reveals that, near $\phi = 0$, G^s behaves like the function G^{ss} given by

$$G^{ss} = \frac{1}{k^3a^3} + \frac{1}{2ka} + \frac{\rho_p\rho'\phi^4}{8k^3a^5} \tag{55}$$

Guided by (55) in our choice of the singular parts of the integrands in (26), we approach method 2 by rewriting (26) as

$$G_1(u) = 2\int_0^\pi (G(u,\phi)\sin^2(\phi/2)\cos(n\phi) - \frac{\phi^2}{4k^3a^3})d\phi + \int_0^\pi \frac{\phi^2}{2k^3a^3}\,d\phi \tag{56a}$$

$$G_2(u) = \int_0^\pi (G(u,\phi)\cos\phi\cos(n\phi)\ \frac{1}{k^3a^3} - \frac{1}{2ka} + \frac{(n^2+1)\phi^2}{2k^3a^3} - \frac{\rho_p\rho'\phi^4}{8k^3a^5})d\phi$$

$$+ \int_0^\pi (\frac{1}{k^3a^3} + \frac{1}{2ka} - \frac{(n^2+1)\phi^2}{2k^3a^3} + \frac{\rho_p\rho'\phi^4}{8k^3a^5})d\phi \tag{56b}$$

$$G_3(u) = \int_0^\pi (G(u,\phi)\sin\phi\sin(n\phi) - \frac{n\phi^2}{k^3a^3})d\phi + \int_0^\pi \frac{n\phi^2}{k^3a^3}\,d\phi \tag{56c}$$

There are two integrals on the right-hand side of each of equations (56a), (56b), and (56c). If Gaussian quadrature is applied to the first integral and if the second integral is evaluated analytically by using formulas 200.01., 200.03., and sequel in [12], then (56) becomes

$$G_1(u) = \pi\sum_{\ell=1}^{n_\phi} A_\ell^{(n_\phi)}\,(G(u,\phi_\ell)\sin^2(\tfrac{1}{2}\phi_\ell)\cos(n\phi_\ell) - \frac{\phi_\ell^2}{4k^3a_\ell^3})$$

$$-\frac{1}{2k^3(\rho_p\rho')^{3/2}}\,[\frac{w}{r} - \log(w+r)] \tag{57a}$$

$$G_2(u) = \frac{\pi}{2}\sum_{\ell=1}^{n_\phi} A_\ell^{(n_\phi)}\Big(G(u,\phi_\ell)\cos\phi_\ell\cos(n\phi_\ell) - \frac{1}{k^3a_\ell^3} - \frac{1}{2ka_\ell} + \frac{(n^2+1)\phi_\ell^2}{2k^3a_\ell^3} - \frac{\rho_p\rho'\phi_\ell^4}{8k^3a_\ell^5}\Big)$$

$$+ \frac{w^3}{\pi^2k^3(\rho_p\rho')^{3/2}r} + \frac{\log(w+r)}{2k(\rho_p\rho')^{1/2}} + \frac{(n^2+1)}{2k^3(\rho_p\rho')^{3/2}}\left[\frac{w}{r} - \log(w+r)\right] -$$

$$- \frac{1}{8k^3(\rho_p\rho')^{3/2}}\left[\frac{w(3+4w^2)}{3r^3} - \log(w+r)\right] \qquad (57b)$$

$$G_3(u) = \frac{\pi}{2}\sum_{\ell=1}^{n_\phi} A_\ell^{(n_\phi)}\Big(G(u,\phi_\ell)\sin\phi_\ell\ \sin(n\phi_\ell) - \frac{n\phi_\ell^2}{k^3a_\ell^3}\Big) - \frac{n}{k^3(\rho_p\rho')^{3/2}}\left[\frac{w}{r} - \log(w+r)\right] \qquad (57c)$$

where a_ℓ is the right-hand side of (53a) evaluated at $\phi = \phi_\ell$. In (57),

$$w = \frac{\pi\sqrt{\rho_p\rho'}}{\sqrt{(\rho'-\rho_p)^2 + (z'-z_p)^2}} \qquad (58a)$$

$$r = \sqrt{1 + w^2} \qquad (58b)$$

Equation (57) is used only if the minimum value $\sqrt{(\rho'-\rho_p)^2+(z'-z_p)^2}$ of $R(u,\phi)$ with respect to ϕ in (26) satisfies

$$\sqrt{(\rho'-\rho_p)^2 + (z'-z_p)^2} < c_\phi\rho_q \qquad (59)$$

The distance $R(u,\phi)$ enters (26) through (27). If (59) is not true, then $G_m(u)$ is approximated by the pure Gaussian quadrature formulas (36). In method 2, $G_{m\alpha}$ is obtained by substituting either (57) or (36) into (35).

If

$$p = q \left.\right\} \begin{matrix}\text{Case 4}\\ \text{Method 3}\end{matrix} \qquad (60)$$

then method 3 is used to obtain $G_{m\alpha}$. Since p=q, only G_{11}, G_{12}, G_{13}, G_{32}, and G_{33} are needed in order to calculate (24). From (40) and (41), these subscripted G's are given by

$$G_{1\alpha} = 2\left(\frac{2}{\Delta_q}\right)^{\alpha} \int_0^{\pi} d\phi \int_{-\frac{1}{2}\Delta_q}^{\frac{1}{2}\Delta_q} du\, u^{\alpha-1} G(u,\phi) \sin^2(\phi/2) \cos(n\phi), \quad \alpha = 1,2,3 \tag{61a}$$

$$G_{3\alpha} = \left(\frac{2}{\Delta_q}\right)^{\alpha} \int_0^{\pi} d\phi \int_{-\frac{1}{2}\Delta_q}^{\frac{1}{2}\Delta_q} du\, u^{\alpha-1} G(u,\phi) \sin\phi \sin(n\phi), \quad \alpha = 2,3 \tag{61b}$$

where $G(u,v)$ is given by (27) with

$$R(u,\phi) = \sqrt{u^2 + 4\rho_q(\rho_q + u \sin v_q)\sin^2(\phi/2)} \tag{62}$$

Substitution of (38) for $G(u,\phi)$ in (61) reveals that, in (61), the only integrand which is not bounded in the vicinity of $u = \phi = 0$ is the integrand for $\alpha = 1$ in (61a). In method 3, the singular part of this integrand is integrated analytically with respect to both u and ϕ, the remaining part is integrated by means of method 1, and then method 1 is applied directly to the integrals (40) and (41) for G_{12}, G_{13}, G_{32}, and G_{33}.

Equation (61a) for G_{11} is rewritten as

$$G_{11} = I_a + I_b \tag{63}$$

where

$$I_a = \frac{4}{\Delta_q} \int_0^{\pi} d\phi \int_{-\frac{1}{2}\Delta_q}^{\frac{1}{2}\Delta_q} du \left(G(u,\phi)\sin^2(\phi/2)\cos(n\phi) - \frac{\phi^2}{4k^3(u^2+\rho_q^2\phi^2)^{3/2}} \right) \tag{64}$$

$$I_b = \frac{1}{\Delta_q} \int_0^{\pi} d\phi \int_{-\frac{1}{2}\Delta_q}^{\frac{1}{2}\Delta_q} du \frac{\phi^2}{k^3(u^2 + \rho_q^2\phi^2)^{3/2}} \tag{65}$$

It is evident from (38) and (62) that the integrand in (64) is bounded. Application of formulas 200.03. and 200.01. of [12] to (65) gives

$$I_b = \frac{1}{k^3\rho_q^3} \log\left[\frac{2\rho_q\pi}{\Delta_q} + \sqrt{1 + (\frac{2\rho_q\pi}{\Delta_q})^2}\right] \tag{66}$$

Integration with respect to u of the second term in (64) by means of formula 200.03. of [12] gives

$$I_a = 2\int_0^\pi H_1(\phi)\sin^2(\phi/2)\cos(n\phi)d\phi - \frac{1}{k^3\rho_q^3}\int_0^\pi \frac{d\phi}{\sqrt{\phi^2 + (\frac{\Delta_q}{2\rho_q})^2}} \tag{67}$$

where $H_1(\phi)$ is given by (41). The first integral in (67) is the right-hand side of (40a) for $\alpha = 1$. Application of method 1 to this integral and to those in (40) and (41) for G_{12}, G_{13}, G_{32}, and G_{33}, evaluation of the second integral with respect to ϕ in (67) by means of Gaussian quadrature, and use of (63) and (66) give

$$G_{11} = \pi\sum_{\ell=1}^{n_\phi} A_\ell^{(n_\phi)} H_1(\phi_\ell)\sin^2(\tfrac{1}{2}\phi_\ell)\cos(n\phi_\ell) - \frac{\pi}{2k^3\rho_q^3}\sum_{\ell=1}^{n_\phi}\frac{A_\ell^{(n_\phi)}}{\sqrt{\phi_\ell^2 + (\frac{\Delta_q}{2\rho_q})^2}}$$

$$+ \frac{1}{k^3\rho_q^3}\log\left[\frac{2\rho_q\pi}{\Delta_q} + \sqrt{1 + (\frac{2\rho_q\pi}{\Delta_q})^2}\right] \tag{68a}$$

$$G_{1\alpha} = \pi\sum_{\ell=1}^{n_\phi} A_\ell^{(n_\phi)} H_\alpha(\phi_\ell)\sin^2(\tfrac{1}{2}\phi_\ell)\cos(n\phi_\ell) \tag{68b}$$

$$\alpha = 2,3$$

$$G_{3\alpha} = \frac{\pi}{2}\sum_{\ell=1}^{n_\phi} A_\ell^{(n_\phi)} H_\alpha(\phi_\ell)\sin\phi_\ell \sin(n\phi_\ell) \tag{68c}$$

where $H_\alpha(\phi_\ell)$ is given by either (44) or (49) depending on whether (48) is true.

Equations (68b) and (68c) and the first sum in (68a) were taken directly from (50). The rest of the right-hand side of (68a) is due to

the manipulations (63)-(67). The numerical integration with respect to ϕ required to obtain (68a) is of the bounded integrand in (64) rather than of the unbounded integrand in (40a). Hence, the portion of (68a) in excess of (50a) fortifies the numerical integration with respect to ϕ. Having been obtained through analytical integration with respect to u, this portion of (68a) does not affect the accuracy of the numerical integration with respect to u.

IV. EVALUATION OF THE PLANE WAVE EXCITATION VECTOR

The column vector which appears on the right-hand side of (10) and whose elements are given by (11) is called the excitation vector. In this section, the elements (11) are evaluated for the case in which $\underline{H}^i$ is the magnetic field of either a θ polarized or a ϕ polarized incident plane wave.

Consider a θ polarized incident plane wave defined by

$$\underline{E}^{i\theta} = \underline{u}_\theta^t \, k\eta \, e^{-j\underline{k}_t \cdot \underline{r}} \tag{69a}$$

$$\underline{H}^{i\theta} = -\underline{u}_\phi^t \, k \, e^{-j\underline{k}_t \cdot \underline{r}} \tag{69b}$$

and also a ϕ polarized incident plane wave defined by

$$\underline{E}^{i\phi} = \underline{u}_\phi^t \, k\eta \, e^{-j\underline{k}_t \cdot \underline{r}} \tag{70a}$$

$$\underline{H}^{i\phi} = \underline{u}_\theta^t \, k \, e^{-j\underline{k}_t \cdot \underline{r}} \tag{70b}$$

where k is the propagation constant, η is the intrinsic impedance of space, $\underline{r}$ is the radius vector from the origin, and

$$\begin{aligned} \underline{k}_t &= -\underline{u}_x \sin\theta_t - \underline{u}_z \cos\theta_t \\ \underline{u}_\theta^t &= \underline{u}_x \cos\theta_t - \underline{u}_z \sin\theta_t \\ \underline{u}_\phi^t &= \underline{u}_y \end{aligned} \tag{71}$$

where $\underline{u}_x$, $\underline{u}_y$, and $\underline{u}_z$ are unit vectors in the x, y, and z directions, respectively. In (71), the letter t stands for transmitter. The origin is on the axis of the body of revolution and is in the vicinity of the body of revolution although not necessarily centered inside it. In (69) and (70), the $\underline{E}$'s are electric fields and the $\underline{H}$'s are magnetic fields.

Each of the incident plane waves (69) and (70) comes from the direction for which $\theta = \theta_t$ and $\phi = 0$. Here, θ and ϕ are standard spherical coordinates. θ is measured from the positive z axis. ϕ is the angle that the projection onto the xy plane makes with the positive x axis. At the aspect ($\theta = \theta_t$, $\phi = 0$), the unit vectors $\underline{u}_\theta^t$ and $\underline{u}_\phi^t$ reduce to the unit vectors in the θ and ϕ directions, respectively. Because of the circular symmetry of the body of revolution, no generality is lost by confining $\underline{k}_t$ to the xz plane. If $\underline{k}_t$ were rotated through an angle ϕ_t from $\phi = 0$ to $\phi = \phi_t$, the response would also rotate through the same angle ϕ_t.

In view of (70a), substitution of (69b) for $\underline{H}^i$ in (11) gives

$$I_{ni}^{it\theta} = \frac{-1}{\eta} \int dt\ T_i(t) \int_0^{2\pi} d\phi\ (\underline{u}_\phi \cdot \underline{E}^{i\phi}) e^{-jn\phi} \tag{72a}$$

$$I_{ni}^{i\phi\theta} = \frac{1}{\eta \rho_i} \int dt\, \rho\, P_i(t) \int_0^{2\pi} d\phi\ (\underline{u}_t \cdot \underline{E}^{i\phi}) e^{-jn\phi} \tag{72b}$$

The additional superscript θ on the left-hand sides of (72) indicates the θ polarized incident plane wave. In view of (69a), substitution of (70b) for $\underline{H}^i$ in (11) gives

$$I_{ni}^{it\phi} = \frac{1}{\eta} \int dt\ T_i(t) \int_0^{2\pi} d\phi\ (\underline{u}_\phi \cdot \underline{E}^{i\theta}) e^{-jn\phi} \tag{73a}$$

$$I_{ni}^{i\phi\phi} = \frac{-1}{\eta \rho_i} \int dt\, \rho\, P_i(t) \int_0^{2\pi} d\phi\ (\underline{u}_t \cdot \underline{E}^{i\theta}) e^{-jn\phi} \tag{73b}$$

The third superscript on the left-hand sides of (73) indicates the ϕ polarized incident plane wave.

Substitution of (9) for the $\underline{W}$'s and (69a) for $\underline{E}^i$ in (7) and (8) of [1] reveals that the elements $V_{ni}^{t\theta}$ and $V_{ni}^{\phi\theta}$ considered in Section IV of [1] are given by

$$V_{ni}^{t\theta} = \frac{1}{\eta} \int dt\ T_i(t) \int_0^{2\pi} d\phi\ (\underline{u}_t \cdot \underline{E}^{i\theta}) e^{-jn\phi} \tag{74a}$$

$$V_{ni}^{\phi\theta} = \frac{1}{\eta\rho_i} \int dt\, \rho\, P_i(t) \int_0^{2\pi} d\phi\ (\underline{u}_\phi \cdot \underline{E}^{i\theta}) e^{-jn\phi} \tag{74b}$$

Substitution of (9) for the $\underline{W}$'s and (70a) for $\underline{E}^i$ in (7) and (8) of [1] gives

$$V_{ni}^{t\phi} = \frac{1}{\eta} \int dt\ T_i(t) \int_0^{2\pi} d\phi\ (\underline{u}_t \cdot \underline{E}^{i\phi}) e^{-jn\phi} \tag{75a}$$

$$V_{ni}^{\phi\phi} = \frac{1}{\eta\rho_i} \int dt\, \rho\, P_i(t) \int_0^{2\pi} d\phi\ (\underline{u}_\phi \cdot \underline{E}^{i\phi}) e^{-jn\phi} \tag{75b}$$

Comparison of (72) with (75) shows that if $T_i(t)$ and $(\rho P_i(t))/\rho_i$ were interchanged in (75), then

$$I_{ni}^{it\theta} = -\ V_{ni}^{\phi\phi} \tag{76a}$$

$$I_{ni}^{i\phi\theta} = \ V_{ni}^{t\phi} \tag{76b}$$

Comparison of (73) with (74) shows that if $T_i(t)$ and $(\rho P_i(t))/\rho_i$ were interchanged in (74), then

$$I_{ni}^{it\phi} = \ V_{ni}^{\phi\theta} \tag{76c}$$

$$I_{ni}^{i\phi\phi} = -\ V_{ni}^{t\theta} \tag{76d}$$

Now, $T_i(t)$ is responsible for both the asterisk on the left-hand sides of (120) and (122) of [1] and the factor

$$\frac{1}{2}\left(1 + \frac{(-1)^{p-i}\, 2(t-t_p)}{\Delta_p}\right)$$

on the right-hand sides of (120) and (122) of [1]. Also, $(\rho P_i(t))/\rho_i$ appears as the factor

$$1 + \frac{(t-t_p)\sin v_p}{\rho_p}$$

in (121) and (123) of [1]. Hence,

$$\overset{*}{I}{}^{it\theta}_{ni} = -\frac{j^{n+1}\pi k}{2}\int_{t_p^-}^{t_{p+1}^-}\left(1 + \frac{(-1)^{p-i}\, 2(t-t_p)}{\Delta_p}\right)(J_{n+1} - J_{n-1})e^{jkz\cos\theta_t}\,dt \tag{77a}$$

$$I^{i\phi\theta}_{np} = -j^n\pi k\int_{t_p^-}^{t_{p+1}^-}\left(1 + \frac{(t-t_p)\sin v_p}{\rho_p}\right)(J_{n+1} + J_{n-1})\sin v_p\, e^{jkz\cos\theta_t}\,dt \tag{77b}$$

$$\overset{*}{I}{}^{it\phi}_{ni} = \frac{j^n\pi k}{2}\int_{t_p^-}^{t_{p+1}^-}\left(1 + \frac{(-1)^{p-i}\, 2(t-t_p)}{\Delta_p}\right)(J_{n+1} + J_{n-1})\cos\theta_t\, e^{jkz\cos\theta_t}\,dt \tag{77c}$$

$$I^{i\phi\phi}_{np} = -j^n\pi k\int_{t_p^-}^{t_{p+1}^-}\left(1 + \frac{(t-t_p)\sin v_p}{\rho_p}\right)[j\sin v_p\cos\theta_t\,(J_{n+1} - J_{n-1})$$

$$-2\cos v_p\sin\theta_t J_n]e^{jkz\cos\theta_t}\,dt \tag{77d}$$

where J_n, ρ, and z are given by (115), (130) and (131) of [1]. The asterisk on the left-hand sides of (77a) and (77c) indicates that the right-hand sides of (77a) and (77c) are not all of $I^{it\theta}_{ni}$ and $I^{it\phi}_{ni}$ but only the contributions due to the region of integration for which $t_p^- \le t \le t_{p+1}^-$. Both (77a) and (77c) are valid for $i = p-1$ and $i = p$.

Equation (77) can be rewritten as

$$\overset{*}{I}{}^{it\theta}_{ni} = -\frac{j^{n+1}\pi k\Delta_p}{4}(F_{n+1,a} - F_{n-1,a}) - \frac{(-1)^{p-i} j^{n+1}\pi k\Delta_p}{4}(F_{n+1,b} - F_{n-1,b}) \tag{78a}$$

$$I^{i\phi\theta}_{np} = -\frac{j^{n}\pi k\Delta_p \sin v_p}{2}\left[F_{n+1,a} + F_{n-1,a} + \frac{\Delta_p \sin v_p}{2\rho_p}(F_{n+1,b} + F_{n-1,b})\right] \tag{78b}$$

$$\overset{*}{I}{}^{it\phi}_{ni} = \frac{j^{n}\pi k\Delta_p \cos\theta_t}{4}(F_{n+1,a} + F_{n-1,a}) + \frac{(-1)^{p-i} j^{n}\pi k\Delta_p \cos\theta_t}{4}(F_{n+1,b} + F_{n-1,b}) \tag{78c}$$

$$\begin{aligned} I^{i\phi\phi}_{np} = &-\frac{j^{n+1}\pi k\Delta_p \sin v_p \cos\theta_t}{2}\left[(F_{n+1,a} - F_{n-1,a}) + \frac{\Delta_p \sin v_p}{2\rho_p}(F_{n+1,b} - F_{n-1,b})\right] \\ &+ j^{n}\pi k\Delta_p \cos v_p \sin\theta_t\left[F_{na} + \frac{\Delta_p \sin v_p}{2\rho_p}F_{nb}\right] \end{aligned} \tag{78d}$$

where the F's are given by (128) and (129) of [1]. The n_T point Gaussian quadrature formulas for them are

$$\left.\begin{aligned} F_{ma} &= \sum_{\ell=1}^{n_T} A_\ell^{(n_T)} J_m(k\hat{\rho}_\ell \sin\theta_t)e^{jk\hat{z}_\ell \cos\theta_t} && (79a) \\ F_{mb} &= \sum_{\ell=1}^{n_T} A_\ell^{(n_T)} x_\ell^{(n_T)} J_m(k\hat{\rho}_\ell \sin\theta_t)e^{jk\hat{z}_\ell \cos\theta_t} && (79b) \end{aligned}\right\} m=n-1,n,n+1$$

where J_m is the Bessel function of the first kind and where $\hat{\rho}_\ell$ and $\hat{z}_\ell$ are given by (134) and (135) of [1]. The abscissas $x_\ell^{(n_T)}$ and weights $A_\ell^{(n_T)}$ are tabulated in Appendix A of [10] for several values of n_T.

V. NUMERICAL RESULTS

Computed results for the electric currents induced by an axially incident wave on a sphere, a cone-sphere, and a finite cylinder are presented in Figs. 1-14. For axial incidence, θ_t is either 0° or 180° and the only non-zero excitation vectors for the θ polarized plane wave (69) are

$$\begin{bmatrix} \vec{I}^{it}_{-1} \\ \\ \vec{I}^{i\phi}_{-1} \end{bmatrix} = \begin{bmatrix} \vec{I}^{it}_{1} \\ \\ -\vec{I}^{i\phi}_{1} \end{bmatrix} \tag{80}$$

It is evident from (12) and (13) that

$$\begin{bmatrix} Y^{tt}_{-1} & Y^{t\phi}_{-1} \\ \\ Y^{\phi t}_{-1} & Y^{\phi\phi}_{-1} \end{bmatrix} = \begin{bmatrix} Y^{tt}_{1} & -Y^{t\phi}_{1} \\ \\ -Y^{\phi t}_{1} & Y^{\phi\phi}_{1} \end{bmatrix} \tag{81}$$

In consequence of (80), (81), and (10), the only non-zero column vectors $\vec{I}^t_n$ and $\vec{I}^\phi_n$ are given by

$$\begin{bmatrix} \vec{I}^{t}_{-1} \\ \\ -\vec{I}^{\phi}_{-1} \end{bmatrix} = \begin{bmatrix} \vec{I}^{t}_{1} \\ \\ \vec{I}^{\phi}_{1} \end{bmatrix} \tag{82}$$

where the column vector on the right-hand side of (82) satisfies (10) for $n = 1$.

In view of (3), substitution of (82) into (2) and subsequent division by k give

$$\frac{\underline{J}}{|\underline{H}^i|} = 2\, \underline{u}_t \cos\phi \left(\sum_j I^t_{1j} \frac{T_j(t)}{k\rho}\right) + 2j\underline{u}_\phi \sin\phi \left(\sum_j I^\phi_{1j} \frac{P_j(t)}{k\rho_j}\right) \tag{83}$$

The $|\underline{H}|^i$ written instead of k on the left-hand side of (83) is the

magnitude of the incident magnetic field. This magnitude is indeed equal to k. At $t = t^-_{p+1}$, the t component of (83) reduces to

$$\frac{J_t}{|\underline{H}^i|} = \frac{2I^t_{1p}}{k\rho(t^-_{p+1})} \cos \phi, \quad p=1, 2, \ldots P-2 \tag{84}$$

where $\rho(t^-_{p+1})$ is the value of ρ at $t = t^-_{p+1}$. At $t = t_p$, the ϕ component of (83) reduces to

$$\frac{J_\phi}{|\underline{H}^i|} = \frac{2jI^\phi_{1p} \sin \phi}{k\rho_p}, \quad p = 1,2,\ldots P-1 \tag{85}$$

Here, J_t and J_ϕ are, respectively, the t and ϕ components of the electric current $\underline{J}$. In Figs. 1-14, $\frac{|J_t|}{|\underline{H}^i|}$ in the $\phi = 0°$ plane is plotted with squares and $\frac{|J_\phi|}{|\underline{H}^i|}$ in the $\phi = 90°$ plane is plotted with octagons. These currents are plotted versus t/λ where t is the arc length along the generating curve and λ is the wavelength. The horizontal axes in Figs. 1-14 were labeled T/λ because the lower case letter t could not be drawn by the plotter.

Figures 1-4 display computed values of electric current induced on a conducting sphere of radius $.2\lambda$ illuminated by a plane wave. Figure 1 shows the H-field solution of [2], Fig. 2 shows the present H-field solution, Fig. 3 shows the E-field solution of [2], and Fig. 4 shows the E-field solution of [1]. The squares and octagons represent computed values of $\frac{|J_t|}{|\underline{H}^i|}$ and $\frac{|J_\phi|}{|\underline{H}^i|}$, respectively. The solid curves represent the Mie series solution [13]. In Figs. 1 and 3, the squares and octagons are horizontally located at the peaks of the triangles used [2]. In Figs. 2 and 4, the squares are placed at the peaks of the triangles (5) and the octagons are placed at the centers of the pulses (6). That is why the squares and the

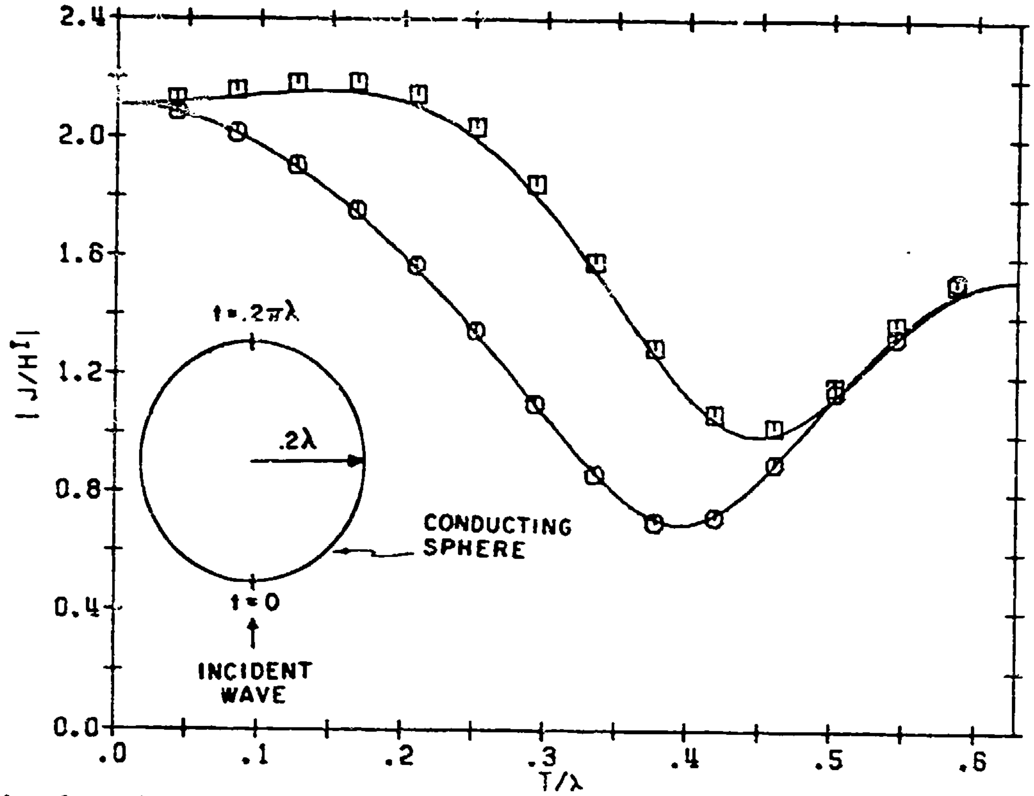

Fig. 1. Electric current on a conducting sphere of radius 0.2λ. The squares and octagons represent the H-field solution of [2]. The solid curves represent the Mie series solution.

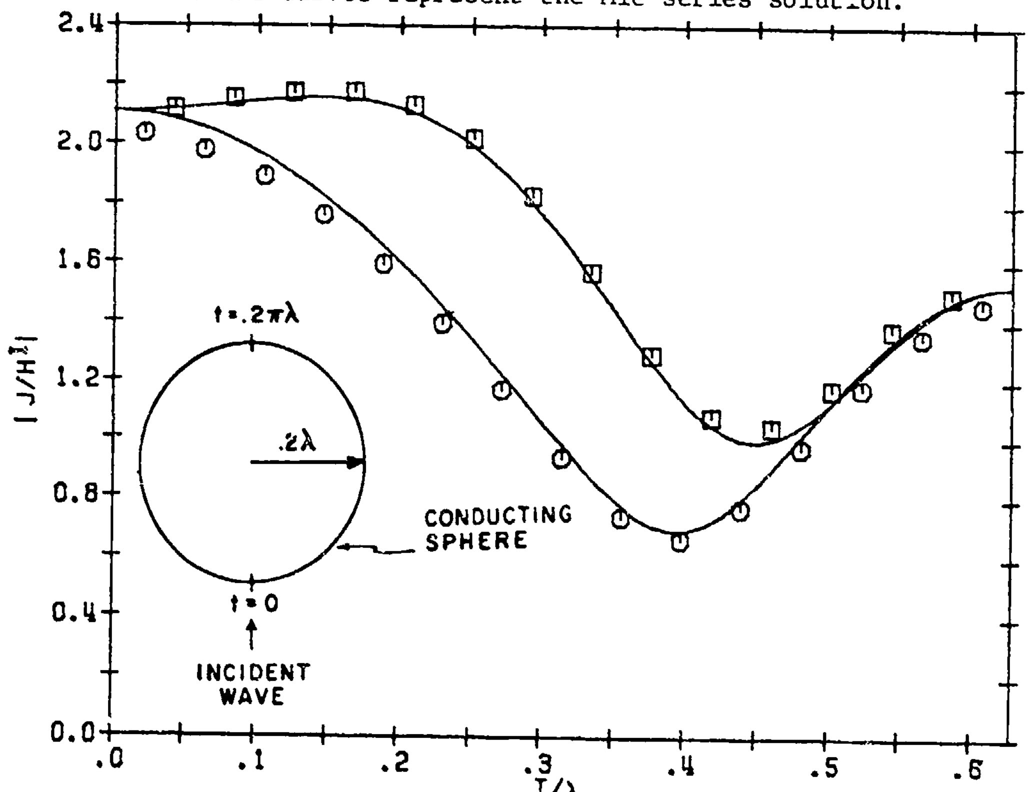

Fig. 2. Electric current on a conducting sphere of radius 0.2λ. The squares and octagons represent the present H-field solution. The solid curves represent the Mie series solution.

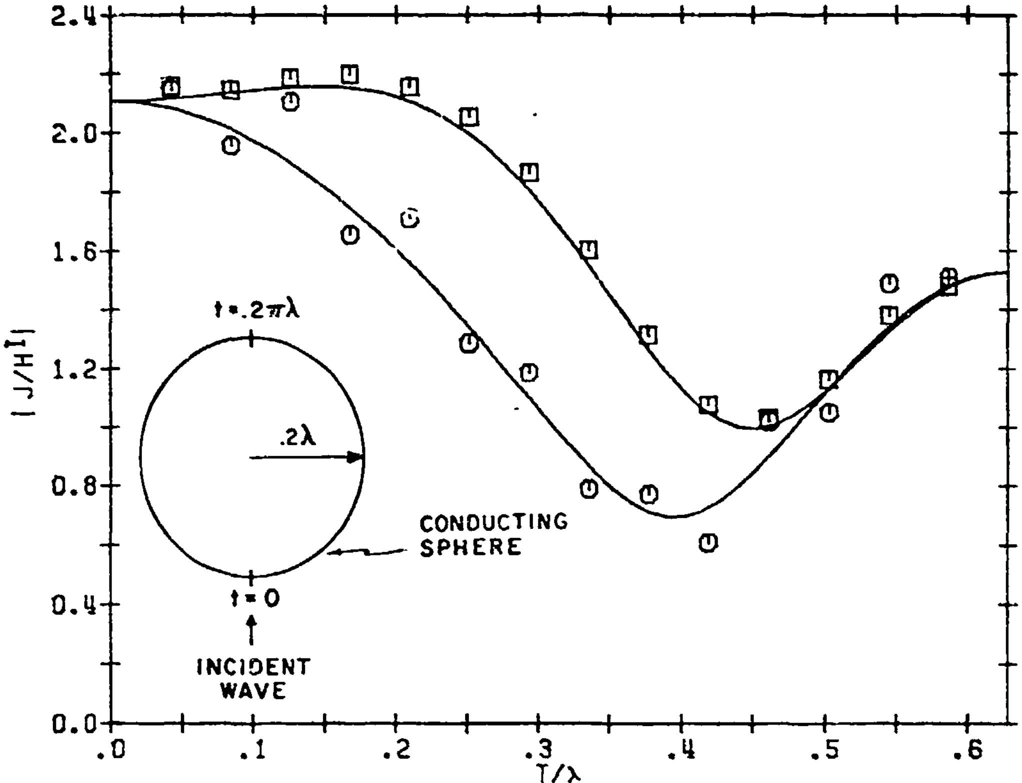

Fig. 3. Electric current on a conducting sphere of radius 0.2λ. The squares and octagons represent the E-field solution of [2]. The solid curves represent the Mie series solution.

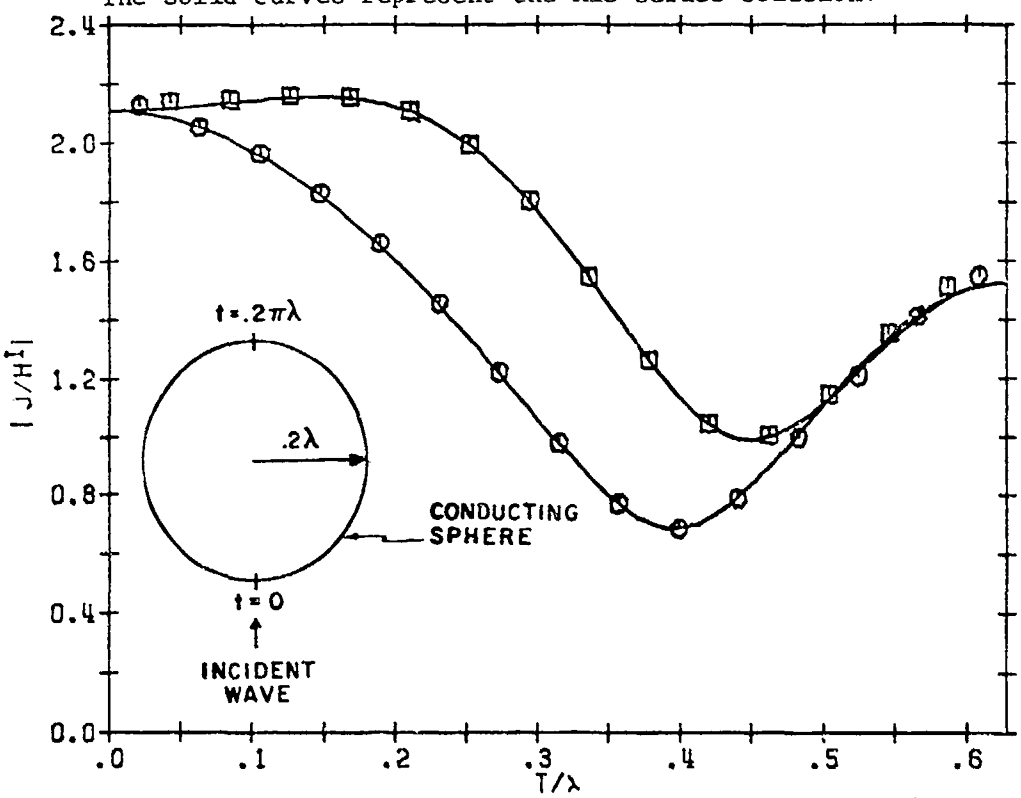

Fig. 4. Electric current on a conducting sphere of radius 0.2λ. The squares and octagons represent the E-field solution of [1]. The solid curves represent the Mie series solution.

octagons line up with each other in Figs. 1 and 3 but are staggered in Figs. 2 and 4. The oscillations of the octagons about the solid curve in Fig. 3 are not surprising because the particular size of the sphere places the electric current error in Fig. 5 on page 32 of [2] near one of its peaks.

Figures 5-10 display computed values of electric current induced on a cone-sphere by plane waves incident from both axial directions. The squares represent $\frac{|J_t|}{|\underline{H}^i|}$ and the octagons represent $\frac{|J_\phi|}{|\underline{H}^i|}$. These symbols are connected by straight lines in order to improve readability. The currents in Figs. 5 and 6 agree reasonably well with those in Fig. 7 of [1]. Likewise, the currents in Figs. 8 and 9 agree reasonably well with those in Fig. 8 of [1]. The jagged nature of the ϕ components of current in Figs. 7 and 10 is probably spurious.

Finally, Figs. 11-14 display computed values of the electric currents induced on a closed cylinder of length .5λ and radius .25λ by an axially incident plane wave.

The currents in Figs. 2,4,6,9,12, and 14 were calculated with

$$\left.\begin{aligned} n_t = n_T &= 2 \\ n_\phi &= 20 \end{aligned}\right\}$$

The currents in the rest of the figures were calculated with $n_\phi = 20$ in [2]. The IBM System 370/155 under WATFIV took 29 seconds of execution time to calculate the H-field solution in Fig. 6. The subroutine YMAT was used for this calculation. The joint calculation of the H-field solution in Fig. 6 and the E-field solution of [1] in Fig. 7 of [1] took 45 seconds of execution time. The subroutine YZ was used for this calculation. The joint calculation of the H-field solution of [2] in Fig. 5 and th E-field solution of [2] in Fig. 7 took 39 seconds of execution time using the subroutine YZ of [14]. Hence, the present H-field solution and the E-field solution of [1] are slightly slower than the H-field and E-field solutions in [2].

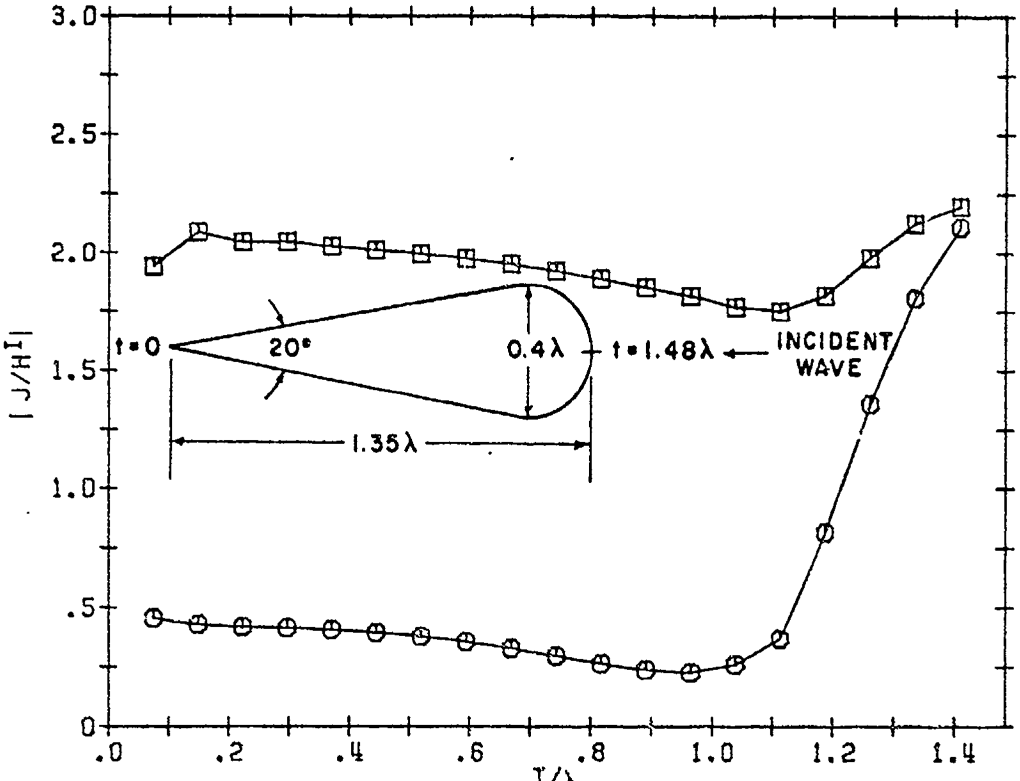

Fig. 5. Electric current induced on a cone-sphere by an axially incident plane wave. Incidence on sphere, H-field solution of [2].

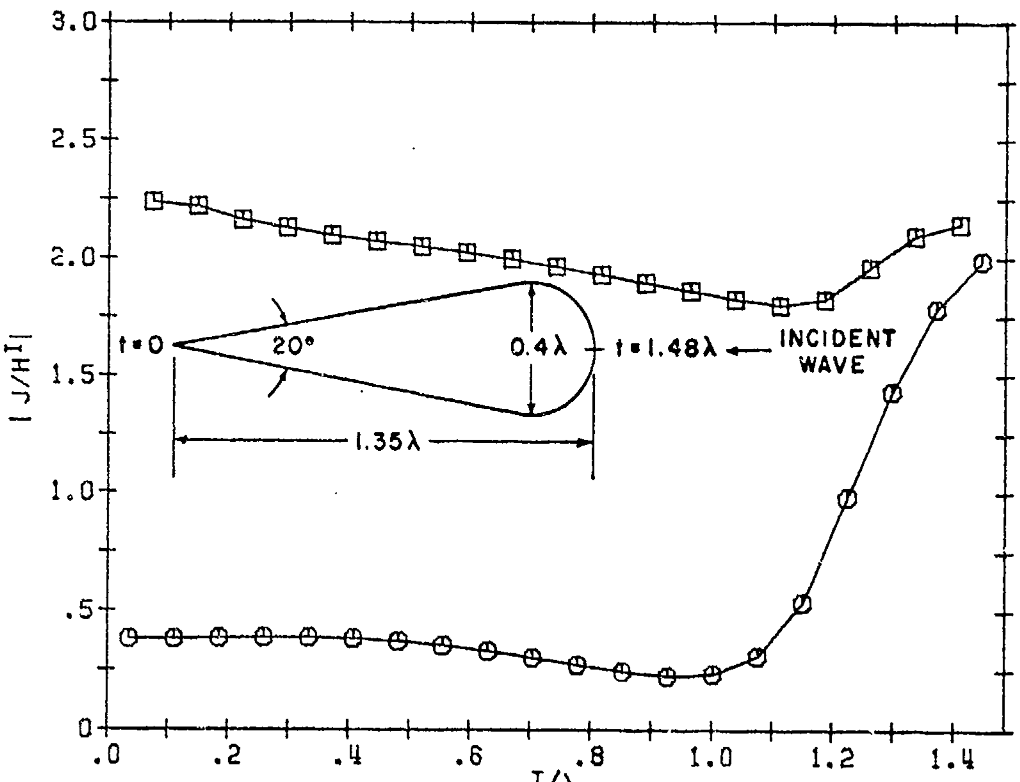

Fig. 6. Electric current induced on a cone-sphere by an axially incident plane wave. Incidence on sphere, present H-field solution.

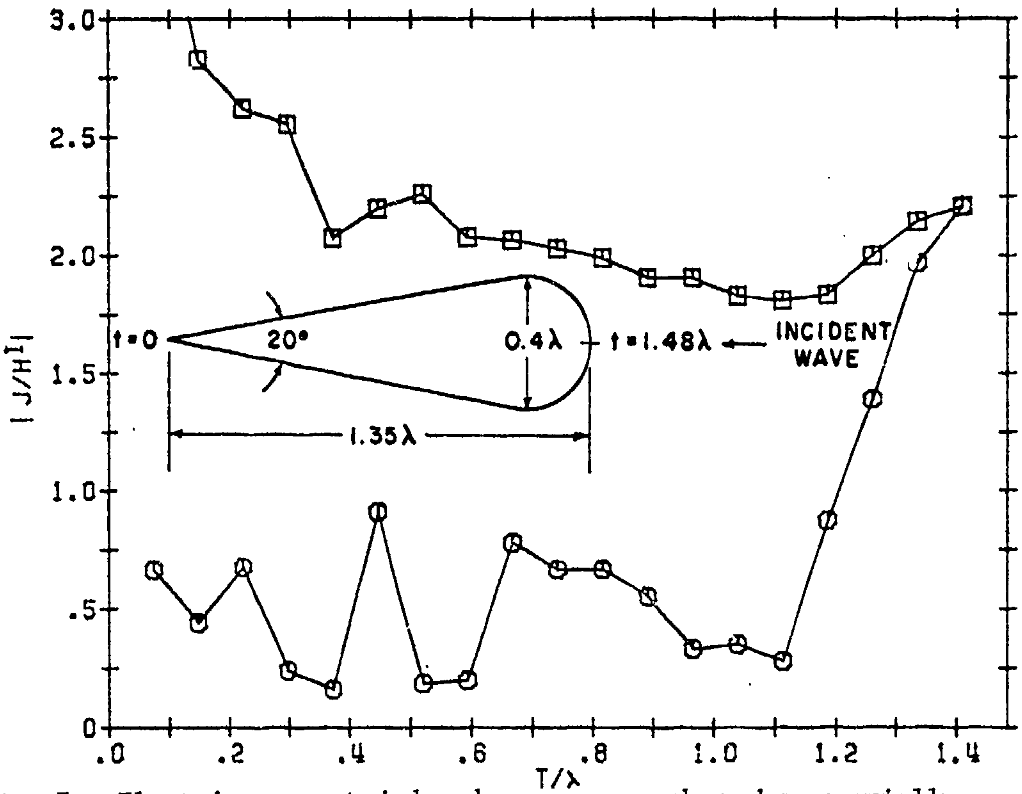

Fig. 7. Electric current induced on a cone-sphere by an axially incident plane wave. Incidence on sphere, E-field solution of [2].

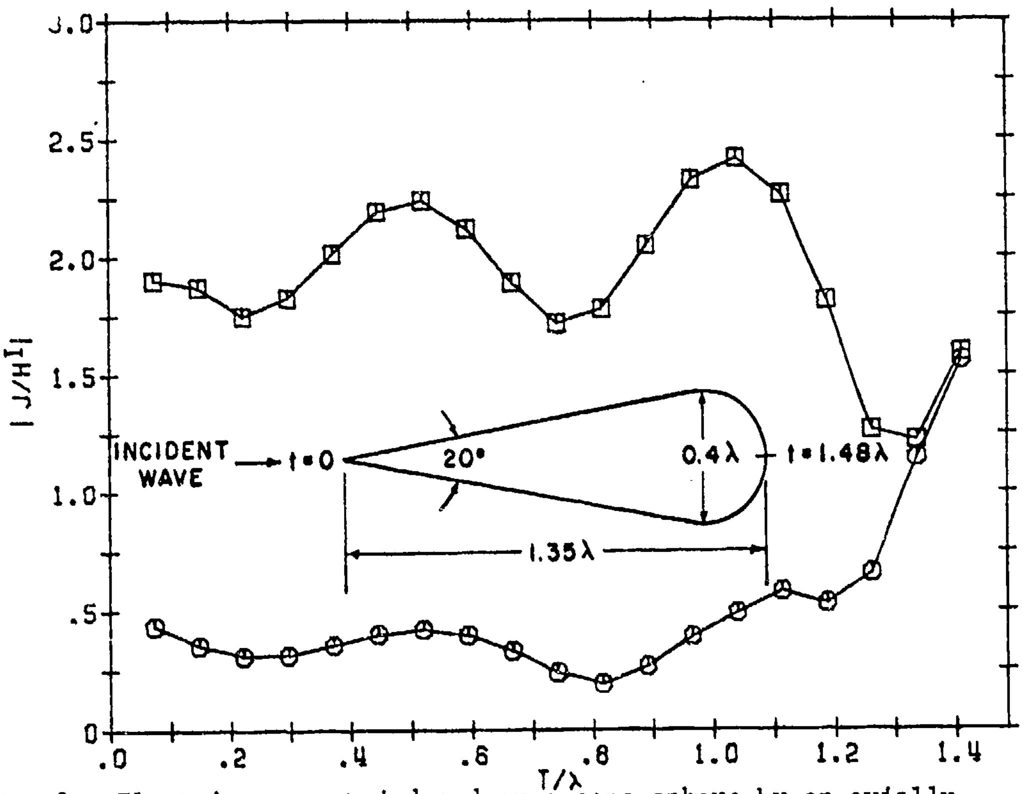

Fig. 8. Electric current induced on a cone-sphere by an axially incident plane wave. Incidence on tip, H-field solution of [2].

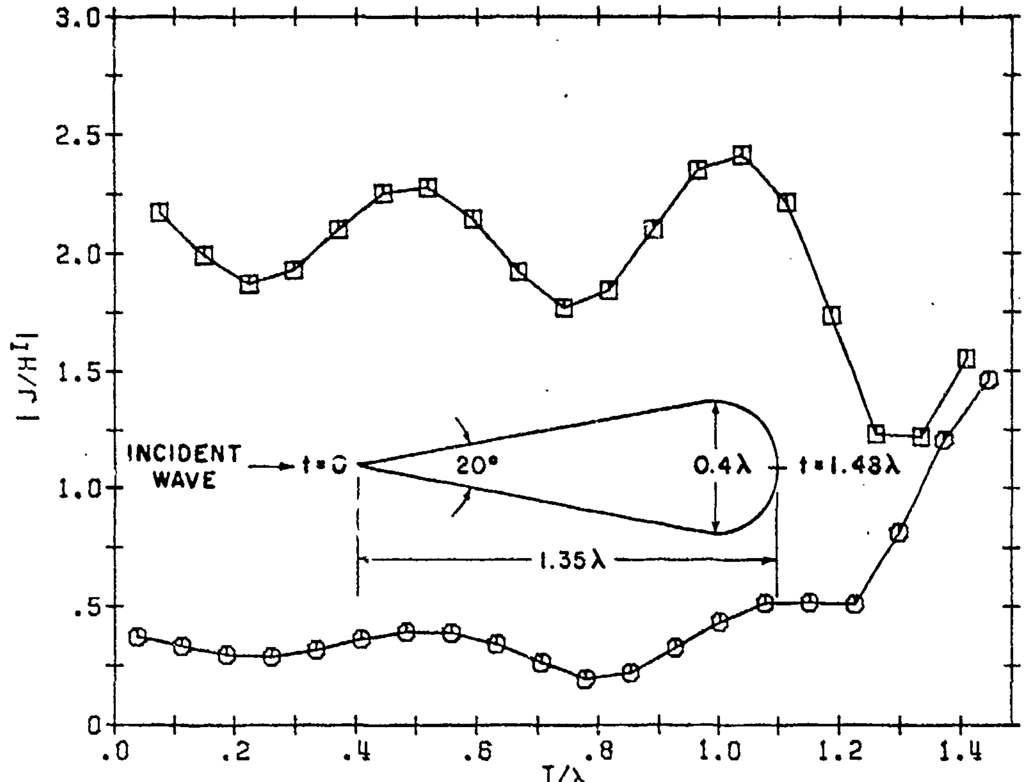

Fig. 9. Electric current induced on a cone-sphere by an axially incident plane wave. Incidence on tip, present H-field solution.

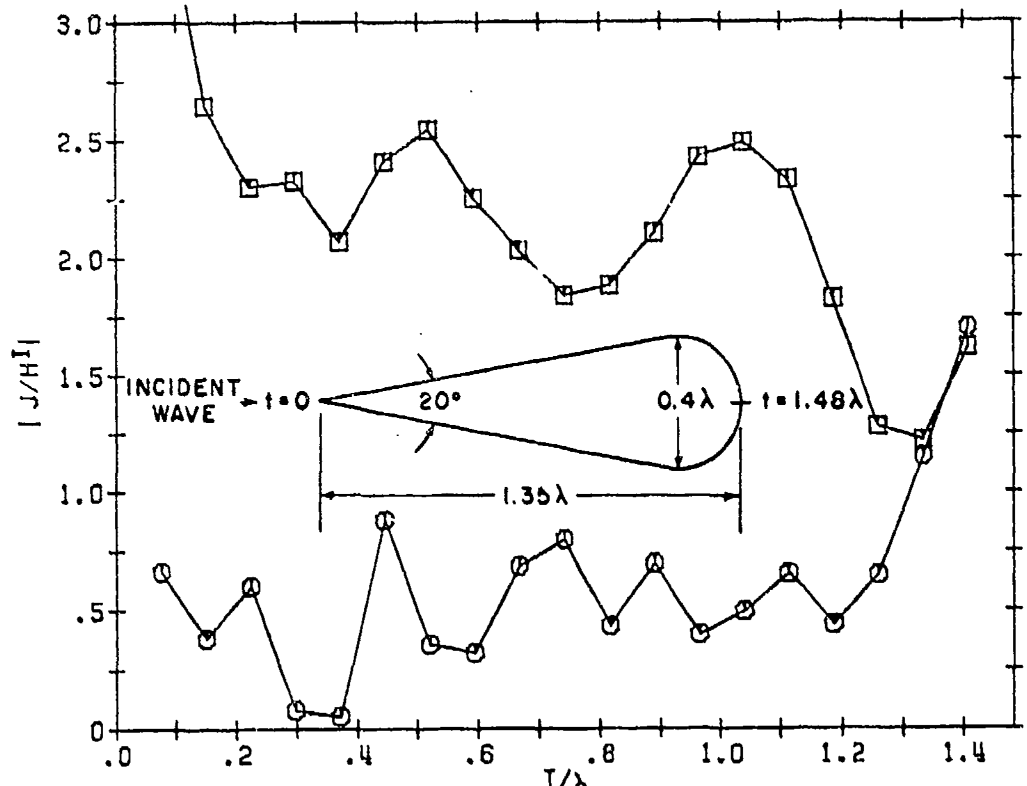

Fig. 10. Electric current induced on a cone-sphere by an axially incident plane wave. Incidence on tip, E-field solution of [2].

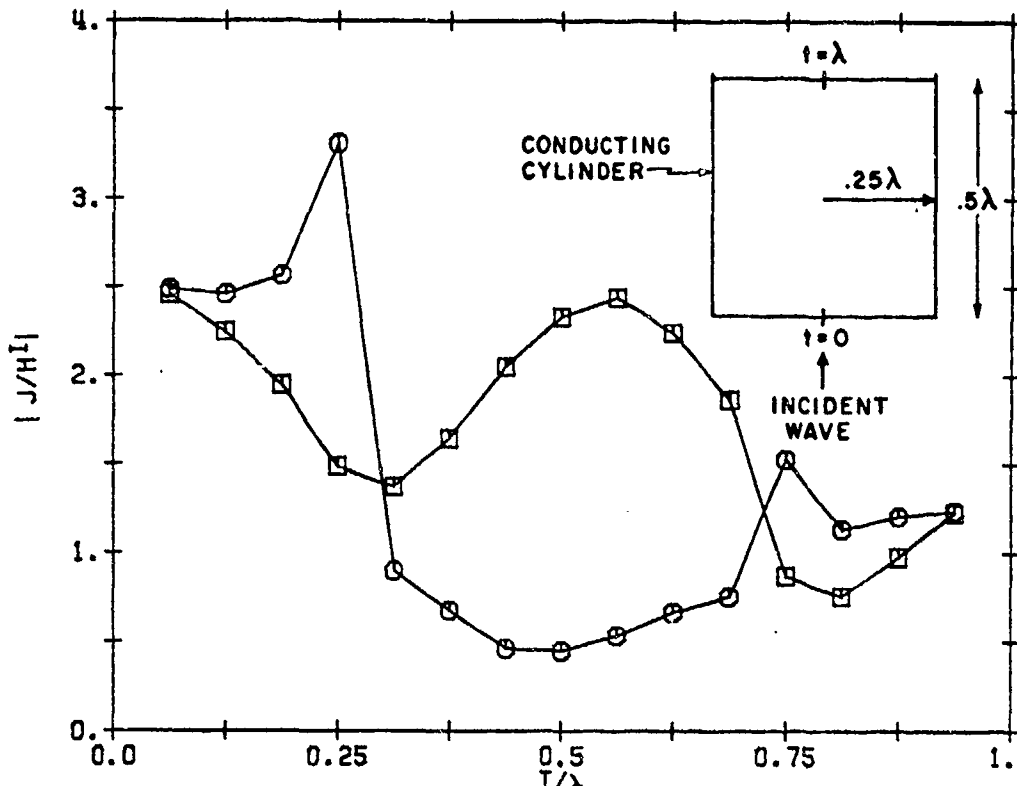

Fig. 11. Electric current induced on a closed cylinder of length 0.5λ and radius 0.25λ by an axially incident plane wave. H-field solution of [2].

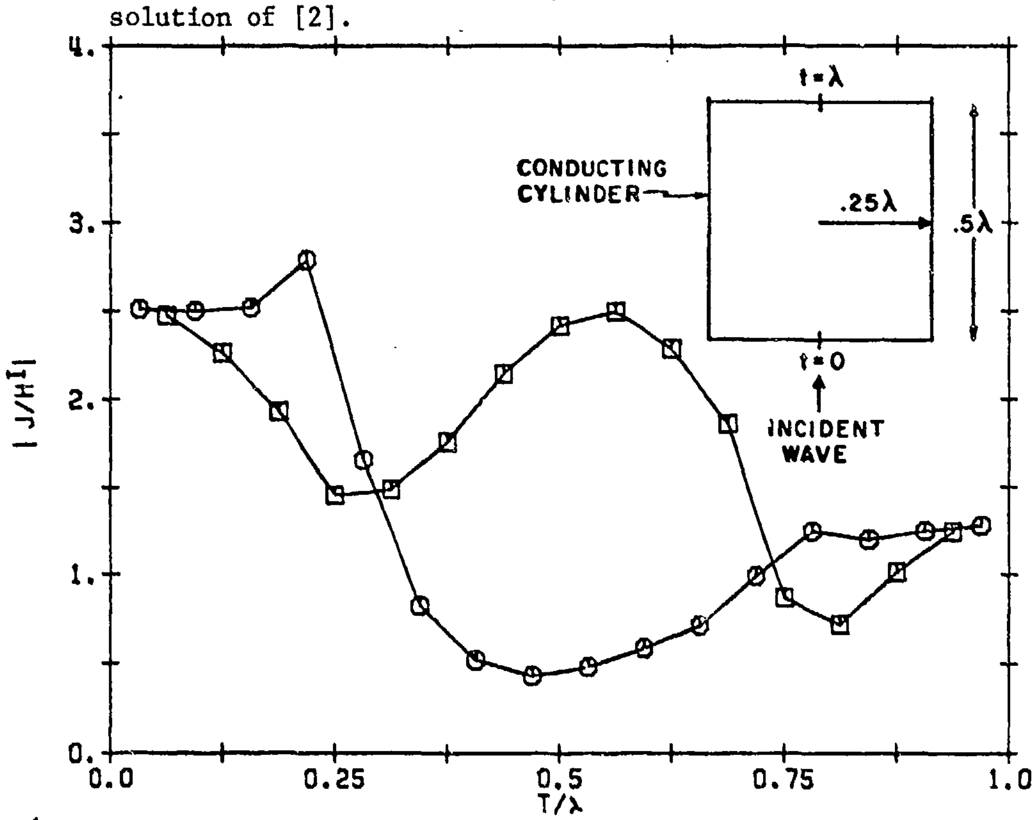

Fig. 12. Electric current induced on a closed cylinder of length 0.5 λ and radius 0.25λ by an axially incident plane wave. Present H-field solution.

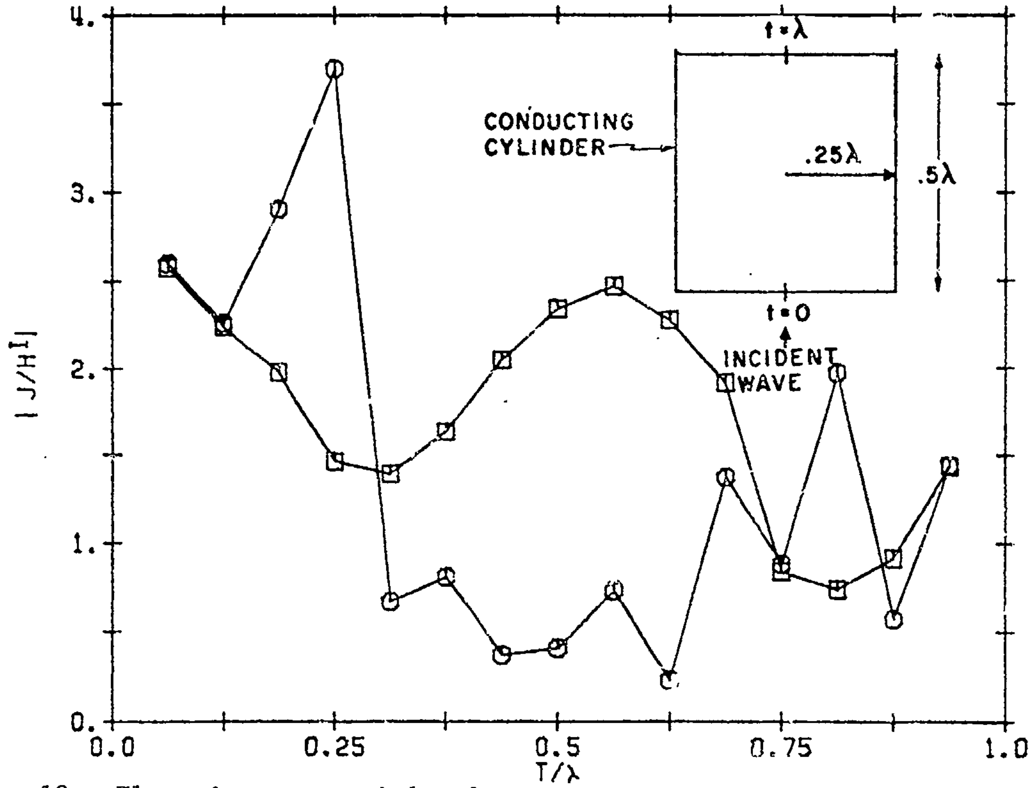

Fig. 13. Electric current induced on a closed cylinder of length 0.5λ and radius 0.25λ by an axially incident plane wave. E-field solution of [2].

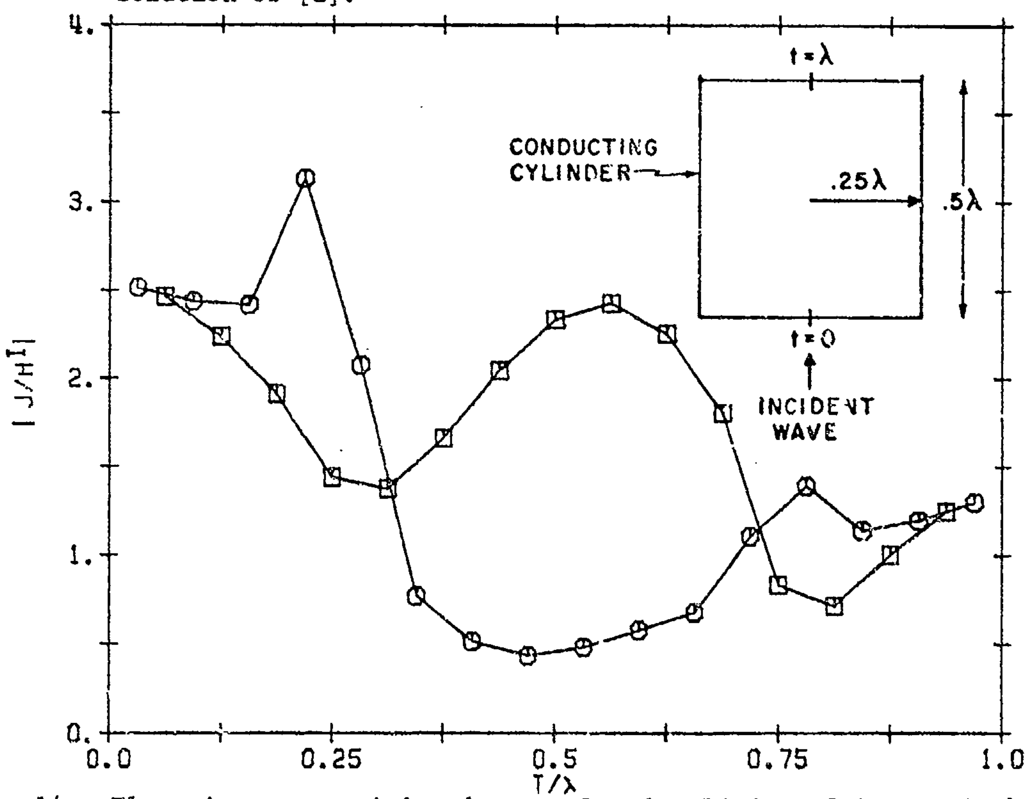

Fig. 14. Electric current induced on a closed cylinder of length 0.5λ and radius 0.25λ by an axially incident plane wave. E-field solution of [1].

The results of calculation of the present H-field solution and E-field solution of [1] for the sphere, cone-sphere and finite cylinder examples with

$$\left.\begin{aligned} n_t = n_T &= 4 \\ n_\phi &= 48 \end{aligned}\right\}$$

were so close to the results in Figs. 2,4,6,9,12, and 14 that distinction was impossible.

PART TWO

COMPUTER PROGRAMS

I. INTRODUCTION

A computer program which implements the present H-field solution is described and listed in Part Two. This program consists of the subroutine YMAT, the function BLOG, the subroutines PLANE, DECOMP, and SOLVE, and the main program for the H-field solution. The subroutine YMAT calculates the elements (12) of the moment matrix in (10). The function BLOG is called by YMAT. The subroutine PLANE uses (78) to calculate the excitation vector on the right-hand side of (10) for a θ polarized incident plane wave. The subroutine PLANE also calculates the excitation vector for a ϕ polarized plane wave, but this vector is not used in the main program. The subroutines DECOMP and SOLVE solve the matrix equation (10) for $\vec{I}_n^t$ and $\vec{I}_n^\phi$. The main program for the H-field solution obtains the electric current induced on a conducting body of revolution by an axially incident plane wave. The subroutines YMAT and PLANE are designed not only for axial incidence but also for oblique incidence. For axial incidence, $n = \pm 1$ and θ_t of (71) is either 0° or 180°. The subroutines YMAT and PLANE admit $n = M1, M1+1, \ldots M2$ where $M2 \geq M1 \geq 0$. The subroutine PLANE also admits arbitrary values of θ_t. Formulas on pages (28) and (29) of [2] obviate calculation of moment matrices and plane wave excitation vectors for negative values of n.

A computer program which implements both the present H-field solution and the E-field solution of [1] is also described and listed in Part Two. This program consists of the previously mentioned subprograms BLOG, PLANE, DECOMP, SOLVE, a new subroutine YZ, and the main program for both the H-field and E-field solutions. The subroutine YZ calculates the moment matrices in (10) of the present report and in (6) of [1]. The subroutine YZ calls the function BLOG. The subroutine PLANE calculates the excitation vector on the right-hand side of (10) for the θ polarized plane wave. PLANE also calculates the elements

$V_{ni}^{t\theta}$ and $-V_{ni}^{\phi\theta}$ of (74) for use on the right-hand side of (6) of [1]. In addition, PLANE calculates excitation vectors for the ϕ polarized plane wave but these vectors are not used in the main program. The subroutines DECOMP and SOLVE solve the matrix equations (10) of the present report and (6) of [1]. The main program for both the H-field and E-field solutions obtains both the present H-field solution and the E-field solution of [1] for the electric current induced on a conducting body of revolution immersed in an axially incident plane wave.

II. THE SUBROUTINE YMAT

With regard to (10), the subroutine YMAT(M1, M2, NP, NPHI, NT, IN, RH, ZH, X, A, XT, AT, Y) puts in Y the moment matrices Y_n defined by

$$Y_n = \begin{bmatrix} Y_n^{tt} & Y_n^{t\phi} \\ Y_n^{\phi t} & Y_n^{\phi\phi} \end{bmatrix}, \quad n = M1, M1+1, \ldots M2 \tag{86}$$

Storage in Y is such that the ith column of Y_n goes from Y((i-1)*N + (n-M1)*N*N+1) to Y(i*N+(n-M1)*N*N) where

$$N = 2*NP - 3 \tag{87}$$

The only output argument of YMAT is Y. The rest of the arguments of YMAT are input arguments. The input argument IN generalizes YMAT for use with problems other than conducting body problems. The term $(\pi\Delta_q)/\rho_q$ in (22d) and the quantities $\dot{Y}_n^{tt}$ in (23) are multiplied by IN in the subroutine YMAT. Thus, the argument IN should be 1 for the present H-field solution. In this solution, the magnetic field is evaluated just inside S. Magnetic field evaluation just outside S can be obtained by setting IN = -1.

Each of the input arguments except M1, M2, and IN represents a variable in Part One of the text. The correspondence is tabulated as

Input Argument	Text Variable		Equation Number
NP	P		3
NPHI	n_ϕ		36
NT	n_t		35
RH	$k\rho(\bar{t}_j)$,	$j = 1,2,\ldots P$	21
ZH	$kz(\bar{t}_j)$,	$j = 1,2,\ldots P$	21
X	$x_\ell^{(n_\phi)}$,	$\ell = 1,2,\ldots n_\phi$	37
A	$A_\ell^{(n_\phi)}$,	$\ell = 1,2,\ldots n_\phi$	36
XT	$x_{\ell'}^{(n_t)}$,	$\ell' = 1,2,\ldots n_t$	35
AT	$A_{\ell'}^{(n_t)}$,	$\ell' = 1,2,\ldots n_t$	35

Here, $\rho(\bar{t}_j)$ and $z(\bar{t}_j)$ are the values of ρ and z at $t=\bar{t}_j$ on the generating curve and k is the propagation constant. The generating curve starts at $t = \bar{t}_1$ and ends at $t = \bar{t}_P$. The input argument P must be a positive integer not less than 3. The input arguments NPHI, NT, X, A, XT, and AT are Gaussian quadrature data. Lines 11 and 12 put c_t and c_ϕ of (31) in CT and CP, respectively. The subroutine YMAT calls the function BLOG which is described and listed in Section III of Part Two.

Minimum allocations are given by

```
COMPLEX  Y(M3*N*N), GA(NPHI), GB(NPHI), GC(NPHI),
    G1A(M3), G2A(M3), G3A(M3), G1B(M3), G2B(M3),
    G3B(M3), G1C(M3), G2C(M3), G3C(M3)

DIMENSION  RH(NP), ZH(NP), X(NPHI), A(NPHI),
    XT(NT), AT(NT), RS(NP-1), ZS(NP-1), D(NP-1),
    DR(NP-1), DZ(NP-1), C2(NPHI), C3(NPHI),
    C4(M3*NPHI), C5(M3*NPHI), C6(M3*NPHI),
    R2(NT), Z2(NT), R7(NT), Z7(NT)
```

where N is given by (87) and

$$M3 = M2 - M1 + 1 \tag{88}$$

The elements of Y_n are calculated from (23) and (24) with $G_{m\alpha}$ evaluated as in Section III of Part One. DO loop 11 puts ϕ_ℓ^2 in C2 and $4\sin^2(\frac{1}{2}\phi_\ell)$ in C3. ϕ_ℓ is given by (37) and $4\sin^2(\frac{1}{2}\phi_\ell)$ is needed in order to evaluate (15) at $\phi = \phi_\ell$. With regard to (36), inner DO loop 29 puts

$$\pi A_\ell^{(n_\phi)} \sin^2(\tfrac{1}{2}\phi_\ell)\cos(n\phi_\ell) \quad \text{in} \quad C4,$$

$$\frac{\pi}{2} A_\ell^{(n_\phi)} \cos\phi_\ell \cos(n\phi_\ell) \quad \text{in} \quad C5,$$

and

$$\frac{\pi}{2} A_\ell^{(n_\phi)} \sin\phi_\ell \sin(n\phi_\ell) \quad \text{in} \quad C6.$$

The index JQ of DO loop 15 obtains q in (23) and (24). With regard to (22d), line 69 puts $(IN)*(\pi\Delta_q)/\rho_q$ in P2. DO loop 12 puts $k\rho'$ and kz' of (29) in R2 and Z2, respectively. DO loop 12 also accumulates the products of IN with (23a), (23b), and (23c) in P1A, P1B, and P1C, respectively. The index IP of DO loop 16 obtains p in (24). Lines 106-112 put kd_o of (32) in D6. If either case 1 of (30) or case 3 of (51) is obtained, branch statement 26 sends execution to statement 41. If either case 2 of (39) or case 4 of (60) is obtained, execution proceeds to line 114. Lines 114-235 calculate $G_{m\alpha}$ for case 2 and case 4. Lines 237-308 calculate $G_{m\alpha}$ for case 1 and case 3. Here, $G_{m\alpha}$ is defined by (25). In cases 2 and 4, the integration with respect to t' is done first. In cases 1 and 3, the integration with respect to ϕ is done first. In all cases,

$$\left.\begin{array}{l} G_{m1} \text{ is stored in } GmA(n-M1+1) \\ G_{m2} \text{ is stored in } GmB(n-M1+1) \\ G_{m3} \text{ is stored in } GmC(n-M1+1) \end{array}\right\} \begin{array}{l} m = 1,2,3 \\ n = M1, M1+1, \ldots M2 \end{array}$$

With regard to (41), DO loop 33 puts

$$\left.\begin{array}{lll} H_1(\phi_K) & \text{in} & GA(K) \\ H_2(\phi_K) & \text{in} & GB(K) \\ H_3(\phi_K) & \text{in} & GC(K) \end{array}\right\} \qquad K = 1,2,\ldots n_\phi$$

where ϕ_K is given by (37). Line 123 is based on (48). DO loop 35 accumulates the H's of (49) in H1A, H2A, and H3A. DO loop 37 accumulates in H1A, H2A, and H3A the sums on ℓ' in (44). If $kR \leq .5$, then the approximation

$$G - \frac{1}{(kR)^3} - \frac{1}{2kR} \approx - \frac{kR}{8}\left(1 - \frac{(kR)^2}{18} + \frac{(kR)^4}{720}\right) - \frac{j}{3}\left(1 - \frac{(kR)^2}{10} + \frac{(kR)^4}{280}\right) \qquad (89)$$

is invoked in order to avoid excessive roundoff error. Lines 152 to 174 put the I's of (47) in W1, W2, and W3. I_1 and I_3 are even in t_o and I_2 is odd in t_o. These three I's are first calculated with t_o replaced by $|t_o|$ and then the sign of I_2 is changed if t_o is negative.

In line 161, d^2 is compared to $10^{-5} r_{pq}^2$. If $d^2 \leq 10^{-5} r_{pq}^2$, then little confidence can be placed in the calculated value of d^2 because r_{pq}^2 and t_o^2 are very close to each other in (46b). If

$$\left.\begin{array}{l} d^2 \leq 10^{-5} r_{pq}^2 \\ |t_o| < \frac{1}{2}\Delta_q \end{array}\right\}$$

then statement 52 stops execution because an accurate value of I_1 can not be obtained. However, if

$$\left.\begin{array}{l} d^2 \leq 10^{-5} r_{pq}^2 \\ |t_o| \geq \frac{1}{2}\Delta_q \end{array}\right\}$$

then accurate calculation of I_1 may be possible. If $|t_o| - \frac{1}{2}\Delta_q$ is

appreciably greater than d^2, then the approximation

$$\left[\frac{w}{k^2 d^2 r}\right]_{|t_o| - \frac{1}{2}\Delta_q}^{|t_o| + \frac{1}{2}\Delta_q} \approx \frac{1}{2k^2}\left[\frac{1}{(|t_o| - \frac{1}{2}\Delta_q)^2} - \frac{1}{(|t_o| + \frac{1}{2}\Delta_q)^2}\right] \tag{90}$$

can be invoked. Line 163 puts the right-hand side of (90) in W4. Lines 166-169 calculate the logarithm term in (47a) according to

$$[\log(w+r)]_{w_1}^{w_2} = \begin{cases} \log\left[\dfrac{(w_2 + r_2)}{(w_1 + r_1)}\right] & , \quad w_1 \geq 0 \\[2ex] \log\left[\dfrac{(w_2 + r_2)(-w_1 + r_1)}{d^2}\right], & w_1 < 0 \end{cases} \tag{91}$$

where

$$\left.\begin{aligned} w_1 &= |t_o| - \frac{1}{2}\Delta_q \\ w_2 &= |t_o| + \frac{1}{2}\Delta_q \\ r_1 &= \sqrt{w_1^2 + d^2} \\ r_2 &= \sqrt{w_2^2 + d^2} \end{aligned}\right\} \tag{92}$$

This logarithm is stored in W.

Nested DO loops 45 and 46 calculate (50) for n = M1 + M-1 where M is the index of DO loop 45. The index K of DO loop 46 obtains ℓ in (50). With regard to (68a), lines 222-228 put

$$\frac{-\pi}{2k^3\rho_q^3} \sum_{\ell=1}^{n_\phi} \frac{A_\ell^{(n_\phi)}}{\sqrt{\phi_\ell^2 + (\frac{\Delta_q}{2\rho_q})^2}} + \frac{1}{k^3\rho_q^3} \log\left[\frac{2\rho_q\pi}{\Delta_q} + \sqrt{1 + (\frac{2\rho_q\pi}{\Delta_q})^2}\right]$$

in D8. DO loop 67 adds D8 to G_{11}. DO loop 67 also sets G_{21}, G_{22}, G_{23}, and G_{31} equal to zero. These four G's are set equal to zero when p = q

because the exact values of the coefficients by which they are multiplied in (24) are zero then.

The index L of DO loop 13 obtains ℓ' in (35). With regard to (36), DO loop 17 puts $G(u,\phi_K)$ in GA(K). If (59) is not true, line 258 sends execution to statement 51. Lines 259-277 calculate the terms in (57) which do not involve $G(u, \phi_\ell)$. DO loop 62 accumulates

$$\sum_{\ell=1}^{n_\phi} \frac{A_\ell^{(n_\phi)} \phi_\ell^2}{k^3 a_\ell^3} \quad \text{in D6}$$

and

$$\sum_{\ell=1}^{n_\phi} A_\ell^{(n_\phi)} \left(\frac{1}{k^3 a_\ell^3} + \frac{1}{2ka_\ell} + \frac{\rho_p \rho' \phi_\ell^4}{8k^3 a_\ell^5}\right) \quad \text{in D7.}$$

Line 275 puts the coefficient of n in (57c) in D8. Line 276 puts the portion of (57a) which does not involve $G(u,\phi_\ell)$ in D6. Line 277 puts in D7 the portion of (57b) which involves neither $G(u,\phi_\ell)$ nor $(n^2 + 1)$. DO loop 32 accumulates G_1, G_2, and G_3 of (36) in H1A, H2A, and H3A, respectively. The index M of outer DO loop 30 obtains $n = M + M1-1$. If (59) is true, lines 295-297 add to H1A, H2A, and H3A the terms in (57) which are not present in (36). Lines 298-306 do the sums with respect to ℓ' in (35).

Lines 309-385 use the previously calculated $G_{m\alpha}$ to obtain the contributions (23) and (24) to the elements of the moment matrices Y_n. The index M of DO loop 31 obtains $n = M + M1-1$. With regard to lines 348-355, the subscripts K1 to K8 for Y are the same as the subscripts K1 to K8 for Z in Table 2 on page 50 of [1]. The variables UA, UG, UB, UH, and UF incremented for $p = q$ in lines 338-342 are intended for Y(K1), Y(K2), Y(K3), Y(K4), and Y(K8 + MT), respectively. Y(K8 + MT) is reserved for $(Y_n^{\phi\phi})_{pq}$ of (24d).

```
C     LISTING OF THE SUBROUTINE YMAT
C     THE SUBROUTINE YMAT CALLS THE FUNCTION BLOG
      SUBROUTINE YMAT(M1,M2,NP,NPHI,NT,IN,RH,ZH,X,A,XT,AT,Y)
      COMPLEX Y(1600),U,H1A,H2A,H3A,GA(48),GB(48),GC(48),H1B,H2B,H3B
      COMPLEX H1C,H2C,H3C,UA,UB,UC,UD,UE,UF,G1A(10),G2A(10),G3A(10)
      COMPLEX G1B(10),G2B(10),G3B(10),G1C(10),G2C(10),G3C(10),CMPLX
      COMPLEX UG,UH
      DIMENSION RH(43),ZH(43),X(48),A(48),XT(10),AT(10),RS(42),ZS(42)
      DIMENSION D(42),DR(42),DZ(42),C2(48),C3(48),C4(200),C5(200)
      DIMENSION C6(200),R2(10),Z2(10),R7(10),Z7(10)
      CT=2.
      CP=.1
      DO 10 I=2,NP
      I2=I-1
      RS(I2)=.5*(RH(I)+RH(I2))
      ZS(I2)=.5*(ZH(I)+ZH(I2))
      D1=.5*(RH(I)-RH(I2))
      D2=.5*(ZH(I)-ZH(I2))
      D(I2)=SQRT(D1*D1+D2*D2)
      DR(I2)=D1
      DZ(I2)=D2
   10 CONTINUE
      M3=M2-M1+1
      M4=M1-1
      PI2=1.570796
      PP=9.869604
      DO 11 K=1,NPHI
      PH=PI2*(X(K)+1.)
      C2(K)=PH*PH
      SN=SIN(.5*PH)
      C3(K)=4.*SN*SN
      A1=PI2*A(K)
      D4=.5*A1*C3(K)
      D5=A1*COS(PH)
      D6=A1*SIN(PH)
      M5=K
      DO 29 M=1,M3
      PHM=(M4+M)*PH
      A2=COS(PHM)
      C4(M5)=D4*A2
      C5(M5)=D5*A2
      C6(M5)=D6*SIN(PHM)
      M5=M5+NPHI
   29 CONTINUE
   11 CONTINUE
      PN1=.7853982*IN
      PN2=8.*PN1
      U=(0.,1.)
      MP=NP-1
      MT=MP-1
      N=MT+MP
      N2N=MT*N
      N2=N*N
      JN=-1-N
      DO 15 JQ=1,MP
      KQ=2
      IF(JQ.EQ.1) KQ=1
      IF(JQ.EQ.MP) KQ=3
      R1=RS(JQ)
      Z1=ZS(JQ)
```

```
      D1=D(JQ)
      D2=DR(JQ)
      D3=DZ(JQ)
      D4=D2/R1
      D5=D1/R1
      SV=D2/D1
      CV=D3/D1
      P1=PN1*D1
      P2=PN2*D5
      P3=2.*D1
      P4=2.*D4
      P5=D4*D4
      P6=D1*D1
      P7=P6*D1
      T6=CT*D1
      T62=T6+D1
      T62=T62*T62
      R6=CP*R1
      R62=R6*R6
      P1A=0.
      P1B=0.
      P1C=0.
      DO 12 L=1,NT
      D6=XT(L)
      R2(L)=R1+D2*D6
      Z2(L)=Z1+D3*D6
      D7=P1*AT(L)/R2(L)
      D8=1.-D6
      D9=D8*D7
      P1A=P1A+D8*D9
      D6=1.+D6
      P1B=P1B+D6*D9
      P1C=P1C+D6*D6*D7
   12 CONTINUE
      DO 16 IP=1,MP
      R3=RS(IP)
      Z3=ZS(IP)
      R4=R1-R3
      Z4=Z1-Z3
      DO 40 L=1,NT
      D7=R2(L)-R3
      D8=Z2(L)-Z3
      R7(L)=R3*R2(L)
      Z7(L)=D7*D7+D8*D8
   40 CONTINUE
      PH=R4*SV+Z4*CV
      A1=ABS(PH)
      A2=ABS(R4*CV-Z4*SV)
      D6=A2
      IF(A1.LE.D1) GO TO 26
      D6=A1-D1
      D6=SQRT(D6*D6+A2*A2)
   26 IF(IP.NE.JQ.AND.(R6.GT.D6.OR.T6.LE.D6)) GO TO 41
      Z5=R4*R4+Z4*Z4
      R5=R3*R1
      PHM=.5*R3*SV
      DO 33 K=1,NPHI
      A1=C3(K)
      RR=Z5+R5*A1
      H1A=0.
```

```
      H2A=0.
      H3A=0.
      IF(RR.LT.T62) GO TO 34
      DO 35 L=1,NT
      W=Z7(L)+R7(L)*A1
      R=SQRT(W)
      SN=-SIN(R)
      CS=COS(R)
      H1B=AT(L)/(R*W)*CMPLX(CS-R*SN,SN+R*CS)
      H1A=H1B+H1A
      H2B=XT(L)*H1B
      H2A=H2B+H2A
      H3A=XT(L)*H2B+H3A
   35 CONTINUE
      GO TO 36
   34 DO 37 L=1,NT
      W=Z7(L)+R7(L)*A1
      R=SQRT(W)
      IF(R.GT..5) GO TO 14
      CS=R*(W*(.6944444E-2-W*.1736111E-3)-.125)
      SN=W*(.3333333E-1-W*.1190476E-2)-.3333333
      H1B=AT(L)*CMPLX(CS,SN)
      GO TO 43
   14 SN=-SIN(R)
      CS=COS(R)
      H1B=AT(L)/R*((CMPLX(CS-R*SN,SN+R*CS)-1.)/W-.5)
   43 H1A=H1B+H1A
      H2B=XT(L)*H1B
      H2A=H2B+H2A
      H3A=XT(L)*H2B+H3A
   37 CONTINUE
      A1=PH+PHM*A1
      A2=ABS(A1)
      R=RR-A2*A2
      D6=A2-D1
      D7=A2+D1
      D62=D6*D6
      D72=D7*D7
      D8=SQRT(D62+R)
      D9=SQRT(D72+R)
      IF(R-(RR*1.E-5)) 52,52,53
   52 IF(D6.LT.0.) STOP
      W4=.5/D62-.5/D72
      GO TO 54
   53 W4=(D7/D9-D6/D8)/R
   54 IF(D6.GE.0.) GO TO 38
      W=ALOG((D7+D9)*(-D6+D8)/R)
      GO TO 39
   38 W=ALOG((D7+D9)/(D6+D8))
   39 W1=(W4+.5*W)/D1
      W5=A2/D1
      W2=(.5*(D9-D8)-1./D9+1./D8)/P6-W5*W1
      W3=(.25*(D7*D9-D6*D8)+W-R*(W4+.25*W))/P7-W5*(2.*W2+W5*W1)
      IF(A1.LT.0.) W2=-W2
      H1A=W1+H1A
      H2A=W2+H2A
      H3A=W3+H3A
   36 GA(K)=H1A
      GB(K)=H2A
      GC(K)=H3A
```

```
   33 CONTINUE
      K1=0
      DO 45 M=1,M3
      H1A=0.
      H2A=0.
      H3A=0.
      H1B=0.
      H2B=0.
      H3B=0.
      H1C=0.
      H2C=0.
      H3C=0.
      DO 46 K=1,NPHI
      K1=K1+1
      D6=C4(K1)
      D7=C5(K1)
      D8=C6(K1)
      UA=GA(K)
      UB=GB(K)
      UC=GC(K)
      H1A=D6*UA+H1A
      H2A=D7*UA+H2A
      H3A=D8*UA+H3A
      H1B=D6*UB+H1B
      H2B=D7*UB+H2B
      H3B=D8*UB+H3B
      H1C=D6*UC+H1C
      H2C=D7*UC+H2C
      H3C=D8*UC+H3C
   46 CONTINUE
      G1A(M)=H1A
      G2A(M)=H2A
      G3A(M)=H3A
      G1B(M)=H1B
      G2B(M)=H2B
      G3B(M)=H3B
      G1C(M)=H1C
      G2C(M)=H2C
      G3C(M)=H3C
   45 CONTINUE
      IF(IP.NE.JQ) GO TO 47
      A1=D5*D5
      D8=0.
      DO 63 K=1,NPHI
      D8=D8+A(K)/SQRT(C2(K)+A1)
   63 CONTINUE
      A2=3.141593/D5
      D8=(ELOG(A2)-PI2*D8)/(R5*R1)
      DO 67 M=1,M3
      G1A(M)=D8+G1A(M)
      G2A(M)=0.
      G2B(M)=0.
      G2C(M)=0.
      G3A(M)=0.
   67 CONTINUE
      GO TO 47
   41 DO 25 M=1,M3
      G1A(M)=0.
      G2A(M)=0.
      G3A(M)=0.
```

```
      G1B(M)=0.
      G2B(M)=0.
      G3B(M)=0.
      G1C(M)=0.
      G2C(M)=0.
      G3C(M)=0.
   25 CONTINUE
      DO 13 L=1,NT
      R5=R7(L)
      Z5=Z7(L)
      DO 17 K=1,NPHI
      W=Z5+R5*C3(K)
      R=SQRT(W)
      SN=-SIN(R)
      CS=COS(R)
      GA(K)=CMPLX(CS-R*SN,SN+R*CS)/(W*R)
   17 CONTINUE
      IF(R62.LE.Z5) GO TO 51
      D6=0.
      D7=0.
      DO 62 K=1,NPHI
      W2=C2(K)
      W=1./(Z5+R5*W2)
      W1=A(K)*SQRT(W)
      D6=D6+W1*W2*W
      D7=D7+W1*(.5+W*(1.+.125*W*R5*W2*W2))
   62 CONTINUE
      W1=R5/Z5
      W2=PP*W1
      W=SQRT(W2)
      W3=1.+W2
      R=SQRT(W3)
      W4=SQRT(R5)
      W5=ALOG(W+R)
      D8=-PI2*D6-(W/R-W5)/(R5*W4)
      D6=.5*D8
      D7=((W/R*(W1-(.125+.1666667*W2)/W3)+.125*W5)/R5+.5*W5)/W4-PI2*D7
   51 A1=AT(L)
      A2=XT(L)*A1
      A3=XT(L)*A2
      K1=0
      DO 30 M=1,M3
      W=M+M4
      H1A=0.
      H2A=0.
      H3A=0.
      DO 32 K=1,NPHI
      K1=K1+1
      H1B=GA(K)
      H1A=C4(K1)*H1B+H1A
      H2A=C5(K1)*H1B+H2A
      H3A=C6(K1)*H1B+H3A
   32 CONTINUE
      IF(R62.LE.Z5) GO TO 44
      H1A=D6+H1A
      H2A=D7-(W*W+1.)*D6+H2A
      H3A=W*D8+H3A
   44 G1A(M)=A1*H1A+G1A(M)
      G2A(M)=A1*H2A+G2A(M)
      G3A(M)=A1*H3A+G3A(M)
```

```
      G1B(M)=A2*H1A+G1B(M)
      G2B(M)=A2*H2A+G2B(M)
      G3B(M)=A2*H3A+G3B(M)
      G1C(M)=A3*H1A+G1C(M)
      G2C(M)=A3*H2A+G2C(M)
      G3C(M)=A3*H3A+G3C(M)
   30 CONTINUE
   13 CONTINUE
   47 A2=D(IP)
      A3=.5*A2
      W1=A3*(R4*D3-Z4*D2)
      W2=-A3*R3*D3
      A3=DZ(IP)
      D6=DR(IP)
      D7=Z4*D6
      D9=D3*D6
      H1C=(R1*D9-D2*(R3*A3+D7))*U
      H3C=A2*D1*U
      H2C=Z4*H3C
      H3C=D3*H3C
      W3=P3*(R4*A3-D7)
      W4=P3*(D2*A3-D9)
      W5=P3*R1*A3
      JM=JN
      DO 31 M=1,M3
      H2A=G2A(M)
      H1A=G1A(M)
      H2B=G2B(M)
      H1B=G1B(M)
      UC=W1*H2A+W2*H1A
      UB=W1*H2B+W2*H1B
      UF=W3*(H2A+D4*H2B)+W4*(H2B+D4*G2C(M))+W5*(H1A+P4*H1B+P5*G1C(M))
      UA=UC-UB
      UB=UC+UB
      UG=UA
      UH=UB
      IF(IP.NE.JQ) GO TO 48
      UA=P1A+UA
      UG=P1B+UG
      UB=P1B+UB
      UH=P1C+UH
      UF=P2+UF
   48 H3A=G3A(M)
      H3B=G3B(M)
      UC=H1C*H3A
      UD=H1C*H3B
      UF=H2C*(H3A+D4*H3B)+H3C*(H3B+D4*G3C(M))
      K1=IP+JM
      K2=K1+1
      K3=K1+N
      K4=K2+N
      K5=K2+MT
      K6=K4+MT
      K7=K3+N2N
      K8=K4+N2N
      GO TO (18,20,19),KQ
   18 Y(K6)=UC+UD
      IF(IP.EQ.1) GO TO 21
      Y(K3)=Y(K3)+UB
      Y(K7)=Y(K7)+UE
      IF(IP.EQ.MP) GO TO 22
   21 Y(K4)=UH
      Y(K8)=UE
      GO TO 22
   19 Y(K5)=Y(K5)+UC-UD
      IF(IP.EQ.1) GO TO 23
      Y(K1)=Y(K1)+UA
      Y(K7)=Y(K7)+UE
      IF(IP.EQ.MP) GO TO 22
   23 Y(K2)=Y(K2)+UG
      Y(K8)=UE
      GO TO 22
   20 Y(K5)=Y(K5)+UC-UD
      Y(K6)=UC+UD
      IF(IP.EQ.1) GO TO 24
      Y(K1)=Y(K1)+UA
      Y(K3)=Y(K3)+UB
      Y(K7)=Y(K7)+UE
      IF(IP.EQ.MP) GO TO 22
   24 Y(K2)=Y(K2)+UG
      Y(K4)=UH
      Y(K8)=UE
   22 Y(K8+MT)=UF
      JM=JM+N2
   31 CONTINUE
   16 CONTINUE
      JN=JN+N
   15 CONTINUE
      RETURN
      END
```

III. THE FUNCTION BLOG

The function BLOG(x) calculates $\log(x + \sqrt{1 + x^2})$ for $x \geq 0$. The method of calculation is described on page 56 of [1].

```
C     LISTING OF THE FUNCTION BLOG
      FUNCTION BLOG(X)
      IF(X.GT..1) GO TO 1
      X2=X*X
      BLOG=((.075*X2-.1666667)*X2+1.)*X
      RETURN
    1 BLOG=ALOG(X+SQRT(1.+X*X))
      RETURN
      END
```

IV. THE SUBROUTINE PLANE

The subroutine PLANE(M1, M2, NF, NP, IN, NT, RH, ZH, XT, AT, THR, RE, R) obtains the plane wave excitation vectors (72)-(75). If IN $\neq$ 2, PLANE stores the plane wave excitation vectors (72) and (73) for the present H-field formulation in RE. If IN $\neq$ 1, PLANE stores $V_{ni}^{t\theta}$, $-V_{ni}^{\phi\theta}$, $-V_{ni}^{t\phi}$, and $V_{ni}^{\phi\phi}$ of (74) and (75) in R. The minus signs attached to $V_{ni}^{\phi\theta}$ and $V_{ni}^{t\phi}$ transform the V's into plane wave measurement vectors. Plane wave scattering calculations are not done in this report, but if they were done, plane wave measurement vectors would be required. $I_{ni}^{it\theta}$ is put in RE(i+(n-M1)*2*N+(K-1)*(M2-M1+1)*2*N) for

N = 2*NP-3

i = 1,2,...NP-2

n = M1, M1+1,...M2

K = 1,2,...NF

$I_{ni}^{i\phi\theta}$ is displaced forward NP-2 locations from $I_{ni}^{it\theta}$ in RE. For $I_{ni}^{i\phi\theta}$, i = 1,2,...NP-1. $I_{ni}^{it\phi}$ is displaced forward N locations from $I_{ni}^{it\theta}$. $I_{ni}^{i\phi\phi}$ is displaced forward N locations from $I_{ni}^{i\phi\theta}$. The angle of incidence θ_t of (71) is THR(K) radians and K = 1,2,...NF. The storage arrangement of $V_{ni}^{t\theta}$, $-V_{ni}^{\phi\theta}$, $-V_{ni}^{t\phi}$, and $V_{ni}^{\phi\phi}$ in R is the same as that of the I's in RE. The arguments RE and R of PLANE are output arguments. The rest of the arguments of PLANE are input arguments. Some of the input arguments obtain variables in Part One of the text. The correspondence is tabulated as

Input Argument	Text Variable	Equation Number
NP	P	9
NT	n_T	79
RH	$k\rho(\bar{t}_j)$, $j = 1,2,\ldots P$	21
ZH	$kz(\bar{t}_j)$, $j = 1,2,\ldots P$	21
XT	$x_\ell^{(n_T)}$, $\ell = 1,2,\ldots n_T$	79
AT	$A_\ell^{(n_T)}$, $\ell = 1,2,\ldots n_T$	79

Here, k is the propagation constant. Also, $\rho(\bar{t}_j)$ and $z(\bar{t}_j)$ are the values of ρ and z at the point $t = \bar{t}_j$ on the generating curve. This curve starts at $t = \bar{t}_1$ and ends at $t = \bar{t}_P$. It is assumed that P is not less than 3. The input arguments NT, XT, and AT are Gaussian quadrature data.

Minimum allocations are given by

```
COMPLEX RE(2*N*(M2-M1+1)*NF), R(2*N*(M2-M1+1)*NF),
    FA(M2+3), FB(M2+3)
DIMENSION RH(NP), ZH(NP), XT(NT), AT(NT), THR(NF),
    CS(NF), SN(NF), R2(NT), Z2(NT)
```

The I's and V's are calculated from (78) of the present report and (124)-(127) of [1]. The index IP of DO loop 12 obtains p in these equations. With regard to (79), DO loop 13 puts $\frac{1}{2}\,k\hat{\rho}_\ell$ and $k\hat{z}_\ell$ in R2 and Z2, respectively. The index K of DO loop 14 obtains the Kth angle of incidence. Nested DO loops 15 and 25 accumulate $S{*}F_{M-2,a}$ and $S{*}F_{M-2,b}$ in FA(M) and FB(M), respectively. Here, $F_{M-2,a}$ and $F_{M-2,b}$ are given by (79) and S is the normalizing constant for the Bessel functions. According to (9.1.46) on page 361 of [15],

$$S = J_o^u(x) + 2J_2^u(x) + 2J_4^u(x) + \ldots \tag{93}$$

where the superscript u means unnormalized, $J_m(x)$ are the cylindrical Bessel functions of the first kind and

$$x = k\hat{\rho}_\ell \sin \theta_t \tag{94}$$

The logic inside DO loop 15 is the same as that inside the DO loop 15 which appears in the listing of the subroutine PLANE on pages 61 and 62 of [1]. If M1 = 0, lines 88 and 89 use the formulas

$$\left.\begin{aligned} F_{-1,a} &= - F_{1a} \\ F_{-1,b} &= - F_{1b} \end{aligned}\right\} \tag{95}$$

to store $F_{-1,a}$ and $F_{-1,b}$ in FA(1) and FB(1), respectively.

The index M of DO loop 27 obtains n = M-2. In DO loop 27,

$I_{ni}^{*it\theta}$ is added to RE(K1) for i = p-1

$I_{ni}^{*it\theta}$ is put in RE(K2) for i = p

$I_{np}^{i\phi\theta}$ is put in RE(K3)

$I_{ni}^{*it\phi}$ is added to RE(K4) for i = p-1

$I_{ni}^{*it\phi}$ is put in RE(K5) for i = p

$I_{np}^{i\phi\phi}$ is put in RE(K6)

The above I's are given by (78). The V's are given by (124)-(127) of [1]. Location of these V's in R is similar to location of the I's in RE.

```
      LISTING OF THE SUBROUTINE PLANE
      SUBROUTINE PLANE(M1,M2,NF,NP,IN,NT,RH,ZH,XT,AT,THR,RE,R)
      COMPLEX RE(240),R(240),U,U1,FA(10),FB(10),UA,UB,F1A,F1B,F2A,F2B
      COMPLEX U2,U3,U4,U5,CMPLX
      DIMENSION RH(43),ZH(43),XT(10),AT(10),THR(3),CS(3),SN(3),R2(10)
      DIMENSION Z2(10),BJ(50)
      MP=NP-1
      MT=MP-1
      N=MT+MP
      N2=2*N
      DO 11 K=1,NF
      X=THR(K)
      CS(K)=COS(X)
      SN(K)=SIN(X)
   11 CONTINUE
      U=(0.,1.)
      U1=3.141593*U**M1
      M3=M1+1
      M4=M2+3
      IF(M1.EQ.0) M3=2
      M5=M1+2
      M6=M2+2
      DO 12 IP=1,MP
      K2=IP
      I=IP+1
      DR=.5*(RH(I)-RH(IP))
      DZ=.5*(ZH(I)-ZH(IP))
      D1=SQRT(DR*DR+DZ*DZ)
      R1=.25*(RH(I)+RH(IP))
      Z1=.5*(ZH(I)+ZH(IP))
      D2=.5*DR
      DR=D2/R1
      DO 13 L=1,NT
      R2(L)=R1+D2*XT(L)
      Z2(L)=Z1+DZ*XT(L)
   13 CONTINUE
      W1=-.5*D1
      W2=-2.*D2
      DO 14 K=1,NF
      CC=CS(K)
      SS=SN(K)
      D3=D2*CC
      D4=-DZ*SS
      D5=-D1*CC
      W3=-2.*D3
      W4=-2.*D4
      W5=-.5*D5
      DO 23 M=M3,M4
      FA(M)=0.
      FB(M)=0.
   23 CONTINUE
      DO 15 L=1,NT
      X=SS*R2(L)
      IF(X.GT..5E-7) GO TO 19
      DO 20 M=M3,M4
      BJ(M)=0.
   20 CONTINUE
      BJ(2)=1.
      S=1.
      GO TO 18
```

```
   19 M=2.8*X+14.-2./X
      IF(X.LT..5) M=11.8+ALOG10(X)
      IF(M.LT.M4) M=M4
      BJ(M)=0.
      JM=M-1
      BJ(JM)=1.
      DO 16 J=4,M
      J2=JM
      JM=JM-1
      J1=JM-1
      BJ(JM)=J1/X*BJ(J2)-BJ(JM+2)
   16 CONTINUE
      S=0.
      IF(M.LE.4) GO TO 24
      DO 17 J=4,M,2
      S=S+BJ(J)
   17 CONTINUE
   24 S=BJ(2)+2.*S
   18 ARG=Z2(L)*CC
      UA=AT(L)/S*CMPLX(COS(ARG),SIN(ARG))
      UB=XT(L)*UA
      DO 25 M=M3,M4
      FA(M)=BJ(M)*UA+FA(M)
      FB(M)=BJ(M)*UB+FB(M)
   25 CONTINUE
   15 CONTINUE
      IF(M1.NE.0) GO TO 26
      FA(1)=-FA(3)
      FB(1)=-FB(3)
   26 UA=U1
      DO 27 M=M5,M6
      M7=M-1
      M8=M+1
      F2A=UA*(FA(M8)+FA(M7))
      F2B=UA*(FB(M8)+FB(M7))
      UB=U*UA
      F1A=UB*(FA(M8)-FA(M7))
      F1B=UB*(FB(M8)-FB(M7))
      K1=K2-1
      K3=K2+MT
      K4=K1+N
      K5=K2+N
      K6=K3+N
      IF(IN.EQ.2) GO TO 28
      RE(K3)=W2*(F2A+DR*F2B)
      RE(K6)=W3*(F1A+DR*F1B)+W4*UA*(FA(M)+DR*FB(M))
      U2=W1*F1A
      U3=W1*F1B
      U4=W5*F2A
      U5=W5*F2B
      IF(IP.EQ.1) GO TO 21
      RE(K1)=RE(K1)+U2-U3
      RE(K4)=RE(K4)+U4-U5
      IF(IP.EQ.MP) GO TO 22
   21 RE(K2)=U2+U3
      RE(K5)=U4+U5
   22 IF(IN.EQ.1) GO TO 29
   28 R(K3)=D5*(F2A+DR*F2B)
      R(K6)=D1*(F1A+DR*F1B)
      U5=D4*UA
      U2=D3*F1A+U5*FA(M)
      U3=D3*F1B+U5*FB(M)
      U4=D2*F2A
      U5=D2*F2B
      IF(IP.EQ.1) GO TO 30
      R(K1)=R(K1)+U2-U3
      R(K4)=R(K4)+U4-U5
      IF(IP.EQ.MP) GO TO 29
   30 R(K2)=U2+U3
      R(K5)=U4+U5
   29 K2=K2+N2
      UA=UB
   27 CONTINUE
   14 CONTINUE
   12 CONTINUE
      RETURN
      END
```

V. THE SUBROUTINES DECOMP AND SOLVE

The subroutines DECOMP(N, IPS, UL) and SOLVE(N, IPS, UL, B, X) solve a system of N linear equations in N unknowns. The input to DECOMP consists of N and the N by N matrix of coefficients on the left-hand side of the matrix equation stored by columns in UL. The output from DECOMP is IPS and UL. This output is fed into SOLVE. The rest of the input to SOLVE consists of N and the column of coefficients on the right-hand side of the matrix equation stored in B. SOLVE puts the solution to the matrix equation in X.

Minimum allocations are given by

```
COMPLEX UL(N*N)
DIMENSION SCL(N), IPS(N)
```

in DECOMP and by

```
COMPLEX UL(N*N), B(N), X(N)
DIMENSION IPS(N)
```

in SOLVE.

More detail concerning DECOMP and SOLVE is on pages 46-49 of [16].

```
C     LISTING OF THE SUBROUTINES DECOMP AND SOLVE
      SUBROUTINE DECOMP(N,IPS,UL)
      COMPLEX UL(1600),PIVOT,EM
      DIMENSION SCL(40),IPS(40)
      DO 5 I=1,N
      IPS(I)=I
      RN=0.
      J1=I
      DO 2 J=1,N
      ULM=ABS(REAL(UL(J1)))+ABS(AIMAG(UL(J1)))
      J1=J1+N
      IF(RN-ULM) 1,2,2
    1 RN=ULM
    2 CONTINUE
      SCL(I)=1./RN
    5 CONTINUE
      NM1=N-1
      K2=0
      DO 17 K=1,NM1
      BIG=0.
      DO 11 I=K,N
      IP=IPS(I)
      IPK=IP+K2
      SIZE=(ABS(REAL(UL(IPK)))+ABS(AIMAG(UL(IPK))))*SCL(IP)
      IF(SIZE-BIG) 11,11,10
   10 BIG=SIZE
      IPV=I
   11 CONTINUE
      IF(IPV-K) 14,15,14
   14 J=IPS(K)
      IPS(K)=IPS(IPV)
      IPS(IPV)=J
   15 KPP=IPS(K)+K2
      PIVOT=UL(KPP)
      KP1=K+1
      DO 16 I=KP1,N
      KP=KPP
      IP=IPS(I)+K2
      EM=-UL(IP)/PIVOT
   18 UL(IP)=-EM
      DO 16 J=KP1,N
      IP=IP+N
      KP=KP+N
      UL(IP)=UL(IP)+EM*UL(KP)
   16 CONTINUE
      K2=K2+N
   17 CONTINUE
      RETURN
      END
      SUBROUTINE SOLVE(N,IPS,UL,B,X)
      COMPLEX UL(1600),B(40),X(40),SUM
      DIMENSION IPS(40)
      NP1=N+1
      IP=IPS(1)
      X(1)=B(IP)
      DO 2 I=2,N
      IP=IPS(I)
      IPB=IP
      IM1=I-1
      SUM=0.
      DO 1 J=1,IM1
      SUM=SUM+UL(IP)*X(J)
    1 IP=IP+N
    2 X(I)=B(IPB)-SUM
      K2=N*(N-1)
      IP=IPS(N)+K2
      X(N)=X(N)/UL(IP)
      DO 4 IBACK=2,N
      I=NP1-IBACK
      K2=K2-N
      IPI=IPS(I)+K2
      IP1=I+1
      SUM=0.
      IP=IPI
      DO 3 J=IP1,N
      IP=IP+N
    3 SUM=SUM+UL(IP)*X(J)
    4 X(I)=(X(I)-SUM)/UL(IPI)
      RETURN
      END
```

VI. THE MAIN PROGRAM FOR THE H-FIELD SOLUTION

The main program for the H-field solution calculates the H-field solution for the electric current induced on a conducting body of revolution immersed in an incident plane wave. Input data are read according to

```
      READ(1,15) NT, NPHI
15    FORMAT(2I3)
      READ(1,10)(XT(K), K = 1, NT)
      READ(1,10)(AT(K), K = 1, NT)
10    FORMAT(5E14.7)
      READ(1,10)(X(K), K = 1, NPHI)
      READ(1,10)(A(K), K = 1, NPHI)
      READ(1,16) NP, BK, THR(1)
16    FORMAT(I3, 2E14.7)
      READ(1,18)(RH(I), I = 1, NP)
      READ(1,18)(ZH(I), I = 1, NP)
18    FORMAT(10F8.4)
```

The input data obtain variables in Part One of the text. The input data are tabulated versus text variables in the following chart.

Input Data	Text Variable	Equation Number
NT	n_t	35
NPHI	n_ϕ	36
XT	$x_{\ell'}^{(n_t)}$, $\ell' = 1,2,\ldots n_t$	35
AT	$A_{\ell'}^{(n_t)}$, $\ell' = 1,2,\ldots n_t$	35
X	$x_{\ell}^{(n_\phi)}$, $\ell = 1,2,\ldots n_\phi$	37
A	$A_{\ell}^{(n_\phi)}$, $\ell = 1,2,\ldots n_\phi$	36
NP	P	3
BK	k	69
THR(1)	θ_t	71
RH	$\rho(\bar{t}_j)$, $j = 1,2,\ldots P$	21
ZH	$z(\bar{t}_j)$, $j = 1,2,\ldots P$	21

The Gaussian quadrature data $x_{\ell'}^{(n_t)}$, $A_{\ell'}^{(n_t)}$, $x_{\ell}^{(n_\phi)}$, and $A_{\ell}^{(n_\phi)}$ are given in Appendix A of [10]. In the main program for the H-field solution, n_T of (79) is set equal to n_t. NP controls the order of the moment matrix Y_1 of (86). This order is (2*NP-3). THR is in radians. THR should be either 0 or π depending on the direction from which the incident wave approaches. The subscript on THR is for compatibility with the subroutine PLANE. $\rho(\bar{t}_j)$ and $z(\bar{t}_j)$ are the values of ρ and z at the point $t = \bar{t}_j$ on the generating curve of the body of revolution. This curve starts at $t = \bar{t}_1$ and ends at $t = \bar{t}_P$. ρ is the distance from the axis of the body of revolution and z is the coordinate measured along this axis. RH and ZH are in meters.

The main program for the H field solution calls the subroutines YMAT, PLANE, DECOMP, and SOLVE. The function subprogram BLOG is also

needed because it is called by the subroutine YMAT.

Minimum allocations are given by

```
COMPLEX Y(N*N), R(2*N), C(N)
DIMENSION XT(NT), AT(NT), X(NPHI), A(NPHI),
    RH(NP), ZH(NP), IPS(N)
```

where

$$N = 2*NP-3$$

The t and ϕ components of the electric current are calculated from (84) and (85). The coefficients I_{1p}^{t} and I_{1p}^{ϕ} in these equations are the pth elements of the vectors $\vec{I}_1^{t}$ and $\vec{I}_1^{\phi}$ which satisfy the n = 1 equation in (10). DO loop 28 prepares RH and ZH for use in the subroutines YMAT and PLANE by multiplying them by k. With regard to (10) line 41 puts Y_1 of (86) in Y. Line 46 calculates IPS and changes Y. Line 47 puts the excitation vectors $\vec{I}_1^{it}$ and $\vec{I}_1^{i\phi}$ for the θ polarized incident plane wave (69) in R. Line 47 also stores the excitation vectors for the ϕ polarized incident plane wave (70) further on in R but these vectors are not used in the main program. In line 50, the output IPS and Y from the subroutine DECOMP is fed along with N and R into the subroutine SOLVE. SOLVE puts $\vec{I}_1^{t}$ and $\vec{I}_1^{\phi}$ in C.

The pth line printed out under the heading JT contains the real part, the imaginary part, and the magnitude of the normalized t component $(J_t)/|\underline{H}^i|$ of electric current at $\phi = 0°$ and $t = \bar{t}_{p+1}$. The pth line printed out under the heading JP contains the real part, the imaginary part, and the magnitude of the normalized ϕ component $(J_\phi)/|\underline{H}^i|$ of electric current at $\phi = 90°$ and $t = t_p$. According to (69b),

$$|\underline{H}^i| = -\underline{u}_\phi^t \cdot [\underline{H}^i]_{z=0}$$

where $[\underline{H}^i]_{z=0}$ is the incident magnetic field at z = 0. The sample input and output data are for the sphere example of Fig. 2. The input array ZH was constructed so that z = 0 at the center of the sphere.

```
C      LISTING OF THE MAIN PROGRAM FOR THE H-FIELD SOLUTION
C      THE SUBPROGRAMS YMAT,BLOG,PLANE,DECOMP, AND SOLVE ARE NEEDED
//PGM JOB (XXXX,XXXX,1,1),'MAUTZ,JOE',REGION=200K
// EXEC WATFIV
//GO.SYSIN DD *
$JOB            MAUTZ,TIME=5,PAGES=60
       COMPLEX Y(1600),R(240),C(40),U,C1
       DIMENSION XT(10),AT(10),X(48),A(48),RH(43),ZH(43),THR(3),IPS(40)
       READ(1,15) NT,NPHI
    15 FORMAT(2I3)
       WRITE(3,30) NT,NPHI
    30 FORMAT('  NT NPHI'/1X,I3,I5)
       READ(1,10)(XT(K),K=1,NT)
       READ(1,10)(AT(K),K=1,NT)
    10 FORMAT(5E14.7)
       WRITE(3,11)(XT(K),K=1,NT)
       WRITE(3,12)(AT(K),K=1,NT)
    11 FORMAT(' XT'/(1X,5E14.7))
    12 FORMAT(' AT'/(1X,5E14.7))
       READ(1,10)(X(K),K=1,NPHI)
       READ(1,10)(A(K),K=1,NPHI)
       WRITE(3,13)(X(K),K=1,NPHI)
       WRITE(3,14)(A(K),K=1,NPHI)
    13 FORMAT(' X'/(1X,5E14.7))
    14 FORMAT(' A'/(1X,5E14.7))
       READ(1,16) NP,BK,THR(1)
    16 FORMAT(I3,2E14.7)
       WRITE(3,17) NP,BK,THR(1)
    17 FORMAT('  NP',6X,'BK',12X,'THR'/1X,I3,2E14.7)
       READ(1,18)(RH(I),I=1,NP)
       READ(1,18)(ZH(I),I=1,NP)
    18 FORMAT(10F8.4)
       WRITE(3,19)(RH(I),I=1,NP)
       WRITE(3,20)(ZH(I),I=1,NP)
    19 FORMAT(' RH'/(1X,10F8.4))
    20 FORMAT(' ZH'/(1X,10F8.4))
       DO 28 J=1,NP
       RH(J)=BK*RH(J)
       ZH(J)=BK*ZH(J)
    28 CONTINUE
       CALL YMAT(1,1,NP,NPHI,NT,1,RH,ZH,X,A,XT,AT,Y)
       MT=NP-2
       N=2*MT+1
       WRITE(3,29)(Y(J),J=1,N)
    29 FORMAT(' Y'/(1X,6E11.4))
       CALL DECOMP(N,IPS,Y)
       CALL PLANE(1,1,1,NP,1,NT,RH,ZH,XT,AT,THR,R,R)
       WRITE(3,23)(R(J),J=1,N)
    23 FORMAT(' R'/(1X,6E11.4))
       CALL SOLVE(N,IPS,Y,R,C)
       U=(0.,1.)
       WRITE(3,21)
    21 FORMAT('     REAL JT     IMAG JT      MAG JT')
       DO 24 J=1,MT
       C1=2./RH(J+1)*C(J)
       C2=CABS(C1)
       WRITE(3,25) C1,C2
    25 FORMAT(1X,3E11.4)
    24 CONTINUE
       WRITE(3,26)
```

```
   26 FORMAT('     REAL JP     IMAG JP      MAG JP')
      MP=NP-1
      DO 27 J=1,MP
      C1=4./(RH(J)+RH(J+1))*U*C(J+MT)
      C2=CABS(C1)
      WRITE(3,25) C1,C2
   27 CONTINUE
      STOP
      END
$DATA
  2 20
-0.5773503E+00 0.5773503E+00
 0.1000000E+01 0.1000000E+01
-0.9931286E+00-0.9639719E+00-0.9122344E+00-0.8391170E+00-0.7463319E+00
-0.6360537E+00-0.5108670E+00-0.3737061E+00-0.2277859E+00-0.7652652E-01
 0.7652652E-01 0.2277859E+00 0.3737061E+00 0.5108670E+00 0.6360537E+00
 0.7463319E+00 0.8391170E+00 0.9122344E+00 0.9639719E+00 0.9931286E+00
 0.1761401E-01 0.4060143E-01 0.6267205E-01 0.8327674E-01 0.1019301E+00
 0.1181945E+00 0.1316886E+00 0.1420961E+00 0.1491730E+00 0.1527534E+00
 0.1527534E+00 0.1491730E+00 0.1420961E+00 0.1316886E+00 0.1181945E+00
 0.1019301E+00 0.8327674E-01 0.6267205E-01 0.4060143E-01 0.1761401E-01
 16 0.1256637E+01 0.3141593E+01
  0.0000  0.2079  0.4067  0.5878  0.7431  0.8660  0.9511  0.9945  0.9945  0.9511
  0.8660  0.7431  0.5878  0.4067  0.2079  0.0000
 -1.0000 -0.9781 -0.9135 -0.8090 -0.6691 -0.5000 -0.3090 -0.1045  0.1045  0.3090
  0.5000  0.6691  0.8090  0.9135  0.9871  1.0000
$STOP
/*
//
PRINTED OUTPUT
 NT NPHI
  2   20
XT
-0.5773503E+00 0.5773503E+00
AT
 0.1000000E+01 0.1000000E+01
X
-0.9931286E+00-0.9639719E+00-0.9122344 [illegible]-0.8391170E+00-0.7463319E+00
-0.6360537E+00-0.5108670E+00-0.3737061[illegible].2277859E+00-0.7652652E-01
 0.7652652E-01 0.2277859E+00 0.3737061E+0[illegible].5108670E+00 0.6360537E+00
 0.7463319E+00 0.8391170E+00 0.9122344E+00 0.9639719E+00 0.9931286E+00
A
 0.1761401E-01 0.4060143E-01 0.6267208E-01 0.8327675E-01 0.1019301E+00
 0.1181945E+00 0.1316886E+00 0.1420961E+00 0.1491730E+00 0.1527534E+00
 0.1527534E+00 0.1491730E+00 0.1420961E+00 0.1316886E+00 0.1181945E+00
 0.1019301E+00 0.8327675E-01 0.6267208E-01 0.4060143E-01 0.1761401E-01
 NP      BK            THR
 16 0.1256637E+01 0.3141593E+01
RH
  0.0000  0.2079  0.4067  0.5878  0.7431  0.8660  0.9511  0.9945  0.9945  0.9511
  0.8660  0.7431  0.5878  0.4067  0.2079  0.0000
ZH
 -1.0000 -0.9781 -0.9135 -0.8090 -0.6691 -0.5000 -0.3090 -0.1045  0.1045  0.3090
  0.5000  0.6691  0.8090  0.9135  0.9871  1.0000
Y
 0.2486E+01-0.2338E-02 0.4211E+00-0.4919E-02 0.6397E-01-0.8888E-02
 0.5598E-01-0.1382E-01 0.4988E-01-0.1923E-01 0.4455E-01-0.2463E-01
 0.3941E-01-0.2964E-01 0.3432E-01-0.3398E-01 0.2937E-01-0.3752E-01
 0.2475E-01-0.4023E-01 0.2065E-01-0.4217E-01 0.1728E-01-0.4348E-01
 0.1475E-01-0.4458E-01 0.1306E-01-0.4490E-01 0.9666E-03 0.9243E-01
```

```
-0.9622E-03-0.5803E-01-0.4589E-02-0.6791E-01-0.9512E-02-0.5939E-01
-0.1517E-01-0.5297E-01-0.2105E-01-0.4766E-01-0.2668E-01-0.4258E-01
-0.3164E-01-0.3741E-01-0.3578E-01-0.3226E-01-0.3903E-01-0.2732E-01
-0.4137E-01-0.2279E-01-0.4297E-01-0.1891E-01-0.4402E-01-0.1588E-01
-0.4484E-01-0.1362E-01-0.4470E-01-0.1244E-01
R
-0.2834E+00-0.7748E+00-0.3446E+00-0.7491E+00-0.4386E+00-0.6972E+00
-0.5523E+00-0.6097E+00-0.6671E+00-0.4800E+00-0.7609E+00-0.3088E+00
-0.8136E+00-0.1067E+00-0.8136E+00 0.1067E+00-0.7609E+00 0.3088E+00
-0.6671E+00 0.4800E+00-0.5523E+00 0.6097E+00-0.4386E+00 0.6972E+00
-0.3454E+00 0.7550E+00-0.2791E+00 0.7810E+00 0.7758E+00-0.2679E+00
 0.7267E+00-0.2959E+00 0.6295E+00-0.3378E+00 0.4891E+00-0.3684E+00
 0.3236E+00-0.3603E+00 0.1626E+00-0.2931E+00 0.4374E-01-0.1652E+00
 0.0000E+00 0.0000E+00 0.4374E-01 0.1652E+00 0.1626E+00 0.2931E+00
 0.3236E+00 0.3603E+00 0.4891E+00 0.3684E+00 0.6295E+00 0.3378E+00
 0.7281E+00 0.2922E+00 0.7778E+00 0.2620E+00
   REAL JT     IMAG JT      MAG JT
-0.7989E+00-0.1959E+01 0.2115E+01
-0.9480E+00-0.1930E+01 0.2151E+01
-0.1162E+01-0.1836E+01 0.2173E+01
-0.1406E+01-0.1658E+01 0.2175E+01
-0.1630E+01-0.1372E+01 0.2130E+01
-0.1764E+01-0.9802E+00 0.2018E+01
-0.1754E+01-0.5127E+00 0.1827E+01
-0.1569E+01-0.2428E-01 0.1569E+01
-0.1218E+01 0.4228E+00 0.1289E+01
-0.7475E+00 0.7772E+00 0.1078E+01
-0.2294E+00 0.1016E+01 0.1042E+01
 0.2592E+00 0.1146E+01 0.1174E+01
 0.6569E+00 0.1210E+01 0.1377E+01
 0.9016E+00 0.1190E+01 0.1493E+01
   REAL JP     IMAG JP      MAG JP
 0.7731E+00 0.1878E+01 0.2031E+01
 0.8555E+00 0.1782E+01 0.1976E+01
 0.9995E+00 0.1602E+01 0.1888E+01
 0.1148E+01 0.1333E+01 0.1759E+01
 0.1240E+01 0.9997E+00 0.1593E+01
 0.1229E+01 0.6569E+00 0.1394E+01
 0.1106E+01 0.3761E+00 0.1168E+01
 0.9065E+00 0.2217E+00 0.9332E+00
 0.7010E+00 0.2213E+00 0.7351E+00
 0.5589E+00 0.3543E+00 0.6618E+00
 0.5201E+00 0.5631E+00 0.7665E+00
 0.5789E+00 0.7809E+00 0.9721E+00
 0.6903E+00 0.9538E+00 0.1177E+01
 0.8141E+00 0.1078E+01 0.1351E+01
 0.8998E+00 0.1148E+01 0.1459E+01
```

VII. THE SUBROUTINE YZ

With regard to (10), the subroutine YZ(M1, M2, NP, NPHI, NT, IN, RH, ZH, X, A, XT, AT, Y, Z) puts in Y the moment matrices Y_n defined by (86). With regard to (6) of [1], the subroutine YZ puts in Z the moment matrices Z_n defined by

$$Z_n = \begin{bmatrix} Z_n^{tt} & Z_n^{t\phi} \\ & \\ Z_n^{\phi t} & Z_n^{\phi\phi} \end{bmatrix}, \quad n = M1, M1+1, \ldots M2 \qquad (96)$$

The Y obtained by YZ is exactly the same as the Y obtained by the subroutine YMAT which is described and listed in Section II of Part Two. The storage arrangement of the elements of Z_n in Z is the same as the arrangement of the elements of Y_n in Y. The Z obtained by YZ is nearly the same as the Z obtained by ZMAT of [1]. The greatest difference in calculation is that, in accord with (68a), the second sum with respect to ℓ' in (97) of [1] is replaced by the exact value of the corresponding integral with respect to t'. The purpose of the subroutine YZ is to obtain Y and Z more efficiently than by means of YMAT of the present report and ZMAT of [1]. Increased efficiency is possible because several calculations done in YMAT of the present report are repeated in ZMAT of [1].

The only output arguments of YZ are Y and Z. The rest of the arguments of YZ are input arguments. The input arguments of YZ have the same names and meanings as the input arguments of YMAT. Lines 13 and 14 put c_t and c_ϕ of (31) in CT and CP, respectively. The subroutine YZ calls the function BLOG which is described and listed in Section III of Part Two.

Minimum allocations are given by

```
COMPLEX Y(M3*N*N), Z(M3*N*N), GA(NPHI), GB(NPHI),
    GC(NPHI), GD(NPHI), GE(NPHI), G1A(M3), G2A(M3),
    G3A(M3), G1B(M3), G2B(M3), G3B(M3), G1C(M3),
    G2C(M3), G3C(M3), G4A(M3), G5A(M3), G6A(M3)
    G4B(M3), G5B(M3), G6B(M3)
```

```
DIMENSION RH(NP), ZH(NP), X(NPHI), A(NPHI), XT(NT)
     AT(NT), RS(NP-1), ZS(NP-1), D(NP-1), DR(NP-1)
     DZ(NP-1), DM(NP-1), C1(NPHI), C2(NPHI), C3(NPHI)
     C4(M3*NPHI), C5(M3*NPHI), C6(M3*NPHI), R2(NT),
     Z2(NT), R7(NT), Z7(NT)
```

Here, N and M3 are given by (87) and (88), respectively.

The elements of Y_n are calculated from (23) and (24) with $G_{m\alpha}$ evaluated as in Section III of Part One. The elements of Z_n are calculated from (48)-(51) of [1]. DO loop 11 puts ϕ_ℓ in C1, ϕ_ℓ^2 in C2, and $4 \sin^2(\frac{1}{2}\phi_\ell)$ in C3. ϕ_ℓ is given by (37) and $4 \sin^2(\frac{1}{2}\phi_\ell)$ is needed in order to evaluate (15) at $\phi = \phi_\ell$. With regard to (36), inner DO loop 29 puts

$$\pi A_\ell^{(n_\phi)} \sin^2(\tfrac{1}{2}\phi_\ell) \cos(n\phi_\ell) \quad \text{in C4,}$$

$$\frac{\pi}{2} A_\ell^{(n_\phi)} \cos\phi_\ell \cos(n\phi_\ell) \quad \text{in C5,}$$

and

$$\frac{\pi}{2} A_\ell^{(n_\phi)} \sin\phi_\ell \sin(n\phi_\ell) \quad \text{in C6.}$$

The index JQ of DO loop 15 obtains q in (23) and (24) of the present report and in (48)-(51) of [1]. With regard to (22d), line 75 puts $(IN)*(\pi\Delta_q)/\rho_q$ in P2. DO loop 12 puts $k\rho'$ and kz' of (29) in R2 and Z2, respectively. DO loop 12 also accumulates the products of IN with (23a), (23b), and (23c) in P1A, P1B, and P1C, respectively. The index IP of DO loop 16 obtains p in (24) of the present report and in (48)-(51) of [1]. Lines 114-120 put kd_o of (32) in D6. If either case 1 of (30) or case 3 of (51) is obtained, branch statement 26 sends execution to statement 41. If either case 2 of (39) or case 4 of (60) is obtained, execution proceeds to line 122. Lines 122-288 calculate $G_{m\alpha}$ for case 2 and case 4. Lines 290-388 calculate $G_{m\alpha}$ for case 1 and case 3. In cases 2 and 4, the integration with respect to t' is done first. In cases 1 and 3, the integration with respect to ϕ is done first. In all cases,

$$\left.\begin{array}{l} G_{m1} \text{ is stored in GmA(n - M1+1)} \\ G_{m2} \text{ is stored in GmB(n - M1+1)} \\ G_{m3} \text{ is stored in GmC(n - M1+1)} \end{array}\right\} \quad \begin{array}{l} m = 1,2,3 \\ n = M1,\ M1+1,\ldots M2 \end{array} \tag{97}$$

$$\left.\begin{array}{l} G_{ma} \text{ is stored in GmA(n - M1+1)} \\ G_{mb} \text{ is stored in GmB(n - M1+1)} \end{array}\right\} \quad \begin{array}{l} m = 4,5,6 \\ n = M1,\ M1+1,\ldots M2 \end{array} \tag{98}$$

The G's in (97) are defined by (25). The G's in (98) are defined by (56)-(57) of [1].

With regard to (41), DO loop 33 puts

$$\left.\begin{array}{l} H_1(\phi_K) \text{ in GA(K)} \\ H_2(\phi_K) \text{ in GB(K)} \\ H_3(\phi_K) \text{ in GC(K)} \end{array}\right\} \quad K = 1,2,\ldots n_\phi$$

DO loop 33 also evaluates G_a and G_b of (71)-(72) of [1] at $\phi = \phi_K$ and puts them in GD(K) and GE(K), respectively. The branch statement in line 133 is based on (48). DO loop 35 uses (49) to calculate $H_\alpha(\phi_K)$ of (41). The index L of DO loop 35 obtains ℓ' in (49). DO loop 35 uses the Gaussian quadrature formulas

$$G_a = \sum_{\ell'=1}^{n_t} A_{\ell'}^{(n_t)} \frac{e^{-jkR}}{kR} \tag{99a}$$

$$G_b = \sum_{\ell'=1}^{n_t} A_{\ell'}^{(n_t)} x_{\ell'}^{(n_t)} \frac{e^{-jkR}}{kR} \tag{99b}$$

to calculate G_a and G_b of (71)-(72) of [1]. In (99),

$$R = \sqrt{(\rho'-\rho_p)^2 + (z'-z_p)^2 + 4\rho_p\rho'\sin^2(\frac{1}{2}\phi_K)} \tag{100}$$

where

$$\rho' = \rho_q + \frac{\Delta_q x_{\ell'}^{(n_t)} \sin v_q}{2} \tag{101a}$$

$$z' = z_q + \frac{x_{\ell'}^{(n_t)} \Delta_q \cos v_q}{2} \tag{101b}$$

DO loop 35 accumulates $H_1(\phi_K)$, $H_2(\phi_K)$, $H_3(\phi_K)$, G_a, and G_b in H1A, H2A, H3A, H4A, and H5A, respectively. DO loop 37 accumulates the sum on ℓ' in (44) for α = 1, 2, and 3 in H1A, H2A, and H3A, respectively. DO loop 37 accumulates G_{a1} and G_{b1} of (79)-(80) of [1] in H4A and H5A, respectively. If $kR \leq .5$ where R is given by (100), then lines 154-159 use (89) and

$$\frac{e^{-jkR}-1}{kR} \approx kR(-\frac{1}{2} + \frac{(kR)^2}{24} - \frac{(kR)^4}{720}) + j(-1 + \frac{(kR)^2}{6} - \frac{(kR)^4}{120} + \frac{(kR)^6}{5040}) \tag{102}$$

in order to put

$$A_{\ell'}^{(n_t)} (G - \frac{1}{(kR)^3} - \frac{1}{2kR}) \quad \text{in H1B} \tag{103a}$$

and

$$A_{\ell'}^{(n_t)} (\frac{e^{-jkR}-1}{kR}) \quad \text{in H4B} \tag{103b}$$

If $kR > .5$, lines 161-165 calculate H1B and H4B directly from (103). Lines 173-199 put I_α of (47) for α = 1,2, and 3 in W1, W2, and W3, respectively. Lines 173-199 also put G_{a2} and G_{b2} of (87)-(88) of [1] in W4 and W5, respectively. I_1, I_3, and G_{a2} are even in t_o. I_2 and G_{b2} are odd in t_o. I_1, I_2, I_3, G_{a2}, and G_{b2} are calculated with t_o replaced by $|t_o|$ and then the signs of I_2 and G_{b2} are changed if t_o is negative. Line 173 puts kt_o in A1.

In line 182, d^2 is compared to $10^{-5} r_{pq}^2$. If $d^2 \leq 10^{-5} r_{pq}^2$, then little confidence can be placed in the calculated value of d^2 because r_{pq}^2 and t_o^2 are very close to each other in (46b). If

$$\left.\begin{array}{l} d^2 \leq 10^{-5} r_{pq}^2 \\ \\ |t_o| < \frac{1}{2}\Delta_q \end{array}\right\}$$

then statement 52 stops execution because an accurate value of I_1 can not be obtained. However, if

$$\left.\begin{array}{l} d^2 \leq 10^{-5} r_{pq}^2 \\ \\ |t_o| \geq \frac{1}{2}\Delta_q \end{array}\right\}$$

then accurate calculation of I_1 may be possible. If $|t_o| - \frac{1}{2}\Delta_q$ is appreciably greater than d^2, then the approximation (90) can be invoked. Line 184 puts the right-hand side of (90) in W4. Lines 187-190 calculate the logarithm term in (47a) according to (91). This logarithm is stored in W.

Nested DO loops 45 and 46 calculate (50) for n = M1 + M-1 where M is the index of DO loop 45. The index K of DO loop 46 obtains ℓ in (50). Nested DO loops 45 and 46 also calculate (91)-(93) of [1] and (91)-(93) of [1] with a replaced by b. The results of these calculations are stored according to (97) and (98). With regard to (68a), lines 271-279 put

$$\frac{-\pi}{2k^3\rho_q^3} \sum_{\ell=1}^{n_\phi} \frac{A_\ell^{(n_\phi)}}{\sqrt{\phi_\ell^2 + \left(\frac{\Delta_q}{2\rho_q}\right)^2}} + \frac{1}{k^3\rho_q^3} \log\left[\frac{2\rho_q\pi}{\Delta_q} + \sqrt{1 + \left(\frac{2\rho_q\pi}{\Delta_q}\right)^2}\right]$$

in D8. Line 280 puts in D9 the term which is present in G_{5a} in case 4 but not present in case 2. Replacement of the second sum with respect

to ℓ' in (97) of [1] by the exact value of the corresponding integral with respect to t' and use of (99) of [1] give

$$G_{5a} = \frac{\pi}{2} \sum_{\ell=1}^{n_\phi} A_\ell^{(n_\phi)} \cos \phi_\ell \cos(n\phi_\ell) \sum_{\ell'=1}^{n_t} A_{\ell'}^{(n_t)} \frac{e^{-jkR_{p\ell'\ell}}}{kR_{p\ell'\ell}} + D9 \qquad (104)$$

where

$$D9 = -\frac{2\pi}{k\Delta_q} \sum_{\ell=1}^{n_\phi} A_\ell^{(n_\phi)} \log\left[\frac{\Delta_q}{2\rho_q\phi_\ell} + \sqrt{1 + \left(\frac{\Delta_q}{2\rho_q\phi_\ell}\right)^2}\right] + \frac{2}{k\rho_q}\left\{\log\left[\frac{2\pi\rho_q}{\Delta_q} + \sqrt{1 + \left(\frac{2\pi\rho_q}{\Delta_q}\right)^2}\right] + \frac{2\pi\rho_q}{\Delta_q} \log\left[\frac{\Delta_q}{2\pi\rho_q} + \sqrt{1 + \left(\frac{\Delta_q}{2\pi\rho_q}\right)^2}\right]\right\} \qquad (105)$$

Line 280 puts the right-hand side of (105) in D9. DO loop 67 adds D8 to G_{11} and D9 to G_{5a}. DO loop 67 also sets G_{21}, G_{22}, G_{23}, and G_{31} equal to zero. These four G's are set equal to zero when p=q because the exact values of the coefficients by which they are multiplied in (24) are zero then.

The index L of DO loop 13 obtains ℓ' in (35) and in (62)-(63) of [1]. With regard to (36), DO loop 17 puts $G(u,\phi_K)$ in GA(K). With regard to (64)-(66) of [1], DO loop 17 puts $(e^{-jkR_{p\ell'\ell}})/(kR_{p\ell'\ell})$ in GD(K). If (59) is not true, line 318 sends execution to statement 51. Lines 319-340 calculate the terms in (57) which do not involve $G(u,\phi_\ell)$ and the terms in (94) of [1] which do not involve $(e^{-jkR_{p\ell'\ell}})/(kR_{p\ell'\ell})$. DO loop 62 accumulates

$$\sum_{\ell=1}^{n_\phi} \frac{A_\ell^{(n_\phi)} \phi_\ell^2}{k^3 a_\ell^3} \quad \text{in D6,}$$

$$\sum_{\ell=1}^{n_\phi} A_\ell^{(n_\phi)} \left(\frac{1}{k^3 a_\ell^3} + \frac{1}{2ka_\ell} + \frac{\rho_p \rho' \phi_\ell^4}{8k^3 a_\ell^5}\right) \quad \text{in D7,}$$

and

$$\sum_{\ell=1}^{n_\phi} \frac{A_\ell^{(n_\phi)}}{ka_\ell} \quad \text{in D9.}$$

Line 337 puts the coefficient of n in (57c) in D8. Line 338 puts the portion of (57a) which does not involve $G(u,\phi_\ell)$ in D6. Line 339 puts in D7 the portion of (57b) which involves neither $G(u,\phi_\ell)$ nor $(n^2 + 1)$. Line 340 puts in D9 the terms in (94) of [1] which do not involve $(e^{-jkR_{p\ell'\ell}})/(kR_{p\ell'\ell})$. DO loop 32 accumulates G_1, G_2, and G_3 of (36) in H1A, H2A, and H3A, respectively. DO loop 32 also accumulates G_4, G_5, and G_6 of (64)-(66) of [1] in H4A, H5A, and H6A, respectively. The index M of outer DO loop 30 obtains n = M + M1-1. If (59) is true, lines 368-370 add to H1A, H2A, and H3A the terms in (57) which are not present in (36) and line 371 adds to H5A the terms in (94) of [1] which are not present in (65) of [1]. Lines 372-380 do the sums with respect to ℓ' in (35). Lines 381-386 do the sums with respect to ℓ' in (62)-(63) of [1].

Lines 389-509 use the previously calculated G's of (97) and (98) to obtain the contributions (23) and (24) to the elements of the moment matrices Y_n and the contributions (48)-(51) of [1] to the moment matrices Z_n. The index M of DO loop 31 obtains n = M + M1-1. Lines 437-438 put G_{7a} and G_{7b} of (54)-(55) of [1] in H4A and H4B, respectively. The subscripts K1, K2,...K8 defined in lines 452-459 have the same meaning as in Table 2 on page 50 of [1]. The variables UA, UG, UB, UH, and UF incremented for p=q in lines 425-429 are intended for Y(K1), Y(K2), Y(K3), Y(K4), and Y(K9), respectively. Y(K9) is reserved for $(Y_n^{\phi\phi})_{pq}$ of (24d).

```
      LISTING OF THE SUBROUTINE YZ
      THE SUBROUTINE YZ CALLS THE FUNCTION BLOG
      SUBROUTINE YZ(M1,M2,NP,NPHI,NT,IN,RH,ZH,X,A,XT,AT,Y,Z)
      COMPLEX Y(1600),Z(1600),U,U1,U2,U3,U4,U5,U6,H1A,H2A,H3A,GA(48)
      COMPLEX GB(48),GC(48),GD(48),GE(48),H1B,H2B,H3B,H1C,H2C,H3C,H4A
      COMPLEX H5A,H6A,H4B,H5B,H6B,UA,UB,UC,UD,UE,UF,G1A(10),G2A(10)
      COMPLEX G3A(10),G1B(10),G2B(10),G3B(10),G1C(10),G2C(10),G3C(10)
      COMPLEX G4A(10),G5A(10),G6A(10),G4B(10),G5B(10),G6B(10),CMPLX
      COMPLEX UG,UH
      DIMENSION RH(43),ZH(43),X(48),A(48),XT(10),AT(10),RS(42),ZS(42)
      DIMENSION D(42),DR(42),DZ(42),DM(42),C1(48),C2(48),C3(48),C4(200)
      DIMENSION C5(200),C6(200),R2(10),Z2(10),R7(10),Z7(10)
      CT=2.
      CP=.1
      DO 10 I=2,NP
      I2=I-1
      RS(I2)=.5*(RH(I)+RH(I2))
      ZS(I2)=.5*(ZH(I)+ZH(I2))
      D1=.5*(RH(I)-RH(I2))
      D2=.5*(ZH(I)-ZH(I2))
      D(I2)=SQRT(D1*D1+D2*D2)
      DR(I2)=D1
      DZ(I2)=D2
      DM(I2)=D(I2)/RS(I2)
   10 CONTINUE
      M3=M2-M1+1
      M4=M1-1
      PI2=1.570796
      PP=9.869604
      DO 11 K=1,NPHI
      PH=PI2*(X(K)+ .)
      C1(K)=PH
      C2(K)=PH*PH
      SN=SIN(.5*PH)
      C3(K)=4.*SN*SN
      A1=PI2*A(K)
      D4=.5*A1*C3(K)
      D5=A1*COS(PH)
      D6=A1*SIN(PH)
      M5=K
      DO 29 M=1,M3
      PHM=(M4+M)*PH
      A2=COS(PHM)
      C4(M5)=D4*A2
      C5(M5)=D5*A2
      C6(M5)=D6*SIN(PHM)
      M5=M5+NPHI
   29 CONTINUE
   11 CONTINUE
      PN1=.7853982*IN
      PN2=8.*PN1
      U=(0.,1.)
      U1=.5*U
      U2=2.*U
      MP=NP-1
      MT=MP-1
      N=MT+MP
      N2N=MT*N
      N2=N*N
      JN=-1-N
```

```
      DO 15 JQ=1,MP
      KQ=2
      IF(JQ.EQ.1) KQ=1
      IF(JQ.EQ.MP) KQ=3
      R1=RS(JQ)
      Z1=ZS(JQ)
      D1=D(JQ)
      D2=DR(JQ)
      D3=DZ(JQ)
      D4=D2/R1
      D5=D1/R1
      SV=D2/D1
      CV=D3/D1
      P1=PN1*D1
      P2=PN2*D5
      P3=2.*D1
      P4=2.*D4
      P5=D4*D4
      P6=D1*D1
      P7=P5*D1
      T6=CT*D1
      T62=T6+D1
      T62=T62*T62
      R6=CP*R1
      R62=R6*R6
      P1A=0.
      P1B=0.
      P1C=0.
      DO 12 L=1,NT
      D6=XT(L)
      R2(L)=R1+D2*D6
      Z2(L)=Z1+D3*D6
      D7=P1*AT(L)/R2(L)
      D8=1.-D6
      D9=D8*D7
      P1A=P1A+D8*D9
      D6=1.+D6
      P1B=P1B+D6*D9
      P1C=P1C+D6*D6*D7
   12 CONTINUE
      DO 16 IP=1,MP
      R3=RS(IP)
      Z3=ZS(IP)
      R4=R1-R3
      Z4=Z1-Z3
      U3=D2*U1
      U4=D3*U1
      DO 40 L=1,NT
      D7=R2(L)-R3
      D8=Z2(L)-Z3
      R7(L)=R3*R2(L)
      Z7(L)=D7*D7+D8*D8
   40 CONTINUE
      PH=R4*SV+Z4*CV
      A1=ABS(PH)
      A2=ABS(R4*CV-Z4*SV)
      D6=A2
      IF(A1.LE.D1) GO TO 26
      D6=A1-D1
      D6=SQRT(D6*D6+A2*A2)
```

```
   26 IF(IP.NE.JO.AND.(R6.GT.D6.OR.T6.LE.D6)) GO TO 41
      Z5=R4*R4+Z4*Z4
      R5=R3*R1
      PHM=.5*R3*SV
      DO 33 K=1,NPHI
      A1=C3(K)
      RR=Z5+R5*A1
      H1A=0.
      H2A=0.
      H3A=0.
      H4A=0.
      H5A=0.
      IF(RR.LT.T62) GO TO 34
      DO 35 L=1,NT
      W=Z7(L)+R7(L)*A1
      R=SQRT(W)
      SN=-SIN(R)
      CS=COS(R)
      D6=AT(L)/R
      H1B=D6/W*CMPLX(CS-R*SN,SN+R*CS)
      H1A=H1B+H1A
      H2B=XT(L)*H1B
      H2A=H2B+H2A
      H3A=XT(L)*H2B+H3A
      H4B=D6*CMPLX(CS,SN)
      H4A=H4B+H4A
      H5A=XT(L)*H4B+H5A
   35 CONTINUE
      GO TO 36
   34 DO 37 L=1,NT
      W=Z7(L)+R7(L)*A1
      R=SQRT(W)
      IF(R.GT..5) GO TO 14
      CS=R*(W*(.6944444E-2-W*.1736111E-3)-.125)
      SN=W*(.3333333E-1-W*.1190476E-2)-.3333333
      H1B=AT(L)*CMPLX(CS,SN)
      CS=R*(W*(.4166667E-1-.1388889E-2*W)-.5)
      SN=W*(W*(.1984126E-3*W-.8333333E-2)+.1666667)-1.
      H4B=AT(L)*CMPLX(CS,SN)
      GO TO 43
   14 SN=-SIN(R)
      CS=COS(R)
      D6=AT(L)/R
      H1B=D6*((CMPLX(CS-R*SN,SN+R*CS)-1.)/W-.5)
      H4B=D6*CMPLX(CS-1.,SN)
   43 H1A=H1B+H1A
      H2B=XT(L)*H1B
      H2A=H2B+H2A
      H3A=XT(L)*H2B+H3A
      H4A=H4B+H4A
      H5A=XT(L)*H4B+H5A
   37 CONTINUE
      A1=PH+PHM*A1
      A2=ABS(A1)
      R=RR-A2*A2
      D6=A2-D1
      D7=A2+D1
      D62=D6*D6
      D72=D7*D7
      D8=SQRT(D62+R)
```

```
      D9=SQRT(D72+R)
      IF(R-(RR*1.E-5)) 52,52,53
   52 IF(D6.LT.0.) STOP
      W4=.5/D62-.5/D72
      GO TO 54
   53 W4=(D7/D9-D6/D8)/R
   54 IF(D6.GE.0.) GO TO 38
      W=ALOG((D7+D9)*(-D6+D8)/R)
      GO TO 39
   38 W=ALOG((D7+D9)/(D6+D8))
   39 W1=(W4+.5*W)/D1
      W5=A2/D1
      W2=(.5*(D9-D8)-1./D9+1./D8)/P6-W5*W1
      W3=(.25*(D7*D9-D6*D8)+W-R*(W4+.25*W))/P7-W5*(2.*W2+W5*W1)
      W4=W/D1
      W5=(D9-D8-A2*W)/P6
      IF(A1.GE.0.) GO TO 27
      W2=-W2
      W5=-W5
   27 H1A=W1+H1A
      H2A=W2+H2A
      H3A=W3+H3A
      H4A=W4+H4A
      H5A=W5+H5A
   36 GA(K)=H1A
      GB(K)=H2A
      GC(K)=H3A
      GD(K)=H4A
      GE(K)=H5A
   33 CONTINUE
      K1=0
      DO 45 M=1,M3
      H1A=0.
      H2A=0.
      H3A=0.
      H1B=0.
      H2B=0.
      H3B=0.
      H1C=0.
      H2C=0.
      H3C=0.
      H4A=0.
      H5A=0.
      H6A=0.
      H4B=0.
      H5B=0.
      H6B=0.
      DO 46 K=1,NPHI
      K1=K1+1
      D6=C4(K1)
      D7=C5(K1)
      D8=C6(K1)
      UA=GA(K)
      UB=GB(K)
      UC=GC(K)
      UD=GD(K)
      UE=GE(K)
      H1A=D6*UA+H1A
      H2A=D7*UA+H2A
      H3A=D8*UA+H3A
```

```
      H1B=D6*UB+H1B
      H2B=D7*UB+H2B
      H3B=D8*UB+H3B
      H1C=D6*UC+H1C
      H2C=D7*UC+H2C
      H3C=D8*UC+H3C
      H4A=D6*UD+H4A
      H5A=D7*UD+H5A
      H6A=D8*UD+H6A
      H4B=D6*UE+H4B
      H5B=D7*UE+H5B
      H6B=D8*UE+H6B
   46 CONTINUE
      G1A(M)=H1A
      G2A(M)=H2A
      G3A(M)=H3A
      G1B(M)=H1B
      G2B(M)=H2B
      G3B(M)=H3B
      G1C(M)=H1C
      G2C(M)=H2C
      G3C(M)=H3C
      G4A(M)=H4A
      G5A(M)=H5A
      G6A(M)=H6A
      G4B(M)=H4B
      G5B(M)=H5B
      G6B(M)=H6B
   45 CONTINUE
      IF(IP.NE.JQ) GO TO 47
      A1=D5*D5
      D8=0.
      D9=0.
      DO 63 K=1,NPHI
      D8=D8+A(K)/SQRT(C2(K)+A1)
      D9=D9+A(K)*BLOG(D5/C1(K))
   63 CONTINUE
      A2=3.141593/D5
      D8=(BLOG(A2)-PI2*D8)/(R5*R1)
      D9=2./R1*(BLOG(A2)+A2*BLOG(1./A2))-3.141593/D1*D9
      DO 67 M=1,M3
      G1A(M)=D8+G1A(M)
      G2A(M)=0.
      G2B(M)=0.
      G2C(M)=0.
      G3A(M)=0.
      G5A(M)=D9+G5A(M)
   67 CONTINUE
      GO TO 47
   41 DO 25 M=1,M3
      G1A(M)=0.
      G2A(M)=0.
      G3A(M)=0.
      G1B(M)=0.
      G2B(M)=0.
      G3B(M)=0.
      G1C(M)=0.
      G2C(M)=0.
      G3C(M)=0.
      G4A(M)=0.
```

```
      G5A(M)=0.
      G6A(M)=0.
      G4B(M)=0.
      G5B(M)=0.
      G6B(M)=0.
   25 CONTINUE
      DO 13 L=1,NT
      R5=R7(L)
      Z5=Z7(L)
      DO 17 K=1,NPHI
      W=Z5+R5*C3(K)
      R=SQRT(W)
      SN=-SIN(R)
      CS=COS(R)
      GA(K)=CMPLX(CS-R*SN,SN+R*CS)/(W*R)
      GD(K)=CMPLX(CS,SN)/R
   17 CONTINUE
      IF(R62.LE.Z5) GO TO 51
      D6=0.
      D7=0.
      D9=0.
      DO 62 K=1,NPHI
      W2=C2(K)
      W=1./(Z5+R5*W2)
      W1=A(K)*SQRT(W)
      D6=D6+W1*W2*W
      D7=D7+W1*(.5+W*(1.+.125*W*R5*W2*W2))
      D9=D9+W1
   62 CONTINUE
      W1=R5/Z5
      W2=PP*W1
      W=SQRT(W2)
      W3=1.+W2
      R=SQRT(W3)
      W4=SQRT(R5)
      W5=ALOG(W+R)
      D8=-PI2*D6-(W/R-W5)/(R5*W4)
      D6=.5*D8
      D7=((W/R*(W1-(.125+.1666667*W2)/W3)+.125*W5)/R5+.5*W5)/W4-PI2*D7
      D9=W5/W4-PI2*D9
   51 A1=AT(L)
      A2=XT(L)*A1
      A3=XT(L)*A2
      K1=0
      DO 30 M=1,M3
      W=M+M4
      H1A=0.
      H2A=0.
      H3A=0.
      H4A=0.
      H5A=0.
      H6A=0.
      DO 32 K=1,NPHI
      K1=K1+1
      H1B=GA(K)
      W4=C4(K1)
      W5=C5(K1)
      W6=C6(K1)
      H1A=W4*H1B+H1A
      H2A=W5*H1B+H2A
```

```
      H3A=W6*H1B+H3A
      H1B=GD(K)
      H4A=W4*H1B+H4A
      H5A=W5*H1B+H5A
      H6A=W6*H1B+H6A
   32 CONTINUE
      IF(R62.LE.Z5) GO TO 44
      H1A=D6+H1A
      H2A=D7-(W*W+1.)*D6+H2A
      H3A=W*D8+H3A
      H5A=D9+H5A
   44 G1A(M)=A1*H1A+G1A(M)
      G2A(M)=A1*H2A+G2A(M)
      G3A(M)=A1*H3A+G3A(M)
      G1B(M)=A2*H1A+G1B(M)
      G2B(M)=A2*H2A+G2B(M)
      G3B(M)=A2*H3A+G3B(M)
      G1C(M)=A3*H1A+G1C(M)
      G2C(M)=A3*H2A+G2C(M)
      G3C(M)=A3*H3A+G3C(M)
      G4A(M)=A1*H4A+G4A(M)
      G5A(M)=A1*H5A+G5A(M)
      G6A(M)=A1*H6A+G6A(M)
      G4B(M)=A2*H4A+G4B(M)
      G5B(M)=A2*H5A+G5B(M)
      G6B(M)=A2*H6A+G6B(M)
   30 CONTINUE
   13 CONTINUE
   47 A2=D(IP)
      A3=.5*A2
      W1=A3*(R4*D3-Z4*D2)
      W2=-A3*R3*D3
      A3=DZ(IP)
      D6=DR(IP)
      D7=Z4*D6
      D9=D3*D6
      H1C=(R1*D9-D2*(R3*A3+D7))*U
      D8=A2*D1
      H3C=D8*U
      H2C=Z4*H3C
      H3C=D3*H3C
      W3=P3*(R4*A3-D7)
      W4=P3*(D2*A3-D9)
      W5=P3*R1*A3
      A1=DR(IP)
      U5=A1*U3
      U6=A1*U4
      D6=-D2*A2
      D7=D1*A1
      A3=DM(IP)
      JM=JN
      DO 31 M=1,M3
      H2A=G2A(M)
      H1A=G1A(M)
      H2B=G2B(M)
      H1B=G1B(M)
      UC=W1*H2A+W2*H1A
      UB=W1*H2B+W2*H1B
      UF=W3*(H2A+D4*H2B)+W4*(H2B+D4*G2C(M))+W5*(H1A+P4*H1B+P5*G1C(M))
      UA=UC-UB
```

```
      UB=UC+UB
      UG=UA
      UH=UB
      IF(IP.NE.JC) GO TO 48
      UA=P1A+UA
      UG=P1B+UG
      UB=P1B+UB
      UH=P1C+UH
      UF=P2+UF
   48 H3A=G3A(M)
      H3B=G3B(M)
      UC=H1C*H3A
      UD=H1C*H3B
      UE=H2C*(H3A+D4*H3B)+H3C*(H3B+D4*G3C(M))
      H5A=G5A(M)
      H5B=G5B(M)
      H4A=G4A(M)+H5A
      H4B=G4B(M)+H5B
      H6A=G6A(M)
      H6B=G6B(M)
      H3A=U5*H5A+U6*H4A
      H1B=U5*H5B+U6*H4B
      H1A=H3A-H1B
      H2A=H3A+H1B
      H3A=-U1*H4A
      H1B=D6*H6A
      W=M+M4
      A1=W*A3
      H2B=D6*H6B-A1*H4A
      H3B=D7*(H6A+D4*H6B)
      H4A=W*D5*H4A
      K1=IP+JM
      K2=K1+1
      K3=K1+N
      K4=K2+N
      K5=K2+MT
      K6=K4+MT
      K7=K3+N2N
      K8=K4+N2N
      K9=K8+MT
      GO TO (18,20,19),KQ
   18 Y(K6)=UC+UD
      Z(K6)=H1B+H2B
      IF(IP.EQ.1) GO TO 21
      Y(K3)=Y(K3)+UB
      Y(K7)=Y(K7)+UE
      Z(K3)=Z(K3)+H2A-H3A
      Z(K7)=Z(K7)+H3B-H4A
      IF(IP.EQ.MP) GO TO 22
   21 Y(K4)=UH
      Y(K8)=UE
      Z(K4)=H2A+H3A
      Z(K8)=H3B+H4A
      GO TO 22
   19 Y(K5)=Y(K5)+UC-UD
      Z(K5)=Z(K5)+H1B-H2B
      IF(IP.EQ.1) GO TO 23
      Y(K1)=Y(K1)+UA
      Y(K7)=Y(K7)+UE
      Z(K1)=Z(K1)+H1A+H3A
      Z(K7)=Z(K7)+H3B-H4A
      IF(IP.EQ.MP) GO TO 22
   23 Y(K2)=Y(K2)+UG
      Y(K8)=UE
      Z(K2)=Z(K2)+H1A-H3A
      Z(K8)=H3B+H4A
      GO TO 22
   20 Y(K5)=Y(K5)+UC-UD
      Y(K6)=UC+UD
      Z(K5)=Z(K5)+H1B-H2B
      Z(K6)=H1B+H2B
      IF(IP.EQ.1) GO TO 24
      Y(K1)=Y(K1)+UA
      Y(K3)=Y(K3)+UB
      Y(K7)=Y(K7)+UE
      Z(K1)=Z(K1)+H1A+H3A
      Z(K3)=Z(K3)+H2A-H3A
      Z(K7)=Z(K7)+H3B-H4A
      IF(IP.EQ.MP) GO TO 22
   24 Y(K2)=Y(K2)+UG
      Y(K4)=UH
      Y(K8)=UE
      Z(K2)=Z(K2)+H1A-H3A
      Z(K4)=H2A+H3A
      Z(K8)=H3B+H4A
   22 Y(K9)=UF
      Z(K9)=U2*(D8*(H5A+D4*H5B)-A1*H4A)
      JM=JM+N2
   31 CONTINUE
   16 CONTINUE
      JN=JN+N
   15 CONTINUE
      RETURN
      END
```

VIII. THE MAIN PROGRAM FOR BOTH THE H-FIELD AND E-FIELD SOLUTIONS

The main program for both the H-field and E-field solutions obtains the present H-field solution and the E-field solution of [1] for the electric current on a conducting body of revolution immersed in an incident plane wave. Input data are read from punched cards. These input data are the same as those for the main program for the H-field solution which is described and listed in Section VI of Part Two.

The main program for both the H-field and E-field solutions calls the subroutines YZ, PLANE, DECOMP, and SOLVE. The function subprogram BLOG is also needed because it is called by the subroutine YZ

Minimum allocations are given by

```
COMPLEX Y(N*N), Z(N*N), RE(2*N), R(2*N), B(N), C(N)
DIMENSION XT(NT), AT(NT), X(NPHI), A(NPHI), RH(NP),
     ZH(NP), IPS(N), IPT(N)
```

where

$$N = 2*NP-3$$

The t and ϕ components of the present H-field solution for the electric current are calculated from (84) and (85). The t and ϕ components of the E-field solution of [1] for the electric current are also calculated from (84) and (85). In the present H-field solution, the coefficients I^t_{1p} and I^ϕ_{1p} in these equations are the pth elements of the vectors $\vec{I}^t_1$ and $\vec{I}^\phi_1$ which satisfy the n=1 equation in (10). In the E-field solution of [1], these coefficients are the elements of the vectors $\vec{I}^t_1$ and $\vec{I}^\phi_1$ which satisfy the n=1 equation in (6) of [1]. DO loop 28 prepares RH and ZH for use in the subroutines YZ and PLANE by multiplying them by k. With regard to (10), line 42 puts Y_1 of (86) in Y. With regard to (6) of [1], line 42 puts Z_1 of (96) in Z. Line 45 calculates IPS and changes Y. Line 46 calculates IPT and changes Z. With regard to (10), line 47 puts the excitation vectors $\vec{I}^{it}_1$ and $\vec{I}^{i\phi}_1$ for the θ

polarized incident plane wave (69) in RE. With regard to (6) of [1], line 47 puts the vectors $\vec{V}_1^t$ and $-\vec{V}_1^\phi$ for the θ polarized incident plane wave in R. Line 47 also stores vectors for the φ polarized incident plane wave (70) further on in RE and R but these vectors are not used in the main program.

In DO loop 36, JHE = 1 obtains the present H-field solution for the electric current and JHE = 2 obtains the E-field solution of [1] for the electric current. In line 55, the output IPS and Y from the subroutine DECOMP is fed along with N and RE into the subroutine SOLVE. SOLVE puts the solution $\vec{I}_1^t$ and $\vec{I}_1^\phi$ to (10) in C. Lines 59-64 put $\vec{V}_1^t$ and $\vec{V}_1^\phi$ in B. In line 67, the output IPT and Z from the subroutine DECOMP is fed along with N and B into the subroutine SOLVE. SOLVE puts the solution $\vec{I}_1^t$ and $\vec{I}_1^\phi$ to (6) of [1] in C. The t and φ components of the normalized electric current are printed out under the headings JT and JP, respectively. The normalization is the same as in the main program for the H-field solution which is described in Section VI of Part Two. The sample input and output data are for the sphere examples of Figs. 2 and 4.

```
C     LISTING OF THE MAIN PROGRAM FOR BOTH THE H-FIELD AND E-FIELD SOLUTIONS
C     THE SUBPROGRAMS YZ,BLOG,PLANE,DECOMP, AND SOLVE ARE NEEDED
//PGM JOB (XXXX,XXXX,1,1),'MAUTZ,JOE',REGION=200K
// EXEC WATFIV
//GO.SYSIN DD *
$JOB              MAUTZ,TIME=5,PAGES=60
      COMPLEX Y(1600),Z(1600),RE(240),R(240),B(40),C(40),U,CI
      DIMENSION XT(10),AT(10),X(48),A(48),RH(43),ZH(43),THR(3),IPS(40)
      DIMENSION IPT(40)
      READ(1,15) NT,NPHI
   15 FORMAT(2I3)
      WRITE(3,30) NT,NPHI
   30 FORMAT('  NT NPHI'/1X,I3,I5)
      READ(1,10)(XT(K),K=1,NT)
      READ(1,10)(AT(K),K=1,NT)
   10 FORMAT(5E14.7)
      WRITE(3,11)(XT(K),K=1,NT)
      WRITE(3,12)(AT(K),K=1,NT)
   11 FORMAT(' XT'/(1X,5E14.7))
   12 FORMAT(' AT'/(1X,5E14.7))
      READ(1,10)(X(K),K=1,NPHI)
      READ(1,10)(A(K),K=1,NPHI)
      WRITE(3,13)(X(K),K=1,NPHI)
      WRITE(3,14)(A(K),K=1,NPHI)
   13 FORMAT(' X'/(1X,5E14.7))
   14 FORMAT(' A'/(1X,5E14.7))
      READ(1,16) NP,BK,THR(1)
   16 FORMAT(I3,2E14.7)
      WRITE(3,17) NP,BK,THR(1)
   17 FORMAT('  NP',6X,'BK',12X,'THR'/1X,I3,2E14.7)
      READ(1,18)(RH(I),I=1,NP)
      READ(1,18)(ZH(I),I=1,NP)
   18 FORMAT(10F8.4)
      WRITE(3,19)(RH(I),I=1,NP)
      WRITE(3,20)(ZH(I),I=1,NP)
   19 FORMAT(' RH'/(1X,10F8.4))
   20 FORMAT(' ZH'/(1X,10F8.4))
      DO 28 J=1,NP
      RH(J)=BK*RH(J)
      ZH(J)=BK*ZH(J)
   28 CONTINUE
      CALL YZ(1,1,NP,NPHI,NT,1,RH,ZH,X,A,XT,AT,Y,Z)
      MT=NP-2
      N=2*MT+1
      CALL DECOMP(N,IPS,Y)
      CALL DECOMP(N,IPT,Z)
      CALL PLANE(1,1,1,NP,3,NT,RH,ZH,XT,AT,THR,RE,R)
      U=(0.,1.)
      DO 36 JHE=1,2
      GO TO (33,34),JHE
   33 WRITE(3,29)(Y(J),J=1,N)
   29 FORMAT(' Y'/(1X,6E11.4))
      WRITE(3,35)(RE(J),J=1,N)
   35 FORMAT(' R'/(1X,6E11.4))
      CALL SOLVE(N,IPS,Y,RE,C)
      GO TO 32
   34 WRITE(3,31)(Z(J),J=1,N)
   31 FORMAT(' Z'/(1X,6E11.4))
      DO 22 J=1,MT
      B(J)=R(J)
```

```
      J1=J+MT
      B(J1)=-R(J1)
   22 CONTINUE
      B(N)=-R(N)
      WRITE(3,23)(B(J),J=1,N)
   23 FORMAT(' B'/(1X,6E11.4))
      CALL SOLVE(N,IPT,Z,B,C)
   32 WRITE(3,21)
   21 FORMAT('    REAL JT     IMAG JT     MAG JT')
      DO 24 J=1,MT
      C1=2./RH(J+1)*C(J)
      C2=CABS(C1)
      WRITE(3,25) C1,C2
   25 FORMAT(1X,3E11.4)
   24 CONTINUE
      WRITE(3,26)
   26 FORMAT('    REAL JP     IMAG JP     MAG JP')
      MP=NP-1
      DO 27 J=1,MP
      C1=4./(RH(J)+RH(J+1))*U*C(J+MT)
      C2=CABS(C1)
      WRITE(3,25) C1,C2
   27 CONTINUE
   36 CONTINUE
      STOP
      END
$DATA
  2 20
-0.5773503E+00 0.5773503E+00
 0.1000000E+01 0.1000000E+01
-0.9931286E+00-0.9639719E+00-0.9122344E+00-0.8391170E+00-0.7463319E+00
-0.6360537E+00-0.5108670E+00-0.3737061E+00-0.2277859E+00-0.7652652E-01
 0.7652652E-01 0.2277859E+00 0.3737061E+00 0.5108670E+00 0.6360537E+00
 0.7463319E+00 0.8391170E+00 0.9122344E+00 0.9639719E+00 0.9931286E+00
 0.1761401E-01 0.4060143E-01 0.6267205E-01 0.8327674E-01 0.1019301E+00
 0.1181945E+00 0.1316886E+00 0.1420961E+00 0.1491730E+00 0.1527534E+00
 0.1527534E+00 0.1491730E+00 0.1420961E+00 0.1316886E+00 0.1181945E+00
 0.1019301E+00 0.8327674E-01 0.6267205E-01 0.4060143E-01 0.1761401E-01
 16 0.1256637E+01 0.3141593E+01
  0.0000  0.2079  0.4067  0.5878  0.7431  0.8660  0.9511  0.9945  0.9945  0.9511
  0.8660  0.7431  0.5878  0.4067  0.2079  0.0000
 -1.0000 -0.9781 -0.9135 -0.8090 -0.6691 -0.5000 -0.3090 -0.1045  0.1045  0.3090
  0.5000  0.6691  0.8090  0.9135  0.9871  1.0000
$STOP
/*
//
```

PRINTED OUTPUT CONSISTS OF THAT FROM THE MAIN PROGRAM FOR THE H-FIELD SOLUTION IN SECTION VI OF PART TWO PLUS THE FOLLOWING LINES.

```
Z
 0.6733E-01-0.1108E+02 0.6205E-01 0.3162E+01 0.5399E-01 0.8394E+00
 0.4415E-01 0.3112E+00 0.3365E-01 0.1593E+00 0.2345E-01 0.9534E-01
 0.1437E-01 0.6434E-01 0.6919E-02 0.4879E-01 0.1242E-02 0.4132E-01
-0.2739E-02 0.3823E-01-0.5271E-02 0.3745E-01-0.6728E-02 0.3773E-01
-0.7250E-02 0.3855E-01-0.7584E-02 0.3880E-01-0.1503E+02 0.6952E-01
 0.2715E+01 0.6766E-01 0.4763E+00 0.6412E-01 0.1469E+00 0.5914E-01
 0.7427E-01 0.5315E-01 0.5232E-01 0.4656E-01 0.4501E-01 0.3977E-01
 0.4254E-01 0.3317E-01 0.4167E-01 0.2706E-01 0.4120E-01 0.2165E-01
 0.4074E-01 0.1707E-01 0.4026E-01 0.1339E-01 0.3982E-01 0.1064E-01
 0.3996E-01 0.8753E-02 0.3906E-01 0.7696E-02
B
```

```
-0.2754E+00-0.7539E+00-0.3120E+00-0.6811E+00-0.3507E+00-0.5623E+00
-0.3645E+00-0.4085E+00-0.3286E+00-0.2433E+00-0.2313E+00-0.1012E+00
-0.8351E-01-0.1840E-01 0.8351E-01-0.1840E-01 0.2313E+00-0.1012E+00
 0.3286E+00-0.2433E+00 0.3645E+00-0.4085E+00 0.3507E+00-0.5623E+00
 0.3106E+00-0.6817E+00 0.2697E+00-0.7559E+00 0.7801E+00-0.2694E+00
 0.7641E+00-0.3111E+00 0.7268E+00-0.3900E+00 0.6583E+00-0.4958E+00
 0.5505E+00-0.6128E+00 0.3995E+00-0.7201E+00 0.2107E+00-0.7956E+00
-0.0000E+00-0.8227E+00-0.2107E+00-0.7956E+00-0.3995E+00-0.7201E+00
-0.5505E+00-0.6128E+00-0.6583E+00-0.4958E+00-0.7268E+00-0.3900E+00
-0.7764E+00-0.3116E+00-0.7793E+00-0.2626E+00
   REAL JT      IMAG JT      MAG JT
-0.8238E+00-0.1971E+01 0.2137E+01
-0.9777E+00-0.1907E+01 0.2143E+01
-0.1186E+01-0.1802E+01 0.2158E+01
-0.1421E+01-0.1620E+01 0.2154E+01
-0.1629E+01-0.1337E+01 0.2108E+01
-0.1751E+01-0.9546E+00 0.1994E+01
-0.1733E+01-0.5013E+00 0.1804E+01
-0.1545E+01-0.2843E-01 0.1545E+01
-0.1196E+01 0.4045E+00 0.1263E+01
-0.7315E+00 0.7493E+00 0.1047E+01
-0.2198E+00 0.9839E+00 0.1008E+01
 0.2653E+00 0.1116E+01 0.1147E+01
 0.6631E+00 0.1182E+01 0.1355E+01
 0.9285E+00 0.1196E+01 0.1514E+01
   REAL JP      IMAG JP      MAG JP
 0.7997E+00 0.1970E+01 0.2126E+01
 0.9274E+00 0.1833E+01 0.2054E+01
 0.1071E+01 0.1645E+01 0.1963E+01
 0.1221E+01 0.1362E+01 0.1829E+01
 0.1312E+01 0.1014E+01 0.1658E+01
 0.1297E+01 0.6571E+00 0.1454E+01
 0.1166E+01 0.3656E+00 0.1222E+01
 0.9561E+00 0.2058E+00 0.9780E+00
 0.7409E+00 0.2063E+00 0.7691E+00
 0.5921E+00 0.3454E+00 0.6855E+00
 0.5508E+00 0.5635E+00 0.7880E+00
 0.6120E+00 0.7924E+00 0.1001E+01
 0.7237E+00 0.9694E+00 0.1210E+01
 0.8687E+00 0.1113E+01 0.1412E+01
 0.9847E+00 0.1194E+01 0.1547E+01
```

REFERENCES

[1] J. R. Mautz and R. F. Harrington, "An Improved E-Field Solution for a Conducting Body of Revolution," Report RADC-TR-80-194, Rome Air Development Center, Griffiss Air Force Base, New York, June 1980.

[2] J. R. Mautz and R. F. Harrington, "H-Field, E-Field and Combined-Field Solutions for Bodies of Revolution," Report TR-77-2, Department of Electrical and Computer Engineering, Syracuse University, Syracuse, NY, February 1977.

[3] A. J. Poggio and E. K. Miller, "Integral Equation Solutions of Three-dimensional Scattering Problems," Chap. 4 of Computer Techniques for Electromagnetics, edited by R. Mittra, Pergamon Press, 1973.

[4] P.L.E. Uslenghi, "Computation of Surface Currents on Bodies of Revolution," Alta Frequenza, vol. 39, No. 8, 1970, pp. 1-12.

[5] T. K. Wu and L. Tsai, "Scattering from Arbitrarily-shaped Lossy Dielectric Bodies of Revolution," Radio Science, vol. 12, No. 5, September-October 1977, pp. 709-718.

[6] J. R. Mautz and R. F. Harrington, "Electromagnetic Scattering from a Homogeneous Material Body of Revolution," AEÜ, vol. 33, No. 2, February 1979, pp. 71-80.

[7] A. W. Glisson and D. R. Wilton, "Simple and Efficient Numerical Techniques for Treating Bodies of Revolution," Report RADC-TR-79-22, Rome Air Development Center, Griffiss Air Force Base, New York 13441, March 1979, A067361.

[8] L. N. Medgyesi-Mitschang and C. Eftimiu, "Scattering from Axisymmetric Obstacles Embedded in Axisymmetric Dielectrics: The Method of Moments Solution," Appl. Phys., vol. 19, 1979, pp. 275-285.

[9] J. R. Mautz and R. F. Harrington, "A Combined-Source Solution for Radiation and Scattering from a Perfectly Conducting Body," IEEE Trans. Antennas Propagat., vol. AP-27, July 1979, pp. 445-454.

[10] V. I. Krylov, Approximate Calculation of Integrals, translated by A. H. Stroud, Macmillan, New York, 1962.

[11] P. J. Davis and P. Rabinowitz, Methods of Numerical Integration, Academic Press, 1975, p. 139.

[12] H. B. Dwight, Tables of Integrals and Other Mathematical Data, Macmillan, New York, 1961.

[13] J. R. Mautz, "Computer Program for the Mie Series Solution for a Sphere," Report TR-77-12, Department of Electrical and Computer Engineering, Syracuse University, Syracuse, NY, December 1977.

[14] J. R. Mautz and R. F. Harrington, "Computer Programs for H-field, E-field, and Combined Field Solutions for Bodies of Revolution," Report RADC-TR-77-215, Rome Air Development Center, Griffiss Air Force Base, New York 13441, June 1977, A044204.

[15] M. Abramowitz and I. A. Stegun, Handbook of Mathematical Functions, U. S. Government Printing Office, Washington, D.C. (Natl. Bur. Std., U. S. Applied Math. Ser. 55), 1964.

[16] J. R. Mautz and R. F. Harrington, "Transmission from a Rectangular Waveguide into Half Space through a Rectangular Aperture," Interim Technical Report RADC-TR-76-264, Rome Air Development Center, Griffiss Air Force Base, New York 13441, August 1976, A030779.

MISSION
of
Rome Air Development Center

RADC plans and executes research, development, test and selected acquisition programs in support of Command, Control Communications and Intelligence (C^3I) activities. Technical and engineering support within areas of technical competence is provided to ESD Program Offices (POs) and other ESD elements. The principal technical mission areas are communications, electromagnetic guidance and control, surveillance of ground and aerospace objects, intelligence data collection and handling, information system technology, ionospheric propagation, solid state sciences, microwave physics and electronic reliability, maintainability and compatibility.